AN ABSTRACT OF THE DISSERTATION OF

Priscilla Emily Dombek for the degree Doctor of Philosophy in Biochemistry and Biophysics presented on July 18, 1996. Title: Functional Domains of *Agrobacterium tumefaciens* Single-Stranded DNA Binding Protein VirE2.

Abstract approved: Redacted for Privacy

Walt Ream

Agrobacterium tumefaciens is a gram-negative soil bacterium that causes crown gall tumors on dicotyledenous plants. The transferred DNA (T-DNA) portion of the *A. tumefaciens* tumor-inducing (Ti) plasmid enters infected plant cells and integrates into plant nuclear DNA. The T-DNA is accompanied into plant cells by the VirD2 endonuclease covalently attached to its 5' end. VirE2, a cooperative, single-stranded DNA-binding protein is also transported into plant cells during infection by *A. tumefaciens*. VirD2 and VirE2 contain nuclear localization signals (NLSs) and are transported into the plant cell nucleus.

The location of functional domains by the insertion of *Xho*I linker oligonucleotides throughout *virE2* is reported. A ssDNA binding domain was located in the C-terminal half of VirE2, as well two domains involved in cooperative single-stranded DNA binding. Further, we isolated a mutation in the central region of VirE2 that decreased tumorigenicity, but did not affect ssDNA binding.

Functional Domains of *Agrobacterium tumefaciens* Single-Stranded DNA Binding Protein VirE2

by

Priscilla Emily Dombek

A DISSERTATION

submitted to

Oregon State University

in partial fulfillment of
the requirements for the
degree of

Doctor of Philosophy

Presented on July 18, 1996
Commencement June 1997

Doctor of Philosophy dissertation of Priscilla Emily Dombek
presented on July 18, 1996

APPROVED:

Redacted for Privacy

Major Professor, representing Biochemistry and Biophysics

Redacted for Privacy

Chair of Department of Biochemistry and Biophysics

Redacted for Privacy

Dean of Graduate School

I understand that my dissertation will become part of the permanent collection of Oregon State University libraries. My signature below authorizes release of my thesis to any reader upon request.

Redacted for Privacy

Priscilla Emily Dombek, Author

ACKNOWLEDGMENTS

I would like to acknowledge my major professor, Dr. Walt Ream; without his guidance this work would not have been possible. I would also like to acknowledge the members of my committee; Dr. Douglas Barofsky, Dr. Dallice Mills, Dr. Henry Schaup and Dr. Dale Mosbaugh, for their time and suggestions. I would like to thank Larry Hodges for being a friend as well as a fellow lab worker during my years in the Ream Laboratory.

I would like to acknowledge the friendship of Marilyn Walsh and Kay Bransom. Many other people at Oregon State University have offered their help, friendship and suggestions during this work including; Ravi Singh, Ellen Wallace, Becky Russell, Charlotte Rasmussen, Margot Pearson, Peggy Peterson, Dorina Avram, Sam Bennett, Dr. Wil Gamble and Jay Evans. I will also miss Owusuwaa Owusu and the other members of the Inner Strength Gospel Choir; and my friends at the Yawners Toastmasters Club, at Unity Church and at the Tuesday night Yoga class with Janet Hochfeld.

TABLE OF CONTENTS

TABLE OF CONTENTS (continued)

TABLE OF CONTENTS (continued)

TABLE OF CONTENTS (continued)

TABLE OF CONTENTS (continued)

LIST OF FIGURES

LIST OF FIGURES (continued)

LIST OF FIGURES (continued)

LIST OF TABLES

LIST OF APPENDIX FIGURES

FUNCTIONAL DOMAINS OF *AGROBACTERIUM TUMEFACIENS* SINGLE-STRANDED DNA BINDING PROTEIN VIRE2

CHAPTER 1. INTRODUCTION

Overview of the Infection Process

Agrobacterium tumefaciens causes crown gall disease on dicotyledenous plants (DeCleene and DeLey 1976; reviewed in Ream 1989; Winans 1992; Hooykaas & Biejersbergen 1994). The *A. tumefaciens*-plant interactions are diagrammed in Figure 1.1. A wounded plant secretes phenolic compounds, such as acetosyringone, which induce the virulence (*vir*) genes on the *A. tumefaciens* tumor-inducing (Ti) plasmid. The *vir* genes and several chromosomally encoded virulence (*chv*) genes direct the transfer and integration of a region of the bacterial Ti plasmid into the plant genome. This transferred DNA, known as the T-DNA, directs the overproduction of plant growth hormones which leads to the proliferation of infected cells, resulting in crown gall tumor formation.

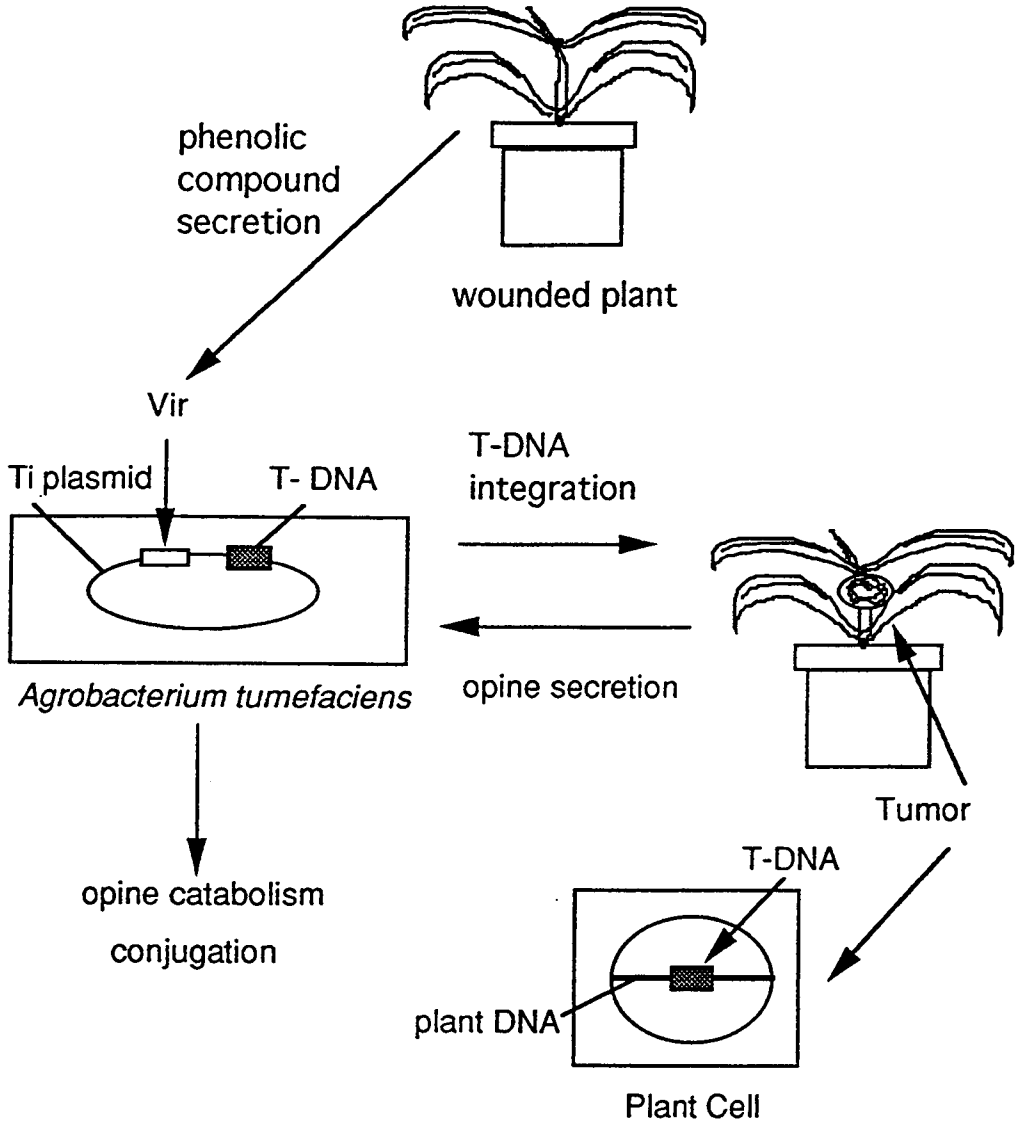

Figure 1.1 Schematic diagram of the *A. tumefaciens*-plant interaction process that leads to tumor development. The open box represents the *vir* operons and the filled box the DNA that is transferred by *A. tumefaciens* to the plant cell nucleus and integrated into the plant genome.

The transformed plant tissue produces novel compounds called opines. Most opines are formed by the condensation of an amino acid with a keto acid or sugar (Dessaux *et al.* 1993). Opines are used as a nutrient source for *A. tumefaciens* and induce conjugal transfer of the Ti plasmid. *A. tumefaciens* is a natural example of plant genetic engineering and is currently the most widely used method of plant transformation. *Agrobacterium* transfers large segments (20 kilobase or more) of DNA (Miranda *et al.* 1992) and protects the incoming DNA from rearrangements and duplications (Grevelding *et al.* 1993). By more fully understanding the transfer process, this research may help to further increase the efficiency of plant transformation using *A. tumefaciens* and since VirE2 protein may play a role in T-DNA integration, an *A. tumefaciens* strain may be developed that can efficiently reintroduce isolated plant genes into their original location by homologous recombination. In addition, this additional understanding of T-DNA transfer may suggest methods to prevent crown gall disease.

A. tumefaciens strains are classified by the opines which they direct the host plant to synthesize. A strain that directs the synthesis of an opine usually has corresponding opine catabolism

genes located on its Ti plasmid. However, many *A. tumefaciens* strains carry plasmids that are non-oncogenic but do have opine catabolism and opine-induced conjugal transfer loci (Kerr and Ellis 1982). Over twenty opines have been classified into mainly four families: octopine, nopaline, mannopine, and agrocinopine. Opines belonging to other families exist and additional opines have been detected in tumors induced by at least three new classes of *A. tumefaciens* strains. These opines are in the process of being characterized and classified (Dessaux *et al.* 1993). An octopine-type Ti plasmid, pTiA6NC, directs the synthesis of octopine, agropine, and mannopine (Winans 1992). A nopaline-type plasmid, pTiC58, directs the synthesis of nopaline and agrocinopines A and B (Winans 1992). The structural formulas of the opines secreted by plants infected by the nopaline- and octopine-type Ti plasmids are shown in Figure 1.2.

Tumor-inducing (Ti) plasmid

A genetic map of an octopine-type Ti plasmid is presented in Figure 1.3. This Ti plasmid has two T-DNA regions that are transferred to the plant (T_L T-DNA and T_R T-DNA).

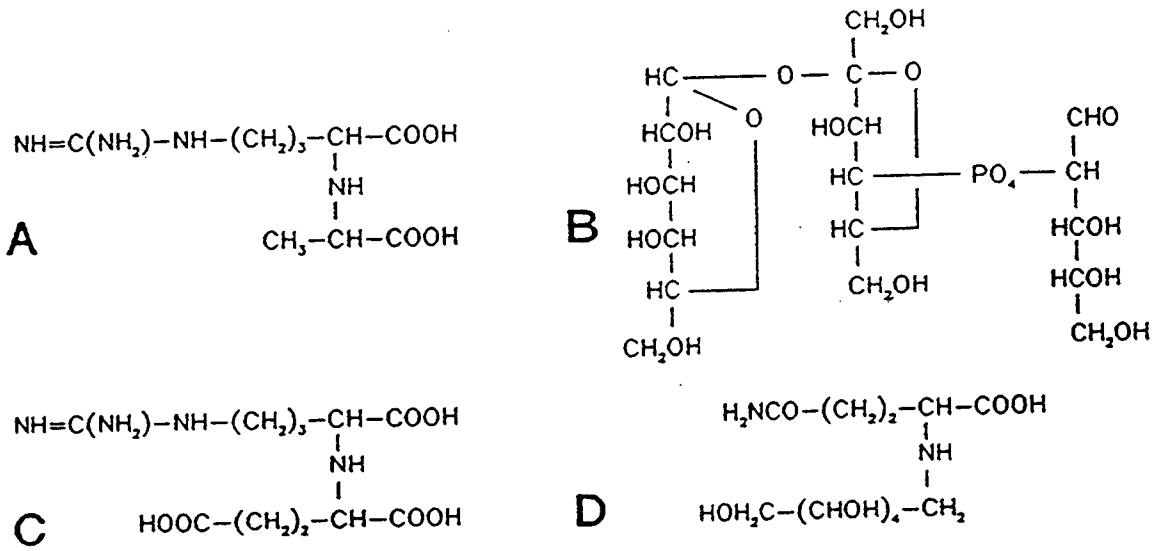

Figure 1.2. Structural formulas of representative opines. a) octopine b) agrocinopine A c) nopaline d) mannopine Synthesis of octopine and mannopine are directed by pTiA6NC. Synthesis of nopaline and agrocinopines A and B are directed by plasmid pTiC58. (Winans 1992)

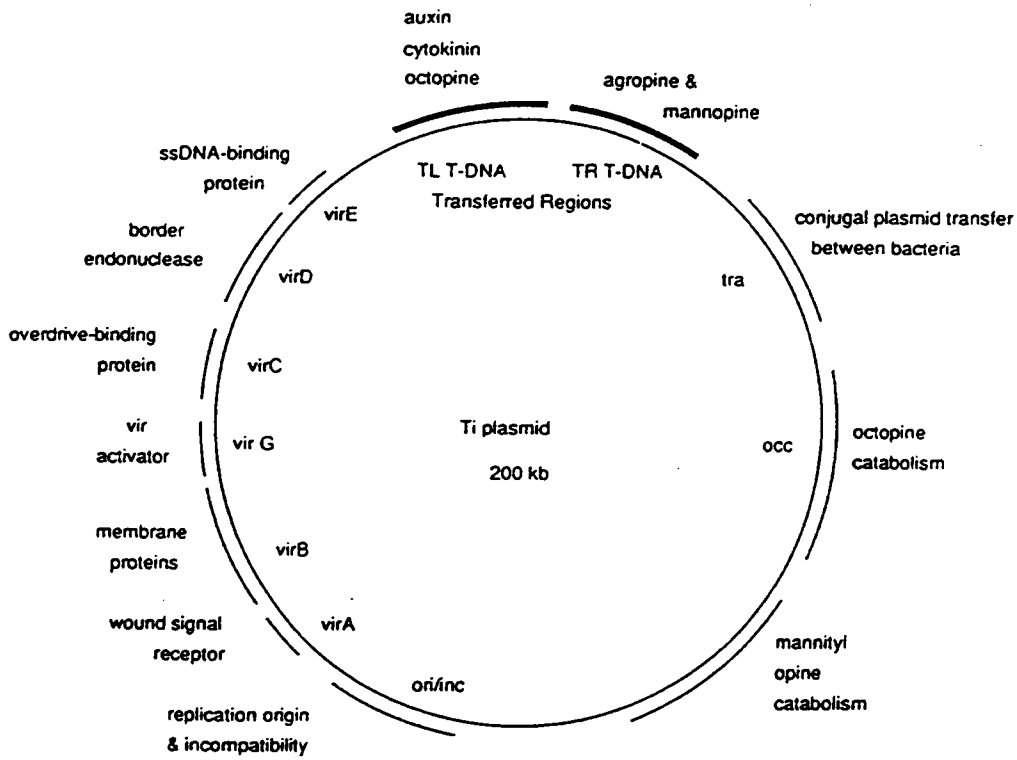

Figure 1.3. Genetic map of an octopine-type Ti plasmid. (Ream 1989). This plasmid has two T-DNA regions that are transferred to the plant, TL-TDNA and TR-TDNA. This transfer is directed by the *vir* (virulence) genes. This Ti plasmid also has *tra* and *occ* regions. The opines synthesized by the infected plant induce conjugal transfer, directed by the *tra* genes and are catabolized by the *occ* genes.

Nopaline Ti plasmids transfer a single T-DNA region. The Ti plasmid also has opine catabolism and conjugal transfer regions.

The *vir* genes on the tumor inducing (Ti) plasmid activate the T-DNA transfer process (Figure 1.3). The *vir* gene products of octopine and nopaline strains are highly homologous (Rogowsky *et al.* 1990). VirA, an environmental sensor protein, phosphorylates VirG (Jin *et al.* 1990a). Phosphorylated VirG binds to the *vir* boxes upstream of the *vir* operons to induce their transcription (Jin *et al.* 1990b; Pazour and Das 1990).

Together the VirD1 and VirD2 proteins form a site-specific endonuclease and nick the border repeats on either side of the T-DNA (Albright *et al.* 1987; Jayaswal *et al.* 1987; Stachel *et al.* 1986; Stachel *et al.* 1987; Veluthambi *et al.* 1987; Wang *et al.* 1987; Yanofsky *et al.* 1986). This results in the release of a single-stranded DNA molecule, known as the T-strand (Albright *et al.* 1987; Jayaswal *et al.* 1987; Stachel *et al.* 1986b).

The VirB proteins and VirD4 form a membrane pore required for T-strand export (Okamoto *et al.* 1991; Berger and Christie 1994; Ward *et al.* 1991; Zambryski 1992).

VirE2, the single-stranded DNA binding protein, is also exported, along with the T strand from *A. tumefaciens* (Otten *et al.* 1984; Citovsky *et al.* 1992; Citovsky *et al.* 1994; Binns *et al.* 1995).

Transferred DNA (T-DNA)

One of the transferred DNA regions from an octopine type plasmid (T_L T-DNA) is diagrammed in Figure 1.4. There are 24-base pair (bp) border repeats on each end, and a sequence, *overdrive*, is adjacent to both right-hand border repeats (Peralta *et al.* 1986). This sequence is required for efficient transfer of both T-DNA regions from octopine-type strains (Peralta *et al.* 1986).

The oncogenes, *iaaM*, *iaaH*, and *ipt* increase the production of the phytohormones, auxin and cytokinin (Schroder *et al.* 1984; Akiyoshi *et al.* 1984). The genes for tryptophan monooxygenase (*iaaM*) and indoleacetamide hydrolase (*iaaH*) encode proteins that convert tryptophan to indoleacetic acid, an auxin (Inze *et al.* 1984). Isopentenyl transferase (*ipt*) catalyzes the last step in the biosynthesis of isopentenyl-AMP which is converted by the plant to *trans*-zeatin and *trans*-ribosyzeatin, both cytokinins (Akiyoshi *et al.* 1984; Barry *et al.* 1984).

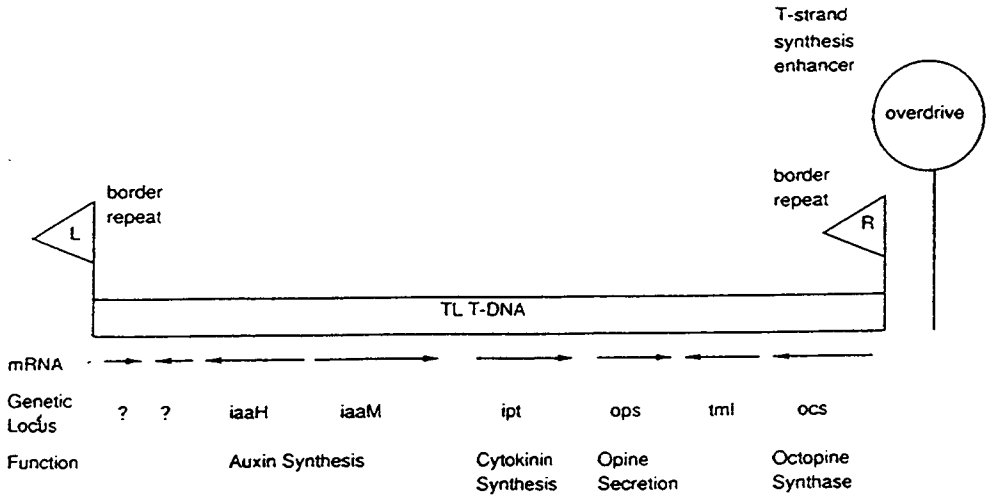

Figure 1.4. Genetic map of the T_L T-DNA of an octopine-type Ti plasmid. The gene symbols indicate indoleacetamide hydrolase (*iaaH*), tryptophan monooxygenase (*iaaM*), isopentenyl transferase (*ipt*), opine secretion (*ops*), tumor morphology large (*tml*), and octopine synthase (*ocs*) (Ream 1989).

family (Kemp 1982). The biosynthesis of a permease that allows opine secretion is directed by *ops* (Messens *et al.* 1985). Mutations in tumor morphology (*tml*) typically result in larger than normal-sized tumors (Ream *et al.* 1983). The other region transferred by octopine-type plasmids, T_R T-DNA, directs the synthesis of two mannopine family opines, mannopine and agropine (Ellis *et al.* 1984).

T-DNA Transfer

T-DNA transfer requires the *vir* genes that lie on the Ti plasmid and some chromosomally encoded genes (reviewed in Ream 1989; Winans 1992; Hooykaas and Bierjersbergen 1994).

Initiation of T-DNA Transfer: VirA/VirG/*chv*

The initiation of T-DNA transfer depends upon *A. tumefaciens* sensing the plant wound environment. Induction of the *vir* genes is influenced by phenolic compounds, sugar molecules, temperature and acidic pH. The plant wound environment contains phenolics and monosaccharides as cell wall precursors (Reisert 1981) and tends to be acidic (Kahl 1982). Phenolic compounds are absolutely required

for induction to occur (Stachel *et al.* 1986a) and efficient induction by these compounds requires pH values between 5.2 and 5.8 (Stachel *et al.* 1986a). Several sugars, including D-galacturonic acid and D-glucuronic acid (both components of plant cell wall polysaccharides), glucose, arabinose, and galactose enhance induction when the concentration of the phenolic compounds is limited (Shimodo *et al.* 1990; Ankenbauer *et al.* 1990).

The *vir* genes are transcribed at extremely low levels until induced by co-cultivation with plant cells or with phenolic compounds (Stachel *et al.* 1986a). VirA and VirG are essential for a response to any of the environmental factors (Stachel and Zambryski 1986) and they share similarities to other bacterial two-component regulatory proteins that detect environmental factors (Parkinson and Kofoid 1992). VirA phosphorylates VirG, which increases its own transcription and that of the other *vir* operons (Powell *et al.* 1988).

VirA expression is increased five- to ten-fold by the phenolic compounds secreted by a wounded plant (Winans *et al.* 1988; Rogowsky *et al.* 1987). The inner membrane spanning VirA protein has its C-terminus extending into the cytoplasm and its N-terminus

into the periplasm (Melchers *et al.* 1989; Winans *et al.* 1989). The periplasmic domain of VirA is similar in sequence to a domain in the *Escherichia coli* Tar protein (Melchers *et al.* 1989) which senses sugars and initiates chemotaxis toward them. Due to the similarities in sequence between these domains, it was thought (Melchers *et al.* 1989) that the periplasmic domain of VirA interacted directly with acetosyringone. However, the periplasmic domain of VirA was deleted without a loss of *vir* gene induction by acetosyringone (Melchers *et al.* 1989; Cangelosi *et al.* 1990; Shimoda *et al.* 1990). In addition, two small cytoplasmic proteins bound an ^{125}I labeled analog of acetosyringone (Lee *et al.* 1992) which did not bind to VirA. These chromosomally-encoded proteins may directly bind to acetosyringone, and then directly interact with VirA in a step prior to VirA/VirG *vir* gene induction. Since mutations in this cytoplasmic domain of VirA eliminate *vir* gene induction by acetosyringone, this domain is thought to be involved in the interaction (Winans *et al.* 1994). Recent genetic evidence suggests that VirA directly senses phenolic compounds (Lee *et al.* 1995). Ti plasmids transferred into isogenic chromosomal backgrounds determined the response of the *A. tumefaciens* strain to individual

phenolic compounds. By subcloning the Ti plasmid, it was also determined that the differences in induction by the phenolic compounds are specifically linked to the *virA* gene (Lee *et al.* 1995). The authors of this paper (Lee *et al.* 1995) mention, in support of their evidence of VirA as the phenolic sensing protein, that neither of the two chromosomally-encoded proteins has been cloned. This genetic evidence is a convincing argument that VirA is indeed the phenolic sensing protein.

Although the periplasmic domain of VirA is not critical for induction by acetosyringone, it is crucial for the enhancement of induction by certain sugars (Shimoda *et al.* 1990). This domain interacts with a periplasmic sugar binding protein, ChvE, that is chromosomally encoded (Cangelosi 1990). ChvE is also required for the chemotaxis of *A. tumefaciens* towards certain sugars.

A. tumefaciens causes tumors on plants only at temperatures below 32°C (Braun 1947). The activity of VirA at elevated temperatures was investigated in an attempt to understand why *A. tumefaciens* does not infect plants at elevated temperatures. Both the autophosphorylation of VirA and the subsequent transfer of this phosphate to VirG does not occur *in vitro* at temperatures above 32°

C (Jin *et al.* 1993a), indicating that VirA might be responsible for this temperature sensitivity. Yet, a *virG* constitutive mutant strain, which activates transcription without VirA, is incapable of infecting plants at temperatures above 32° C (Jin *et al.* 1993a). Consequently, other *A. tumefaciens* proteins may also be inactivated at higher temperatures, or the plant might become resistant to infection under these conditions.

VirG has two domains, a DNA binding domain and a receiver domain (Winans *et al.* 1994). The C-terminal domain binds to the 12-bp *vir* box sequences in *vir* gene promoters (Jin *et al.* 1990b; Pazour and Das 1990; Powell and Kado 1990) and the N-terminal domain is phosphorylated (Jin *et al.* 1990a; Roitsch *et al.* 1990). Three separate research groups have characterized a *virG* mutation that results in constitutive gene expression (Jin *et al.* 1993b; Sheeren-Groot *et al.* 1994; Han and Winans 1994). This mutation (VirGN54D) changes an asparagine at position 54 to an aspartic acid, and the protein cannot be phosphorylated (Jin *et al.* 1993b) because it now has a negative charge near residue 52, the phosphorylation site. Its constitutive phenotype mimics the activity of the wild-type phosphorylated protein. Both VirGN54D and phosphorylated

wild-type VirG bind to a promoter containing two *vir* boxes with 10-fold greater affinity than unphosphorylated VirG (Jin *et al.* 1993b). In a manner similar to other transcriptional activators (Aiba *et al.* 1989), this increase in affinity to DNA may result from cooperative interactions between the phosphorylated receiver domains. Both the wild-type phosphorylated protein and the mutant protein bind to DNA in a cooperative manner, supporting this conclusion.

Since the discovery of *chvE* (Cangelosi *et al.* 1990), several other chromosomally-encoded virulence genes that influence induction have been reported (Mantis and Winans 1993; Charles and Nester 1993; Cooley *et al.* 1994; D'Souza-Ault *et al.* 1993; Gray *et al.* 1993). Another two-component regulatory system, similar to the VirA/VirG system has been identified and the genes have been sequenced (Mantis and Winans 1993; Charles and Nester 1993). Strains with mutations in either *chvI* (the target of phosphorylation) or *chvG* (a protein kinase) are avirulent and have low levels of *vir* gene expression. Their precise functions are unknown. Another chromosomal gene, *ros*, negatively regulates the *virC* and *virD* operons (Close *et al.* 1985; Cooley *et al.* 1994, D'Souza-Ault at al. 1993) which are transcribed in opposite directions. The VirG and

Ros binding sites overlap each other in the common promoter region. After *vir* gene induction, VirG overcomes the repression of gene transcription by Ros. Mutations in another chromosomal gene, *miaA,* which encodes t-RNA: isopentenyl transferase activity, decrease *vir* gene induction two- to ten-fold (Gray *et al.* 1992). Without this tRNA modification enzyme, the translation efficiency of the *vir* genes is reduced.

In summary, *vir* gene induction is a complex process that involves interactions between Ti plasmid and chromosomally-linked genes, and interactions between *A. tumefaciens* genes and plant signal molecules.

T Strand Creation: VirD1/VirD2

After induction of *A. tumefaciens* by acetosyringone, the 24-bp direct repeats flanking the T-DNA are nicked (Albright *et al.* 1987; Wang *et al.* 1987). Border nicks are detected on the bottom strand between the third and fourth base pair in the border repeats of the octopine type Ti plasmid, pTiA6 (Albright *et al.* 1987). The nicks occur within four hours after *vir* gene induction, and both VirD1 and VirD2 are required for border nicking in *A. tumefaciens* and *E. coli*

(Jayaswal *et al.* 1987). The action of this site-specific endonuclease results in the release of a single-stranded DNA molecule, known as the T strand, which is subsequently transferred to the plant.

The release of the T strand has been proposed to occur via DNA replication and strand displacement (Stachel *et al.* 1986b; Albright *et al.* 1987). The nicked bottom strand of the right border provides the 3' OH group for initiation of replication, while the top strand provides a template. Single-stranded DNA transfer also occurs in bacterial conjugation and its similarities with T-DNA transfer will be discussed below. Evidence for the transfer of single-stranded T-strands to plant protoplasts has been presented (Yusibov *et al.* 1994). In these experiments, the bacteria attached to the protoplast cell walls were removed by centrifugation before DNA purification, and T-DNA was amplified using the polymerase chain reaction (PCR), from tobacco protoplasts within 30 minutes after co-cultivation with *A. tumefaciens*. If the template DNA is treated with S1 nuclease, which is specific for single-stranded DNA, prior to the PCR, no PCR product was detected. To verify that the T strands were indeed from the protoplast cytoplasm and not from

contaminating bacteria, several control experiments were performed (Yusibov *et al.* 1994). No detectable PCR product was amplified from the bacteria attached to the protoplast cell walls and then removed by centrifugation or from uninfected plant cells extracted in a similar manner. If the plant protoplasts were mixed with induced bacterial cells and the DNA from the protoplasts was immediately extracted, again no PCR products were observed. Thus, the T-DNA molecules were associated only with infected plant protoplasts after co-cultivation with *A. tumefaciens*. Using PCR primers directed against the Ti plasmid-encoded *virA* gene or an *A. tumefaciens* chromosomal gene, no PCR products were amplified from the infected protoplasts, confirming that bacterial cells did not contaminate the template DNA.

VirD2 covalently attaches to the 5' terminus of the transferred single-stranded T strand molecule (Herrara-Estrella *et al.* 1988; Filichkin and Gelvin 1993; Ward and Barnes 1988; Durrenberger *et al.* 1986; Howard *et al.* 1989; Young and Nester 1988). Evidence for this bond was noticed during the isolation of T strand DNA from induced *A. tumefaciens*. During phenol extraction, T strands are observed in the interphase between the aqueous and

organic phases (Howard *et al.* 1989). This suggests a DNA-protein interaction; this interaction is resistant to boiling in 2% SDS (an ionic detergent), indicating covalent bond formation.

To demonstrate that this protein was VirD2, antisera to VirD2 was used to immunoprecipitate DNA from acetosyringone-induced *A. tumefaciens* cells (Howard *et al.* 1989; Young and Nester 1988). Antisera against VirG did not precipitate any T-DNA molecules, whereas in a related experiment, a 58-kDa protein complexed with DNA was isolated from acetosyringone-induced *A. tumefaciens* cell extracts (Howard *et al.* 1989). The DNA-protein complexes were treated with S1 nuclease, to digest single-stranded DNA, prior to analysis by SDS-polyacrylamide gel electrophoresis and immunoblotting. Immunoblotting identified this protein as VirD2.

In a site-directed mutagenesis experiment, each tyrosine residue in VirD2 was changed to a glycine to eliminate possible phosphodiester bond formation and determine the site of covalent DNA attachment (Vogel and Das 1992a). Tyrosine 29 was found to be essential for endonuclease activity. This amino acid participates in both border nicking and presumably in the formation of the covalent protein-DNA bond, since they are assumed to occur in a one-step

process. The nicked DNA from strains with mutations in each of the other tyrosine residues was covalently bound to protein, again suggesting tyrosine 29 participates in the DNA-protein complex formation.

The activities of both VirD1 and VirD2, individually and together, have been characterized *in vitro*. VirD1 protein may have type I topoisomerase activity as reported by Ghai and Das, 1989, and is able to convert supercoiled DNA to relaxed DNA by cleaving and rejoining the DNA, leading to unwinding. However, other researchers have failed to detect this activity in purified VirD1 (Pansegrau *et al.* 1993a).

At this point, it is difficult to discard either observation. The VirD1 protein was partially purified from *E. coli* by Ghai and Das using sucrose gradient centrifugation. Although not completely purified, protein extracts from cells containing vector only and uninduced cells had no activity. A positive control reaction using calf thymus topoisomerase I was also included. Agarose gels clearly show additional DNA bands corresponding to relaxed DNA in the presence of the protein extract containing VirD1 protein and magnesium.

The VirD1 protein purified by Pansegrau and his group (Scheiffele *et al.* 1995) was able to nick the T-DNA border sequence when combined with purified VirD2 protein. However, it did not exhibit any DNA-relaxing activity. This group as well, purified VirD1 from *E. coli*, and demonstrated that it is an insoluble protein which must be solubilized in urea and renatured. The lack of topoisomerase I activity seen by the second group might be due to a difference in protein refolding during purification. Because border nicking activity was observed when this purified VirD1 protein was in association with purified VirD2 (Scheiffele *et al.* 1995), at least part of the protein must have been correctly renatured.

Purified VirD2 cleaves ssDNA (single-stranded DNA) containing a T-DNA border repeat sequence (Pansegrau *et al.* 1993a) at the same nucleotide sequence as observed in *A. tumefaciens*, and VirD2 also attaches to the 5' end of the cleaved oligonucleotide. Purified VirD1 and VirD2 catalyze the site- and strand-specific cleavage of dsDNA (double-stranded DNA) with a T-DNA border sequence (Scheiffele *et al.* 1995). The reaction requires Mg^{++} ions and supercoiled DNA. Like the reaction of VirD2 with ssDNA, this reaction may also be an equilibrium reaction because when both proteins are in great molar

excess, only 35-40% of the substrate DNA is cleaved. VirD1 either distorts the double-helix exposing the T-DNA border sequence, or alters the specificity of VirD2 from single-stranded to double-stranded DNA.

Overexpression of VirD1 and VirD2 in *A. tumefaciens* by introduction of extra copies on a broad-host-range plasmid results in increased plant transformation efficiency (Wang *et al.* 1990). Tumor size on *Kalanchoe daigremontiana* and carrot increases and more tumors are found on potato discs. Although the initial rate of T strand production is increased, the final T strand level inside *A. tumefaciens* is identical to a wild-type strain.

The *virD* operon has two other open reading frames, *virD3* and *virD4*. A fifth open reading frame, *orf5*, is downstream of *virD4* and has its own promoter (Lin and Kado 1993). Expression of *orf5* is acetosyringone independent. Since VirD4 is a membrane protein, its role in T-DNA transfer will be discussed with the VirB proteins. Neither *virD3* nor *orf5* are required for tumorigenicity on plants (Vogel and Das 1992b; Lin and Kado 1993), and they will not be discussed further.

Overdrive Binding Proteins: VirC

The exact functions of VirC1 and VirC2 proteins are unknown. Evidence suggests VirC1 may bind to the *overdrive* sequence during T-strand transfer (Toro *et al.* 1989). Immediately adjacent to the right T-DNA borders in octopine-type Ti plasmids is a conserved sequence designated *overdrive* that increases tumorigenicity (Peralta and Ream 1985; Peralta *et al.* 1986). This sequence is fully functional on either side of the right border, in either orientation, and when located over 500 bp away (Ji *et al.* 1988; van Haaren *et al.* 1987). Insertion mutations in *virC1* or *virC2* exhibit the same weakly virulent phenotype as an *overdrive* deletion strain (Ji *et al.* 1988). *virC2* and *overdrive* double mutants exhibit this same weakly virulent phenotype suggesting a possible interaction between the proteins of the *virC* operon and the *overdrive* sequence (Ji *et al.* 1988). VirC1 binds specifically to *overdrive* in a gel retardation assay (Toro *et al.* 1989) and in DNA affinity chromatography (Toro *et al.* 1989). VirC2, however, is detected only in the flow-through from the *overdrive* DNA affinity column.

VirC1 possibly also interacts with VirD2. VirD2 protein is retained on DNA affinity columns with either the *overdrive* or right

border sequences, suggesting a possible interaction between VirD2 and VirC1 and other *A. tumefaciens* proteins (Toro *et al.* 1989).

VirC1 increases T-strand production in *E. coli,* but only when quantities of the VirD1/VirD2 endonuclease are limiting (DeVos and Zambryski 1989). The role of *virC* in T-strand production in *A. tumefaciens* remains obscure. Stachel *et al.* (1987) have reported *virC* mutations are unimportant in border nicking, while others notice only a slight decrease in border nicking (Toro *et al.* 1988).

Membrane Pore Proteins: VirB/VirD4

The VirB proteins and VirD4 form a pore structure through which the T-DNA/protein complex is transported. Eleven open reading frames are found in *virB*, the largest *vir* operon (Thompson *et al.* 1988). VirB1, VirB2, VirB4, VirB5, VirB7, VirB8, and VirB9 all have cleavable signal sequences that allow transport across the inner membrane (Beijersbergen *et al.* 1994). VirB2, VirB3, VirB6, VirB8 and VirB10 have hydrophobic domains also designating membrane localization (Beijersbergen *et al.* 1994). Proteins without signal sequences can also be localized to bacterial membranes due to interactions with other proteins (Biejersbergen *et al.* 1994).

Fusions between the *virB* genes and the gene coding for the enzyme alkaline phosphatase (*phoA*) which lacks its signal sequence have been used to determine VirB protein locations. Alkaline phosphate activity is found only after the phosphatase part of a fusion protein is transported across the inner membrane into the periplasmic space (Manoil *et al.* 1990). VirB proteins have also been localized to *A. tumefaciens* cell membranes using specific antiserum to individual VirB proteins. By this method, induced *A. tumefaciens* cells are fractionated into cellular components and immunoblots of these fractions determine the locations of the proteins. Using sequence analysis, alkaline phosphatase fusions and immunoblots, all of the VirB proteins have been localized to one or both *A. tumefaciens* cell membranes (Fernandez *et al.* 1996a, Thorstenson *et al.* 1993; Shirasu and Kado 1993; Beijersbergen *et al.* 1994).

VirB1 was localized to either the inner membrane, or to both the inner and the outer membranes, depending upon the fractionation method applied (Thorstenson *et al.* 1993). VirB2 was localized to both the inner and outer membranes (Shirasu and Kado 1993). The majority of VirB3 was localized to the outer membrane (Shirasu and Kado 1993). VirB4 localized to the inner membrane (Shirasu *et al.*

1994; Thorstenson *et al.* 1993) or to both membranes (Thorstenson *et al.* 1993), again depending upon the fractionation method used. Since VirB4 lacks a hydrophobic domain, its localization may be due to interactions with other VirB proteins (Beijersbergen *et al.* 1994). An active *phoA* fusion with VirB5, indicates a periplasmic location (Beijersbergen *et al.* 1994). Using immunoblots, VirB5 has been localized to both the inner membrane and soluble fractions (containing cytoplasm and periplasm) (Thorstenson *et al.* 1993).

VirB6 has five strongly hydrophobic domains and *phoA* fusion of this protein was active (Beijersbergen *et al.* 1994), leading to the prediction that it is an inner membrane protein with five transmembrane loops. VirB7 has its amino terminus anchored predominantly to the outer membrane and its carboxy domain in the periplasmic space (Fernandez *et al.* 1996a). VirB8 and VirB9 have been localized to both the inner and outer membranes using immunoblot analysis (Thorstenson *et al.* 1993, Shirasu and Kado 1993). However, VirB8 has also been localized solely to the inner membrane using VirB8 antisera and immunogold labeling of thin sections of *A. tumefaciens* (Thorstenson and Zambryski 1994). VirB10 and VirB11 have been localized to the inner membrane (Ward

et al 1990; Christie *et al.* 1989; Thorstenson *et al.* 1993) or to both the inner and outer membranes, depending upon the fractionation method used (Thorstenson *et al.* 1993).

VirB4 and VirB11 have nucleotide binding sites and ATPase activity (Shirasu and Kado 1993; Ward *et al.* 1990), and may provide energy for T-DNA transport. VirB4 must be able to bind ATP to function in T-DNA transfer (Fullner *et al.* 1994). VirB11 belongs to a protein family of nucleotide binding proteins required for secretion in gram-negative bacteria (Pugsley 1993) and mutations in VirB11 that abolish its nucleotide binding site result in an avirulent phenotype (Stephens *et al.* 1995).

VirD4, an essential virulence protein, was detected in the inner membrane fraction and in fractions that sedimented between the inner and outer membrane fractions, as determined by immunoblot analysis and sucrose density gradient centrifugation (Okamoto *et al.* 1991). The N-terminus of VirD4 has a signal sequence, and active PhoA fusions were constructed using the N-terminal region of VirD4. Therefore, the C-terminal region of VirD4 is most likely located in the periplasm, while the N-terminal region anchors VirD4 to the inner membrane.

All of the VirB proteins, except VirB1, are required for virulence (Berger and Christie 1994). Since the VirB proteins and VirD4 are not involved in T strand formation and are essential for virulence, their membrane localization suggests they are essential for T-DNA export. VirB9, VirB10 and VirB11 are tightly associated with the cell membranes and may form a protein complex spanning the inner and outer membranes (Finberg *et al.* 1995). VirB10 exists in *A. tumefaciens* as a membrane-associated protein complex (Ward *et al.* 1990), as treatment of *A. tumefaciens* whole cells or membranes with protein crosslinking reagents results in the formation of higher molecular weight forms of this protein. VirB10 either associates with itself or with other membrane proteins. Recent work indicates VirB7 interacts with and stabilizes the putative T-complex transport apparatus (Fernandez *et al.* 1996b). Without VirB7, the steady-state levels of VirB4, VirB9, VirB10 and VirB11 are reduced. *Trans* expression of VirB7 partially restored the levels of these proteins and *trans* expression of VirB7 and VirB8 fully restored the levels of these proteins to wild-type (Fernandez *et al.* 1996b). Therefore, genetic evidence implicates that VirB4,

VirB7, VirB8, VirB9, VirB10 and VirB11 are involved in the formation of the putative T-complex transport apparatus.

VirE1/VirE2

The *virE* operon encodes two proteins, VirE1 (65 amino acids) and VirE2 (533 amino acids) (Winans *et al.* 1987), and both are needed for tumorigenesis (McBride and Knauf 1988). In the *A. tumefaciens* cell, VirE2 is primarily located in the cytoplasm, although it is also found in the inner and outer membranes and in the periplasm (Christie *et al.* 1988). A third open reading frame further downstream may be important for virulence on some hosts (tomato) but not on others (*K. daigremontiana*) (McBride and Knauf 1988).

VirE2 binds cooperatively and without sequence specificity to single-stranded DNA (Gietl *et al.* 1987; Das 1988; Christie *et al.* 1988; Citovsky *et al.* 1988; Citovsky *et al.* 1989; Sen *et al.* 1989), but does not bind to dsDNA or ssRNA (Sen *et al.* 1989). In cooperative binding, the binding of one molecule of VirE2 facilitates the binding of other VirE2 molecules through a protein/protein interaction between adjacent VirE2 molecules. Cooperative ssDNA binding is supported by gel retardation experiments that give a sharp

transition from free to fully retarded ssDNA probe with increasing VirE2 concentration (Citovsky *et al.* 1989). Electron microscopy of ssDNA with subsaturating amounts of VirE2 protein demonstrated molecules either coated completely with VirE2 or protein-free, also indicating cooperative binding (Sen *et al.* 1989). VirE2 has been reported to convert collapsed ssDNA into extended structures (Citovsky *et al.* 1989; Sen *et al.* 1989) or to increase the diameter of the ssDNA (Sen *et al.* 1989). Two electron micrographs in the Sen paper clearly show the increase in diameter of the ssDNA due to binding of the VirE2 protein, the VirE2 protein coated ssDNA strands are more than twice as thick as the dsDNA. Therefore, VirE2 must increase the diameter of the ssDNA.

VirE2 has traditionally been assigned a protective role in T-DNA transfer (Citovsky *et al.* 1989; Sen *et al.* 1989; Christie *et al.* 1988). Because VirE2 is a ssDNA binding protein, it is assumed to coat the T strand and protect it from nucleases inside the *A. tumefaciens* cell and during its transfer into the plant cell. *In vitro*, VirE2 protects ssDNA from degradation by the nuclease, DNase I (Sen *et al.* 1989). VirE2-specific antiserum immunoprecipitates T-DNA

from the supernatant of induced *A. tumefaciens* cells (Christie *et al.* 1988), although these complexes might form after cell lysis.

In contrast to this view, evidence is accumulating that VirE2 is exported directly into, and functions within, plant cells. First, VirE2 is not required to protect T strands from nucleases inside *A. tumefaciens*, as they accumulate to normal levels in a *virE* mutant strain (Stachel *et al.* 1987, Veluthambi *et al.* 1988). In addition, VirE2 is necessary only inside the plant cells as determined by a VirE2-producing transgenic tobacco plant that forms tumors when inoculated with a *virE2* mutant *A. tumefaciens* strain (Citovsky *et al.* 1992).

VirE2 is exported separately from T-DNA into plant cells during extracellular complementation. In this assay, two *A. tumefaciens* strains, a *virE2* mutant and a *virE*$^+$ strain lacking the T-DNA region, when co-inoculated onto a plant, subsequently formed tumors (Otten *et al.* 1984). Each strain alone is avirulent and unable to exchange genes by conjugation. The *virE*$^+$ strain requires *virA* and *virG* for *vir* gene induction and the membrane proteins of the *virB* operon and *virD4* for VirE2 export (Otten *et al.* 1984). Tight binding to plant cells is required of both strains (Christie *et al.* 1988,

Dombek and Ream, unpublished data), suggesting the direct export of VirE2 into plant cells rather than into the *virE2* mutant *A. tumefaciens* strain. An alternative explanation is that the T-strands are exported into the VirE2-producing *A. tumefaciens* strain and then into plant cells. However, PCR failed to amplify T-strands from *A. tumefaciens* cells that were co-cultivated with tobacco protoplasts (Yusibov *et al.* 1994) suggesting that T-strands are only transferred from *A. tumefaciens* directly into plant cells.

VirE1 is also required for the export of VirE2 in the extracellular complementation assay (Sundberg *et al.* 1996), suggesting an interaction between VirE1 and VirE2. Another observation supports this interaction: although VirE2 is stable in *A. tumefaciens* without VirE1 (Sundberg *et al.* 1996), VirE2 is not stable in *E. coli* without VirE1 (McBride and Knauf 1988; P. Dombek and W. Ream unpublished data). In contrast, T-DNA can be exported from the *virE1* deletion strain in the extracellular complementation assay (Sundberg *et al.* 1996), an example of T-DNA export independent of VirE2 protein.

The broad-host-range plasmid RSF1010 can be exported by *A. tumefaciens* into plant cells (Buchanan-Wollaston *et al.* 1987). This

plasmid prevents tumorigenesis by sequestering VirB proteins required for T-DNA export (Ward *et al.* 1991). Coordinate overexpression of *virB9*, *-10*, and *-11* restored tumorigenesis of this *A. tumefaciens* strain. In the extracellular complementation assay, RSF1010 prevents transfer of VirE2 into plant cells, however it does not block the movement of uncoated T strands from a *virE2* mutant into plant cells (Binns *et al.* 1995). Binns cites this evidence to suggest the direct export of VirE2 into plant cells (Binns *et al.* 1995). Apparently, the RSF1010 intermediate competes with VirE2 for VirB proteins in the transport pore. Nonpolar mutations in *virB* genes 4, 5, 6, 8, 9, or 10 eliminate export to plant cells of both VirE2 and T strands in this assay (Binns *et al.* 1995). Thus, both uncoated T-strands and VirE2 are exported through a common transport apparatus and both interact directly with the VirB proteins. The possible functions of VirE2 inside the plant cell will be discussed in the section on T-DNA integration.

Similarities Between T-DNA Transfer and Bacterial Conjugation

T-DNA transfer from *A. tumefaciens* to plant cells is a process that mimics bacterial conjugation, and this relationship was first noted by Stachel and Zambryski (1986). The broad host-range plasmid RSF1010 can be transferred into plant cells by *A. tumefaciens* (Buchanan-Wollaston *et al.* 1987). Bacterial conjugation is a process that involves cell-to-cell contact and single-stranded DNA transfer (Brock *et al.* 1994). During conjugation, the DNA transferred may be a plasmid or part of the chromosome mobilized by a plasmid. The conjugative plasmid in the donor cell codes for surface structures and proteins required for DNA transfer. The surface structures are called sex pili and they make contact between the donor and recipient cells and recognize receptors on the recipient cell surface. After initial contact, the pili retract and the cells are pulled together, facilitating transmembrane pore formation.

Membrane fusion may occur between the donor and recipient cells. After contact, the conjugal plasmid DNA is nicked in the donor cell and one parental strand is transferred to the recipient. As the

transfer occurs, the donor cell replaces the transferred strand by rolling circle method of DNA replication. A complementary DNA strand to the transferred strand is likewise synthesized in the recipient, and when conjugation is concluded, both donor and recipient cells possess the complete plasmid.

VirD1/VirD2: Similarities to TraJ/TraI

VirD1 and VirD2 share functional similarities with the TraJ and TraI proteins encoded by the plasmid RP4 (Pansegrau and Lanka 1991; Lessl and Lanka 1994; Kado 1994). RP4 is a conjugative broad-host-range plasmid (IncP) that can be transferred to gram-positive and gram-negative bacteria, and also to yeast (Lessl and Lanka 1994). TraI and TraJ form a nucleoprotein complex with the origin of transfer (*oriT*) of RP4 (Pansegrau and Lanka 1991). Both TraI and TraJ are required *in vitro* for site- and strand-specific cleavage of *oriT* (Pansegrau *et al.* 1994). Correspondingly, both VirD1 and VirD2 are required *in vitro* for specific cleavage of the T-DNA borders (Scheiffele *et al.* 1995).

During conjugation, TraJ binds to *oriT* and loads TraI onto the DNA. Similar in size to TraJ, VirD1 may also load VirD2 onto DNA in

an analogous reaction (Lessl and Lanka 1994). As mentioned previously, the function of VirD1 is unclear; one group found that purified VirD1 has topoisomerase activity (Ghai and Das 1988), while another group did not (Scheiffele *et al.* 1995).

There are remarkable similarities between TraI and VirD2. Purified TraI catalyzes a site-specific cleavage and joining reaction on ssDNA containing the *nic* region of *oriT,* and covalently attaches via its tyrosine 22 to the 5' terminus of the nicked DNA (Pansegrau *et al.* 1993b). VirD2 also catalyzes a cleaving and joining reaction on ssDNA containing a border repeat sequence (Pansegrau *et al.* 1993a) and attaches via tyrosine 29 to the 5' end of the transferred DNA (Vogel and Das 1992a). The amino acid sequence of VirD2 shares a relaxase motif with TraI and proteins from other mobilizable plasmids (Pansegrau and Lanka 1991). Consensus nick sequences have been found between the T-DNA border repeat sequences and the RP4 transfer origin (Waters *et al.* 1993). Interestingly, VirD2 can also nick ssDNA containing the *nic* sequence from RP4, whereas, TraI cannot nick the border repeat sequence (Pansegrau *et al.* 1993b). VirD1 may increase the specificity of VirD2 *in vivo* (Pansegrau *et al.* 1993a).

VirB/VirD4 Pore: Similarities to Conjugal Pore and Pilin Production Proteins

It is not clear whether *A. tumefaciens* forms a pilus-like structure, although homologies exist between the VirB proteins and proteins involved in pilus structure and assembly. In addition to TraJ and TraI, other RP4 proteins share similarities in amino acid sequence and genetic organization to Vir proteins. The plasmid RP4 has two regions that direct conjugative transfer, *tra1* and *tra2* (Lessl *et al.* 1993). *tra2* and one protein encoded by *tra1* are required for pilus formation, as determined by electron microscopy. Six of these *tra2*-encoded proteins share between 39% and 53% conserved amino acid sequence to corresponding VirB proteins (Lessl *et al.* 1993) and this similarity extends to gene organization. Most of the Tra2 proteins are also hydrophobic and have N-terminal signal sequences. The amino acid sequences of TrbE and TrbB, *tra2* proteins, share 48% and 52% similarity to the amino acid sequences of VirB4 and VirB11 respectively (Lessl *et al.* 1993; Lessl and Lanka 1994). All four proteins have consensus nucleotide binding sites. In addition, both VirB11 and TrbB possess ATPase and

autophosphorylation activity (Lessl *et al.* 1993). VirB4 also hydrolyzes ATP (Shirasu *et al.* 1994).

Both VirB2 and the *tra2*-encoded TrbC have sequence similarities to the pilus subunit (TraA) of *E. coli* F plasmid (Shirasu and Kado 1993; Kado 1994). VirB2 and TraA have peptidase signal cleavage sites and both are cleaved to generate proteins of 7.2 kDa (Shirasu *et al.* 1990). The 7.2 kDa TraA protein is the pilin structural protein (Frost *et al.* 1984). The F plasmid also requires TraQ and TraX for TraA processing (Maneewannakul *et al.* 1993). Analogous VirB proteins have not been found (Kado 1994).

Four VirB proteins (in addition to VirB2) are similar to proteins encoded by the F plasmid (Kado 1994). These F plasmid proteins are essential for its conjugal transfer. TraL and VirB3 share 42% amino acid similarity while TraC and VirB4 share 46% amino acid similarity. Both TraL and TraC are required for pilus formation and are thought to be involved in pilus assembly (Kado 1994).

In addition, more VirB proteins share amino acid sequence similarities to proteins encoded by the *trw* operon of the IncW broad-host-range plasmid R388 than to any other operon (Kado

1994). Ten of the eleven VirB proteins share between 42% to 59% amino acid sequence similarity to proteins encoded by this operon, which encodes pilin assembly and subunit proteins.

The proteins encoded by the *trb* operon of RP4, the *trW* operon of R388, the *tra* operon of F, and the *virB* operon are similar in amino acid sequence and genetic organization to the *ptl* operon of *Bordetella pertussis*. This bacterial pathogen causes the respiratory disease whooping cough and it secretes a multi-subunit complex known as pertussis toxin. Thus, the VirB protein transmembrane structure could have broad specificity and secrete both proteins and DNA (Kado 1994).

VirD4 shares conserved amino acids with proteins found in the plasmids RP4 and F. Comparing VirD4 and TraG of RP4, 28% of the amino acids are identical (Kado 1994). TraG also has a signal sequence for transport to the inner membrane and is essential for conjugal transfer. Although TraG is not involved in pilus formation, it is thought to be part of a membrane channel. TraD, essential for F plasmid transfer, shares 43% amino acid similarity to VirD4 (Okamoto *et al.* 1991).

Recently, a cluster of conjugal transfer genes from the IncN plasmid, pKM101, that direct the synthesis of the pilus and mating pore was sequenced (Pohlman *et al.* 1994). Using *phoA* gene fusions, 11 of the 18 conjugal transfer proteins were found to be exported from the cytoplasm. *tra* genes with amino acid similarities to *virB1, -2, -3, -6, -8, -9* and *-11* were found, and the operons were similarly arranged. Amino acid sequence similarities were also found between the *tra* operon of pKM101 and the *ptl* operon (Pohlman et al 1994).

VirE2: Similarities to TraC1

VirE2, like the TraC1 primase of RP4 is a non-specific ssDNA binding protein. This primase activity initiates DNA replication in the recipient cell, converting the transferred single-stranded DNA to double-stranded DNA. TraC1 is transported with the transferred single-stranded DNA into recipient cells and protects it from nuclease attack. However, TraC1 and VirE2 do not share any regions of conserved amino acid sequence and VirE2 lacks the primase activity of TraC1 (Schieffele *et al.* 1995).

RSF1010 Transfer by *A. tumefaciens*

As previously mentioned, the broad host-range plasmid RSF1010 can be transferred into plant cells by *A. tumefaciens* (Buchanan-Wollaston *et al.* 1987). Transfer is dependent upon the *mob* genes and the origin of transfer (*ori*T) of RSF1010 (Buchanan-Wollaston *et al.* 1987). The Mob proteins nick the DNA at *oriT* and transfer is dependent upon *A. tumefaciens* Vir proteins encoded by the *virA, virG, virB* and *virD* operons, while mutations in *virC* or *virE* reduce transfer efficiency (Buchanan-Wollaston *et al.* 1988).

Integration of the T-DNA into the Plant Cell Nuclear DNA

VirD2/VirE2: Nuclear Localization Signals

Inside the plant cell, the T-DNA must be targeted into the plant cell nucleus before integration can occur. Both VirD2 and VirE2 contain short stretches of basic amino acids that act as nuclear localization signals (Shurvinton *et al.* 1992; Tinland *et al.* 1992; Howard *et al.* 1992; Citovsky *et al.* 1992; Citovsky *et al.* 1994).

VirD2 has two functional domains, an N-terminal domain for T strand attachment and border nicking and a C-terminal nuclear localization signal (Shurvinton *et al.* 1992; Tinland *et al.* 1992). The VirD2 nuclear localization signal is important for tumorigenesis but not for T strand production (Shurvinton *et al.* 1992). The nuclear localization signal transports the reporter enzymes β-glucuronidase (GUS) and β-galactosidase to the nucleus of both yeast and tobacco cells (Tinland *et al.* 1992; Howard *et al.* 1992). The VirD2 nuclear localization sequence functions in both monocots and dicots. A VirD2- β-glucuronidase fusion protein accumulates in the nuclei of maize leaves and immature maize roots (Citovsky *et al.* 1994).

VirE2 has two nuclear localization signals that function in plants. Either signal, when fused to β-glucuronidase, directs it into tobacco cell nuclei (Citovsky *et al.* 1992). However, in the monocot maize, only the nuclear localization sequence closest to the N-terminus is functional. VirE2 without this sequence no longer transports β-glucuronidase into the nuclei of maize leaves and immature maize roots (Citovsky *et al.* 1994).

In the plant, VirD2 directs the T-strands into the nucleus (Tinland *et al.* 1995). If tobacco seedlings are infected by a *virD2*

mutant *A. tumefaciens* strain without its nuclear localization signal, only 5% of the T-DNA molecules enter the nucleus compared to infection by a wild-type *A. tumefaciens* strain (Tinland *et al.* 1995). In this assay, transient gene expression was measured by inserting the reporter gene (*uidA*) that codes for β-glucuronidase into the T-DNA, and this construct allowed the transient expression of the reporter gene to be measured shortly after infection by *A. tumefaciens*. Three days after infection, the seedlings were incubated in the β-glucuronidase substrate, X-gluc, and transient expression was measured by counting the number of blue spots that appear on each seedling. The *uidA* gene does not necessarily have to be integrated to be transiently expressed. However, it must be converted to double-stranded form and transcribed.

Illegitimate Recombination

Sequence analysis of T-DNA insertions and their respective plant DNA target sites have revealed several commonalties (Bakkeren *et al.* 1989; Ohba *et al.* 1995; Mayerhofer *et al.* 1991; Gheysen *et al.* 1991). However, no consensus sequence has been found that predicts the site of T-DNA integration. The T-DNA

sequence at the left (3') end of the integrated T strand is more variable than the right (5') end. For example, in six of eight transformed tobacco plants the right T-DNA end was conserved (Tinland *et al.* 1995). In contrast, fifteen of eighteen transformants had deletions of up to 52 nucleotides from their 3' ends (Rossi *et al.* 1996; Gheysen *et al.* 1991; Mayerhofer *et al.* 1991). Larger truncations, up to 181 nucleotides, have also been observed (Ohba *et al.* 1995).

Frequently, short sequences (1-7 bp) of homology are found between the T-DNA ends and the pre-insertion sites (Gheysen *et al.* 1991; Mayerhofer *et al.* 1991; Ohba *et al.* 1995) In most cases, additional nucleotides ("filler" DNA) corresponding to duplications of both plant and T-DNA occur at the junction sites (Gheysen *et al.* 1991; Mayerhofer *et al.* 1991; Ohba *et al.* 1995). Short target site deletions (13-73 bp) occur in most cases, although larger target rearrangements have also been observed (Gheysen *et al.* 1991; Mayerhofer *et al.* 1991; Ohba *et al.* 1995).

T-DNA integration occurs by illegitimate recombination (Gheysen *et al.* 1991; Mayerhofer *et al.* 1991; Ohba *et al.* 1995), which is also involved in the integration of viral and transfected

DNA into mammalian cells (for review see Roth and Wilson 1988). T-DNA integration and illegitimate recombination in mammalian cells share several commonalities: the absence of well-defined target sites (only short regions of homology are required), the presence of additional nucleotides at the recombinant junctions, and small deletions or larger rearrangements at the target sites (Gheysen *et al.* 1991). Only 1-6 bp of homology are required between the single-stranded ends of the virus SV40 and the target site of integration in monkey cells (Roth and Wilson 1986). When SV40 integrates into mammalian chromosomes, about 10% of the junctions contain from 1-40 additional nucleotides of filler DNA at the recombinant junctions (Roth *et al.* 1989). In contrast, approximately 40%, of T-DNA junctions contain filler DNA, of up to 40 nucleotides (Gheysen *et al.* 1991). In one example, an 11-bp deletion of the target site occurred upon integration of hepatitis B virus DNA cloned from hepatocellular carcinomas and a region of 5 bp homology was found between the cellular DNA deleted at the target site and the integrated hepatitis B virus DNA (Hino *et al.* 1989).

Illegitimate recombination in *A. tumefaciens* involves T-DNA joining to the free ends of nicked plant DNA (Gheysen *et al.* 1991). Nicks in DNA can occur due to errors during replication or repair, or when ssDNA is exposed during transcription (Roth and Wilson, 1988). T-DNA integrates preferentially into transcriptionally active regions of the plant genome (Koncz *et al.* 1989).

Role of VirD2 in T-DNA Integration

The *in vivo* participation of VirD2 in the integration event is supported. In a recent paper, an *A. tumefaciens* strain with a *virD2* mutation was used to infect tobacco seedlings (Tinland *et al.* 1995). After infection, the integration efficiency of this strain was compared to a wild-type strain and integrated T-DNA molecules were recovered from the infected plants and sequenced. The sequences obtained were compared to T-DNA sequences integrated due to infection by a wild-type *A. tumefaciens* strain.

VirD2 has a motif common to many recombinases (His-(2X)-Arg-(32+/-2X)-Tyr) (Argos *et al.* 1986). The arginine of this motif was changed to a glycine (*virD2*R129G) to disrupt a possible integration function and this construct was used to infect tobacco

plants. The level of T strands produced by this strain was less than 1% of the wild-type level, probably due to a conformational defect in the VirD2 protein.

The integration efficiency of this *virD2*R129G mutant strain was first compared to a wild-type strain (Tinland *et al.* 1995). The integration efficiency was determined by measuring the frequency of T strands integrated into the plant cell nucleus and dividing this number by the frequency of T strands transported into the plant cell nucleus, but not necessarily integrated. For each strain, the integration frequency of the T strands was determined by counting the number of calli that arose on tobacco seedlings after *A. tumefaciens* infection and selection on media containing kanamycin. T strand transport to the nucleus was determined by measuring the transient expression of a β-glucuronidase reporter gene as the number of blue spots that appeared on tobacco seedlings three days after *A. tumefaciens* infection. Using these methods, the integration efficiency was found to be unaffected by this *virD2* mutation (Tinland *et al.* 1995).

Although the integration efficiency was reported to be unchanged, changes were noticed when the T-DNA from plants

transformed by this strain was sequenced (Tinland *et al.* 1995). The precise ligation of the T-DNA right border to the plant DNA did not occur in any of the eight transformed plants (Tinland *et al.* 1995). In six of the eight plants transformed with a wild-type strain, the right border junction was intact. In four of the plants transformed with the *virD2* mutant, multimers of the complete plasmid were found, suggesting a mechanism of rolling circle replication during T-DNA transfer. This indicates that VirD2 participates in the ligation of the T-DNA to the plant DNA and is required for the precise integration of the right T-DNA border into the plant DNA (Tinland *et al.* 1995).

If VirD2 does participate in the ligation step, as postulated by Tinland *et al.* (1995) it appears unlikely that the integration efficiency is not decreased using the *virD2*R129G mutant strain. The efficiency of both T-DNA transfer to the plant cell nucleus (measured by blue spots per seedling) and T-DNA integration (measured by calli formed per seedling) was decreased in the *virD2*R129G mutant strain to approximately equal a 1:250 dilution of a wild-type strain with a completely avirulent *A. tumefaciens* strain (Tinland *et al.* 1995). This *A. tumefaciens* strain, with a

deletion in *virD2*, is avirulent, as T-DNA border nicking and T strand formation do not occur. Therefore, approximately 250-fold fewer T strands are transferred into the plant cell nucleus by the *virD2*R129G mutant strain compared to a wild-type strain.

The integration efficiencies were determined for 1:100, 1:250 and 1:500 dilutions of a wild-type strain mixed with the *virD2* deletion strain and compared with the integration efficiency of the undiluted *virD2*R129G mutant strain (Tinland *et al.* 1995). The integration efficiencies obtained for the three dilutions of the wild-type strain in three separate experiments were 0.14 +/- 0.03, 0.032 +/- 0.006, 0.07 +/-0.008 (mean +/- standard deviation). The three experiments have over a 4-fold variation in integration efficiency (from 0.032 to 0.14) casting doubt on the ability of this procedure to accurately determine integration efficiency. For the *virD2*R129G strain the integration efficiencies obtained in the three experiments were 0.108, 0.013 and 0.087 respectively (Tinland *et al.* 1995). Wide variability (over 7-fold from 0.013 to 0.108) is again seen in these experiments. The *virD2*R129G mutation had a slightly lower integration efficiency in the first two experiments and a slightly higher integration efficiency in the third experiment. In all three

cases the value for the *virD2*R129G strain was outside the standard deviation of the mean value found using the diluted wild-type strain (Tinland *et al.* 1995). Therefore, it appears unconvincing on the basis of three widely differing experiments to conclude that the *virD2*R129G strain does not change the efficiency of T-DNA integration. Another more consistent method needs to be developed or more than three separate experiments need to be performed.

Role of VirE2 in T-DNA Integration

To assess the influence of *virE2* on T-DNA integration in plants, a *virE2* deletion strain was used to infect tobacco seedlings (Rossi *et al.* 1996). This experiment was executed by the same group that infected the tobacco seedlings with the *virD2* mutant (Tinland *et al.* 1995) using an identical procedure to the one described in the preceding section. The efficiency of integration was also found to be *virE2* independent.

It appears likely that VirE2, like VirD2, does change the integration efficiency. In the next section, evidence will be presented implicating VirE2 protein in T-DNA integration. The efficiency of T-DNA transfer from *A. tumefaciens* to the plant cell

nucleus (measured by blue spots per seedling) matches a 1:2500 to 1:5000 dilution of a wild-type strain diluted with a strain containing a deletion in *virD2* (Rossi *et al.* 1996). The number of blue spots that appeared per seedling after inoculation with the *virE2* deletion strain was fewer than 1 per seedling. In one of the three experiments performed, the number of calli formed after inoculation with the *virE2* deletion strain was less than 1 per 100 seedlings (Rossi *et al.* 1996). Therefore, in the integration efficiency experiments with the *virE2* deletion strain the limit of accurately detectable T-DNA transfer and integration events may have been exceeded. This might have also been the case using the *virD2*R129G mutant strain which was 250-fold less efficient than wild-type in T-DNA transfer (Tinland *et al.* 1995).

In three independent experiments using 1:500, 1:1000 and 1:5000 dilutions of a wild-type strain, with the *virD2* deletion strain, the integration efficiencies were 0.045 +/- 0.01, 0.040 +/- 0.005, 0.34 +/- 0.21 (Rossi *et al.* 1996). A large variation, over 8-fold from 0.04 to 0.34, is again seen in the transfer efficiencies obtained in the three experiments. The integration efficiencies of the *virE2* deletion strain were 0.028, 0.092, and 0.5, respectively

(Rossi *et al.* 1996). The first value, and the second value are lower and higher respectively, than the mean values determined for the wild-type strain in the first two experiments. The third value is within the mean value plus the standard deviation of the wild-type strain. Therefore, as with VirD2, the results seem inconclusive due to the large variation in the integration efficiency values obtained.

Sequence analysis of the T-DNAs integrated after infection with the *virE2* deletion strain were compared to T-DNAs obtained after infection with a wild-type strain (Rossi *et al.* 1996). Twenty-one transgenic plants infected with the *virE2* mutant *A. tumefaciens* strain were regenerated and their T-DNAs analyzed. Seventeen of the plants had precise T-DNA/right border junctions. A similar percentage of plants infected with a wild-type strain also had this precise junction. VirE2, therefore, does not influence the integration pattern of the 5' end of the T-DNA. As previously discussed, VirD2 protein is needed for a precise 5' junction.

However, when the left-end junctions were analyzed, only four of the twenty-one plants had deletions of fewer than 52 bp, and were therefore similar to the left-end junctions found in the four plants transformed with a wild-type strain (Rossi *et al.* 1996). The

remaining seventeen plants transformed with the *virE2* mutant had left-end truncations of up to 1 kb. Plants with larger deletions may have been present but were not selected because truncations greater than 1430 bp also deleted part of the kanamycin resistance gene and therefore would not be detected.

The authors propose that VirE2 protects ssDNA from nucleases inside the plant cell and, therefore, is needed for integration of full-length copies of T-DNA (Rossi *et al.* 1996). Without *virE2*, the transfer efficiency of the T-DNA into the plant cell nucleus, as determined by the transient expression assay, was only 0.02-0.04% of wild-type (Rossi *et al.* 1996). The quantity of T strands formed inside the *virE2* mutant was identical to that observed in a wild-type strain (Rossi *et al.* 1996), which supports previous reports (Stachel *et al.* 1987; Veluthambi *et al.* 1988). Therefore, these left hand truncations may have occurred inside the plant cell. The transient expression of the reporter gene encoding β-glucuronidase in seedlings infected with a *virE2* mutant strain was lower (Rossi *et al.* 1996), as expected, because fewer T-DNA molecules are detected in the cytoplasm of protoplasts co-cultivated with a *VirE2* mutant as compared to wild-type (Yusibov *et al.* 1994).

T-DNA degradation inside the plant cell due to a lack of VirE2 is also supported by the following observation: when tobacco seedlings were infected by co-inoculating the *virE2* deletion strain with a *virE*$^{+}$ strain, the integrated T-DNAs in four of the five plants had left end T-DNA truncations of less than 52 bp and were therefore similar to plants infected by wild-type *A. tumefaciens* (Rossi *et al.* 1996). Therefore, VirE2 can be exported from *A. tumefaciens* and still protect the T strand from degradation.

The authors state that the *A. tumefaciens* proteins VirD2 and VirE2 are responsible for the transport and precise integration of full-length T-DNA copies (Rossi *et al.* 1996). The sequencing results support this conclusion, since without a fully-functional VirD2 protein, the 5' end of the integrated T-DNA molecule is truncated and without VirE2, the 3' end is truncated more extensively (up to 1 kb) than it would ordinarily be (less than 52 bp).

It has been suggested that VirE2 may also participate in T-DNA integration (Gardner and Knauf 1986) in addition to protecting the T-DNA from nucleases inside the plant cell (Rossi *et al.* 1996). In a unique experiment, plant viroid genes were inserted into the T-DNA (Gardner and Knauf 1986). Mutations in the *vir* genes were made to

assess their effect on viroid and T-DNA transfer. Mutations in the *virB* or *virD* operons prevented tumor formation and viroid symptoms. Mutations in *virE2* resulted in viroid symptoms but no tumors (Gardner and Knauf 1986). This indicates that the T-DNA entered the plant nuclei but did not integrate. The authors suggested VirE2 is involved in T-DNA integration. However, since viroid symptoms are a sensitive assay of T-DNA transfer, an alternative explanation (that fewer T strands were transferred and therefore integration did not occur) is also possible.

Genetic evidence has shown that VirE2 can mediate homologous genetic recombination in *E. coli* (W. Ream unpublished data). This experiment utilized an *E. coli* strain containing two copies of the *lac* operon in its bacterial chromosome and a deletion of the region including *recA*. The copies of the *lac* operon had non-overlapping deletions in *lacZ*, the gene encoding the enzyme β-galactosidase, and its activity was used to screen for recombination events. Only when a complete copy of *lacZ* is created, by homologous recombination, is β-galactosidase activity present. A plasmid containing the *virE* operon under control of the IPTG-inducible

promoter, *trc*, was introduced into this *E. coli* strain to determine if VirE2 could substitute for RecA.

RecA is the major recombination protein of *E. coli*, which like VirE2, binds cooperatively and without sequence specificity to ssDNA. In homologous recombination, RecA binds ssDNA and, without regard to sequence homology, binds dsDNA in a second binding site (Roca and Cox 1990). This process is known as co-aggregation. RecA then searches for homologous regions between the ss and dsDNA. If homology is found, RecA displaces one of the strands of dsDNA and replaces it with homologous ssDNA in the strand exchange process (Roca and Cox 1990).

In the recombination experiments, *E. coli* cells were grown overnight in the presence of IPTG to induce the *virE* genes and plated on lactose minimal medium containing X-gal. *E. coli* cells with a functional copy of *lacZ* will be able to utilize lactose and grow on the lactose minimal plates. X-gal is a substrate for β-galactosidase, and is converted to a blue-colored compound in its presence. When *virE* was present, blue colonies arose on the lactose minimal plates. No colonies grew using the same *E. coli* strain

containing the vector alone or containing *virE* with a truncated *virE1* gene.

PCR (polymerase chain reaction) primers were designed so that only when they were brought into close proximity to one another by a recombination event would a product be obtained. The DNA from several blue colonies resulting from VirE2-mediated recombination was amplified using these primers, and products of the expected sizes were generated. Sequencing revealed the wild-type *lacZ* sequence, verifying that VirE2 can mediate genetic recombination in *E. coli.*

Some differences were observed between recombination mediated by VirE2 and that mediated by RecA. The frequency of recombination was much less in the *virE*-containing strain, with 10^6 fewer colonies generated, and the *virE*-mediated recombinants were also unstable. If a blue colony arising from *virE* mediated recombination was grown in broth and re-plated on lactose minimal medium, only a fraction of the cells survived. The *virE*-mediated recombination intermediates were not properly resolved in *E. coli.*

VirE2 has an identical site-specific recombinase motif (His_{229}-2X-Arg_{226}-32+/-2X-Tyr_{192}) to one found in VirD2. Site-

specific recombination, unlike homologous recombination, requires only very short regions of homologous DNA. This motif (Argos *et al.* 1986) is found in a family of conservative site-specific recombination proteins encoded by seven different bacteriophage systems: λ, ϕ80, P22, P2, 186, P4, and P1 (reviewed by Nash 1981). Each system has a different site-specificity, which might account for the large diversity seen in the overall protein sequences (Argos *et al.* 1986).

In the first six systems, recombination occurs between specific *att* sites on the phage and bacterial chromosomes. This event is carried out by the phage-encoded integrase (Int) protein (Nash 1981; Yu and Haggard-Ljungquist 1993; Pierson and Kahn 1984). In the P1 system, P1 is maintained as a bacterial plasmid and Cre protein resolves dimer copies of this plasmid into daughter cells during bacterial replication (Austin *et al.* 1981). Flp is a eukaryotic protein similar to Cre, that also shares this motif (McLeod *et al.* 1984). This yeast protein is involved in recombination between copies of the 2μ plasmid.

In vitro, the recombinase proteins Cre, Flp, and λ integrase generate staggered nicks in the DNA (Craig and Nash 1983; Andrews

et al. 1985; Hoess and Abremski 1985). There is no evidence that VirE2 nicks DNA. VirD2 may generate the nicks in the plant DNA or the T-DNA may preferentially integrate into nicked DNA. Cre, Flp, and λ integrase then attach transiently to the 3' end of the DNA via a phosphodiester bond during strand cleavage and rejoining (Craig and Nash 1983; Andrews *et al.* 1985; Hoess and Abremski 1985). This bond energy is conserved during strand exchange, as no high energy co-factor is required.

VirD2, VirE2 and Flp lack the less-highly conserved amino acids that surround this integrase motif and are shared by some of the bacteriophage proteins (P. Dombek unpublished data). VirE2, however, does have a Thr_{471}-Gly_{470}-X-Arg_{468} motif that occurs about 100 amino acids away from the integrase motif in five of the bacteriophage proteins. Roles for all three amino acids in the integrase motif have been proposed (Argos *et al.* 1986). The histidine hydrogen bonds with specific DNA sequences, the arginine ionically interacts with the DNA phosphate backbone, and the tyrosine forms a transient phosphodiester linkage with the DNA.

To determine whether this motif in *virE2* is important in T-DNA integration, site-directed mutagenesis could be used to change

inactivate a possible recombination function, as it would be expected to eliminate transient phosphodiester bond formation between the protein and DNA. The mutant VirE2 protein should retain the ability to bind ssDNA, as this motif is in the N-terminal half of the protein. The ability of this mutant VirE2 protein to mediate genetic recombination in *E. coli* and infect plants could also be tested to determine the significance of this motif.

VirE2 could also be purified and tested for both strand exchange and co-aggregation activities. VirE2, like RecA during co-aggregation, may bind to dsDNA in the presence of both ssDNA and magnesium.

Research Objectives

At 533 amino acids in length, VirE2 protein is larger than *E. coli* RecA (353 amino acids) (Cox and Lehman 1987), *E. coli* SSB (178 amino acids) (Chase and Williams 1986), and bacteriophage T4 (301 amino acids) (Alberts and Frey 1970). All three proteins bind cooperatively and non-specifically to ssDNA (Alberts and Frey 1970; Chase and Williams 1986; Cox and Helman 1987). Both RecA (Cox and Lehman 1987; Gardner *et al.* 1995) and gp32 (Casas-Finet *et al.*

1992; Hurley *et al.* 1993) are multi-functional proteins and it is likely VirE2 may also have several functional domains. VirE2 has one or more domains involved in binding ssDNA and since this binding to ssDNA is cooperative, it also has one or more cooperativity domains. VirE2 participates in other protein-protein interactions since its export from *A. tumefaciens* requires six of the *virB* proteins, as well as VirD4 and VirE1 (Binns *et al.* 1995; Otten *et al.* 1984; Sundberg *et al.* 1996). Therefore, a domain or domains that interact with these other *vir* proteins is expected. Since VirE2 can also mediate genetic recombination, a region of VirE2 may participate in T-DNA integration.

Therefore, the main objective of this research was to identify the domains required for ssDNA binding and cooperativity. Additionally, this research may identify other domains that did not affect ssDNA binding but are important for other functions of the VirE2 protein.

The approach taken utilized linker-insertion mutagenesis (Goff and Prasad 1991) to add two amino acids throughout the protein, to minimize the probability that the mutations would introduce large three-dimensional conformational changes that would destabilize

the protein and lead to a total loss of activity. These insertions were intended to perturb only a portion of the protein, which could indicate its function. Additionally, a ten amino acid deletion was created in a serine-rich region of VirE2 that shares 66% amino acid identity with a region in gp32 (P. Dombek unpublished data). This region in gp32 is surrounded by acidic amino acids and participates in protein-protein interactions with other proteins that participate in bacteriophage T4 replication (Hurley *et al.* 1993; Krassa *et al.* 1991). Therefore, it was hoped this deletion could eliminate the interaction of VirE2 with one or more other *A. tumefaciens* proteins or plant proteins.

E. coli protein extracts containing the wild-type and mutant VirE2 proteins were used to determine their ssDNA binding abilities in electrophoretic mobility shift assays. Immunoblot analysis was used to determine the amount of VirE2 protein in each extract, and the binding to ssDNA was quantitated using a phosphorimager. This approach allowed for the detection of small differences in the DNA binding abilities between the wild-type and mutant VirE2 proteins.

Virulence assays were also performed using *A. tumefaciens* strains containing the wild-type and mutant VirE2 proteins to

correlate changes in DNA binding with changes in phenotype. VirE2 is a plant-host-range determining protein by using transposon mutagenesis to construct truncated versions of VirE2 (Hirooka and Kado 1986). Consequently, plants from several families were infected.

The results of this research demonstrated that the C-terminal half of VirE2 contains a domain critical for ssDNA binding; two insertions in the N-terminal half identified cooperativity domains. An insertion in the central region of VirE2 decreased tumorigenicity but did not affect ssDNA binding or the stability of VirE2 in *A. tumefaciens*. This mutation might define another functional domain. Surprisingly, the 10 amino acid deletion did not change ssDNA binding or virulence. Chou and Fasman (1978) secondary structural predictions of the linker insertion mutants suggested only localized changes in the secondary structure of VirE2 due to these insertions. Consequently, linker insertion mutagenesis is a potential method for determining protein functional domains.

CHAPTER 2. EXPERIMENTAL PROCEDURES

Bacterial Strains, Plasmids, and Growth Conditions

Listed in Table 2.1 are the bacterial strains and plasmids used in this study. All *A. tumefaciens* strains were derived from A348, which harbors the octopine-type Ti plasmid pTiA6NC in the C58 chromosomal background (Garfinkel *et al.* 1981). *Escherichia coli* cells (MM294, DH5α, SK1592) were grown in L-broth (Maniatis *et al.* 1982) containing appropriate antibiotics at 37°C. *A. tumefaciens* cells were grown in YEP (Garfinkel *et al.* 1981) containing appropriate antibiotics at 28°C.

Construction of *virE2* Mutants

Linker Insertion Mutagenesis

The linker inserted into *virE2* in pGR1 was the 12-bp oligonucleotide 5'-dCTCGAGCTCGAG-3') which contains two *Xho*I sites (one of which is underlined).

Table 2.1 Bacterial Strains and Plasmids

Strain or plasmid	Characteristics	Reference
E. coli		
DH5α	F⁻ *recA1 gyrA96 thi*-1 *hsdR17 supE44 relA1 deoR* φ80*dlacZ*Δ*M15* λ- Δ(*lacZYA-argF*)*U169*	Clontech
CJ236	*dut-1 ung-1 thi-1 relA1*/pCJ105(*F' cat*)	Joyce and Gridley 1984
JC10,289	F⁻ del(*srl-recA*)306::Tn*10 thr-1 leuB6 thi-1 lacY1 galK2 ara-14 xyl-15 proA2 his-4 argE3 rpsL31 tsx-33 supE44 mtl-1*	Csonka and Clark 1979
MM294	F⁻ *endA1 thi-1 hsdR17 supE44*	Bachmann 1987
A. tumefaciens		
A348	C58 chromosomal background containing pTiA6NC	Garfinkel *et al.* 1981
WR5000	2.4 kb *Hinc*II fragment containing *neo* from Tn*5* replacing *virE2* in pTiA6NC	This study
WR5100	pPD100 transformed into WR5000: *virE1*⁺ *virE2*⁺/*virE::neo*	This study

WR5101-WR5108	pPD101-pPD108 transformed into WR5000	This study
WR5110	pPD110 transformed into WR5000	This study
Plasmids		
pBL17	pTrc99A with only one *Sph*I site	This study
pGR1	3.2 kb *Xho*I fragment containing *virE* from pTiA6NC inserted into *Sal*I site of pUC18	Sundberg *et al.* 1996
pPD1	*Xho*I linker inserted into *Stu*I site 30 bp from *virE2* start in pGR1	This study
pPD2	*Xho*I linker inserted into *Xmn*I site 281 bp from *virE2* start in pGR1	This study
pPD3	*Xho*I linker inserted into *Rsa*I site 638 bp from *virE2* start in pGR1	This study
pPD4	*Xho*I linker inserted into *Nae*I site 768 bp from *virE2* start in pGR1	This study
pPD5	*Xho*I linker inserted into *Nru*I site 1133 bp from *virE2* start in pGR1	This study
pPD6	*Xho*I linker inserted into *Rsa*I site 1414 bp from *virE2* start in pGR1	This study
pPD7	*Xho*I linker inserted into *Pvu*II site 1489 bp from *virE2* start in pGR1	This study
pPD8	*Xho*I linker inserted into *Nae*I site 1526 bp from *virE2* start in pGR1	This study

Table 2.1 (continued)

pPD10	codons 56-65 of *virE2* deleted from pGR1	This study
pPD15	2.4 kb *Hinc*II fragment containing *neo* from Tn*5* replacing *virE2* in pGR1	This study
pPD16	*Bam*H1-cut pPD15 inserted into *Bam*H1 site of pRK310	This study
pPD20	1.9 kb *Eco*R1 fragment from pGR1 inserted into the *Eco*R1 site of pUC118	This study
pPD25	codons 56-65 of *virE2* deleted in pPD20	This study
pPD100	*Bam*H1-cut pGR1 inserted into *Bam*H1 site of pRK310	This study
PPD101-108	*Bam*H1-cut pPD1-pPD8 inserted into *Bam*H1 site of pRK310	This study
pPD110	*Bam*H1-cut pPD10 inserted into *Bam*H1 site of pRK310	This study
pPD201-208	*Sph*I fragments containing *virE2* from pPD1-pPD8 in *Sph*I site of pWR223	This study
pPD210	*Sph*I fragment containing *virE2* from pPD10 in *Sph*I site of pWR223	This study
pRK310	broad-host-range *tetA lacZ'* pUC9 multiple cloning site	Ditta *et al.* 1985

Table 2.1 (continued)

pTrc99A	*trcP* vector *lacI*^{q} pUC18 *Eco*RI-*Hin*dIII polylinker region	Amann *et al.* 1988 Pharmacia
pWR223	annealed *Nco*I/*Sph*I oligonucleotides containing the first 10 codons of *virE1* (through *Sph*I site) with *Nco*I and *Sph*I compatible ends inserted into *Nco*I-*Sph*I-cut pBL17 (Fig. 3.6)	This study
pWR225	*Sph*I fragment containing the *virE* operon from the *Sph*I site in *virE1* through the end of *virE2* (from pGR1) in *Sph*I site of pWR223	This study

Table 2.1 (continued)

This linker was designed so that it would not change the reading frame or add a stop codon when inserted into *virE2*. The plasmid pGR1 was first linearized with one of the following blunt-cutting restriction enzymes; *Nae*I, *Rsa*I, *Stu*I, *Pvu*II, *Xmn*I which cut throughout *virE2* and within the vector. The resulting linearized DNA was then gel purified and ligated to the oligonucleotide linkers. Restriction endonuclease reactions contained 5-10 µg pGR1 plasmid DNA, 8.8 µl 10X restriction enzyme buffer (0.5 M Tris-HCl (pH 8.0), 100 mM $MgCl_2$), 2 µl RNase (5 mg/ml stock), plus dH_2O to 88 µl total volume. Two µl ethidium bromide (1 mg/ml stock) was then added to maximize the number of DNA molecules that would be cut only once (Goff and Prasad 1991). Twenty units of the blunt-cutting restriction enzyme of choice was then added to the digest. The reaction was incubated at 37°C for 70 minutes, followed by inactivation of the enzyme by heating to 65°C for 10 minutes. The digested DNA was subjected to electrophoresis through an 1% agarose gel using pGR1 (linearized with *Bam*HI) as a marker for the migration of full-length linear molecules. The linearized DNA was purified from agarose as described in the DNA methods section

(section 2.3). The purified DNA was then concentrated by ethanol precipitation and resuspended in 20 µl water.

The 5' ends of the oligonucleotide linkers (1.7 µg linker DNA) were phosphorylated in 30 µl of buffer consisting of 0.1M Tris-HCl (pH 8.0), 10 mM $MgCl_2$, 5 mM dithiothreitol, and 0.43 mM ATP. One µl (10 units) T4 polynucleotide kinase (Bethesda Research Laboratories) was then added and the reaction was incubated at 37°C for 45 minutes. The phosphorylated linkers were then ligated to the gel-purified linearized DNA by adding 1 µg DNA to 1.7 µg oligonucleotide linkers, 17 µl 5X T4 DNA ligase buffer (330 mM Tris-HCl (pH 7.6), 33 mM $MgCl_2$, 50 mM dithiothreitol, 330 mM ATP) (Bethesda Research Laboratories), 4 µl (4 units) T4 DNA ligase (Bethesda Research Laboratories), and dH_2O to bring the total volume of the reaction mix to 85 µl. The reaction was incubated overnight at 15°C.

To ensure that only a single *Xho*I site was inserted into the ligated DNA, the ligation reaction was digested with *Xho*I, which cleaves within the 12 bp linker sequence. The DNA in the ligation mix was extracted with an equal volume of phenol/chloroform (1:1) and then extracted again with an equal volume of

chloroform/isoamyl alcohol (24:1). The DNA was then ethanol precipitated, resuspended in 27 µl of 1X restriction enzyme buffer (50 mM Tris-HCl (pH 7.4), 10 mM Mg Cl_2, 50 mM NaCl) and 3 µl *Xho*I (30 units), then incubated at 37°C for one hour. This typically resulted in the insertion of just 6 bp (two codons, CTCGAG) indicating complete *Xho*1 digestion.

Excess linkers were separated from the linearized DNA by electrophoresis through a 1% Sea Plaque low-melting temperature agarose gel (FMC Bioproducts) which resolved two bands; an upper band of linearized DNA and a diffuse lower band of linker DNA. The linearized DNA band was excised and ligated without purification from the agarose as follows. The DNA-containing agarose, containing about 0.7 µg DNA, was first melted at 70°C. Using 10 µl of molten agarose, 4 µl 5X ligation buffer (330 mM Tris-HCl (pH 7.6), 33 mM $MgCl_2$, 50 mM dithiothreitol, 330 mM ATP), 4.5 µl water, and 1.5 µl T4 DNA ligase (1.5 units), the DNA was re-ligated overnight at room temperature. The ligation reaction was heated to 70°C and 10 µl used to transform 200 µl competent cells (described in section 2.3 on DNA methods).

The resultant *E. coli* colonies were screened to determine the site of the linker insertion. Miniprep DNA was isolated and digested with *Xho*I and *Bam*HI. *Bam*HI cuts once in the multiple cloning site of pGR1, approximately 300 bp upstream from the start of *virE1*, and *Xho*I cuts only at the site of the mutation. To show that other alterations did not occur during linker insertion, the Central Services Laboratory (Oregon State University) sequenced each mutation with an Applied Biosystems Model 373 sequencer using the dye-terminator method.

Site-directed Mutagenesis

To prepare single-stranded template DNA, the DNA fragment to be mutagenized was cloned into pUC118 which has an M13 origin of replication. The *virE* containing plasmid, pGR1 was cut with *Eco*RI and the 1967 bp *Eco*RI fragment containing both *virE1* and the N-terminal half of *virE2* was ligated into pUC118, previously linearized with *Eco*RI. The resulting plasmid, pPD20, was transformed into *E. coli* strain CJ236 (chloramphenicol resistant) and plated on L agar plates containing both ampicillin (50 μg/ml) and chloramphenicol (30 μg/ml). The cells were grown overnight in L

Broth plus antibiotics, and 25 µl of this culture was used to inoculate 2 ml of L Broth supplemented with 0.001% thiamine. Ampicillin (25 µg/ml) was added and the culture was incubated at 37°C with shaking for 30 minutes. Forty µl of M13KO7 helper phage (at a concentration of 0.5-5 x 10^{11} pfu/ml) was added to the culture which was then incubated for an additional two hours at 37°C with shaking. The entire culture was added to 8 ml of L Broth supplemented with 0.001% thiamine, 25 µg/ml ampicillin, and 50 µg/ml kanamycin. Kanamycin selected for cells infected by the helper phage.

Cells were shaken for 16 hours at 37°C and the bacterial debris was pelleted by centrifugation at 12,100 x g for 10 minutes. Three ml of 2.5 M NaCl/20% PEG was added to 9 ml of the phage supernatant and the solution was placed at 4°C overnight. The solution was centrifuged in an SS34 rotor at 12,100 x g for 10 minutes which resulted in a beige-colored, round pellet of phage particles containing single-stranded pPD20 DNA. The supernatant was removed from the pellet as completely as possible.

The pellet was resuspended in 0.5 ml of TE and 2 µl RNaseA (5 mg/ml) was added. The DNA was incubated at 37°C for 20 minutes

and then was extracted twice with phenol/chloroform and extracted once with chloroform/isoamyl alcohol. Each extraction was re-extracted by adding 200 µl of TE to the leftover phenol/chloroform or chloroform/isoamyl alcohol which doubled the yield of DNA. The DNA was ethanol precipitated, washed in 75% ethanol, allowed to air-dry and resuspended in 100 µl of TE. One µl of the single-stranded DNA was analyzed by electrophoresis through an 0.8% agarose gel, with supercoiled double-stranded DNA as a control. A single band of single-stranded DNA was visible at a lower position than the supercoiled plasmid DNA. The single-stranded DNA concentration was determined by measuring the OD_{260}.

Prior to synthesis of second strand DNA, an oligonucleotide primer (200 pmol) was phosphorylated in 30 µl of buffer consisting of 0.1 M Tris-HCl (pH 8.0), 10 mM $MgCl_2$, 5 mM dithiothreitol, and 0.43 mM ATP. To delete codons 55-66 from *virE2*, an oligonucleotide primer corresponding to codons 50-54 and 65-69 in *virE2* was designed and synthesized (5'-GGA-TCG-GTC-GAT-TCC-GGA-AAT-CAA-GCT-GAG-3'). This primer contains a *Bsp*E1 site (underlined) which is not found in *virE* or pUC118. Five units of T4 polynucleotide kinase (Bethesda Research Laboratories) were added

and the solution was incubated at 37°C for 45 minutes and then incubated at 65°C for 10 minutes to inactivate the enzyme. Three µl of TE were added to bring the oligonucleotide to a final concentration of 6 pmol/µl. The phosphorylated primer was stored frozen.

The phosphorylated primer was then annealed to the single-stranded DNA template. One µg of template DNA, 1 µl of phosphorylated oligonucleotide primer (6 pmol), 2 µl of 5X Sequenase buffer (200 mM Tris-HCl (pH 7.5), 100 mM $MgCl_2$, 250 mM NaCl) (United States Biochemical), and 6 µl of dH_2O were added to a microfuge tube. An identical reaction was set up without the oligonucleotide primer and with 7 µl of dH_2O instead of 6 µl. Both reactions were placed in a beaker of H_2O at 70°C and the water was allowed to cool to 30-35°C. To each of the 10 µl annealing reactions (with and without the oligonucleotide primer) 20 µl of buffer consisting of 20 mM Tris-HCl (pH 7.5), 10 mM $MgCl_2$, 25 mM NaCl, 75 mM APT, 5 mM dithiothreitol, 100 mM dATP, 100 mM dTTP, 100 mM dCTP, 100 mM dGTP, 1.6 units of Version 2.0 Sequenase DNA polymerase (United States Biochemical), and 0.33 units of T4 DNA ligase (Bethesda Research Laboratories) were added on ice. The

reactions were incubated at room temperature for 5 minutes and then incubated at 37°C for 75 minutes to complete the synthesis of second strands.

Two µl of each reaction was analyzed by agarose gel electrophoresis with single-stranded template DNA and supercoiled plasmid DNA as controls. In the control reaction without the oligonucleotide primer, little DNA corresponding to the double-stranded supercoiled plasmid was visible, whereas in the reaction with the oligonucleotide added, considerably more DNA corresponding to the double-stranded plasmid DNA was observed. Two µl of each reaction was used to transform *E. coli.* Three times more colonies were seen when using the primer-added reaction to transform the *E. coli*, as compared to a transformation using the unprimed reaction.

The transformants were screened by digesting the DNA with *Bsp*E1, to verify that this new restriction site was created at the site of the deletion. The resultant plasmid was named pPD25 (Table 1). This mutation, designated *virE2*Δ1, was excised from pPD25 as a 536 bp *Stu*I-*Bgl*II restriction fragment and inserted into pGR1, replacing the corresponding wild-type fragment. To verify that

other alterations had not occurred during mutagenesis, the insert was sequenced by the Central Services Laboratory (Oregon State University).

Construction of a *virE2* null Strain of *A. tumefaciens*

An *A. tumefaciens* strain was created with *virE2* deleted from the Ti plasmid to use as a background strain for virulence assays. This strain was transformed with broad host-range plasmids containing either a wild-type *virE2* gene or plasmids with a mutant *virE2* gene to assay for tumorigenesis. To create this *A. tumefaciens virE2* null strain, a deletion in a cloned *virE2* gene was first created in *E. coli*. The *virE2* sequence was replaced with a gene encoding kanamycin resistance so that in a later step, an *A. tumefaciens* strain containing the *virE2* deletion could be selected by its resistance to kanamycin. Details of the plasmid construction follow.

The *virE* operon of pTiA6NC lies within a 3.2 kb *Xho*I restriction fragment (Garfinkel *et al.* 1981); this fragment was inserted into the *Sal*I site of pUC18 such that *lacZ* and *virE* are transcribed in the same direction in the resulting plasmid, pGR1

(Sundberg *et al.* 1996). The 1497 bp of the coding region of the *virE2* gene in pGR1 was replaced with the kanamycin resistance gene (*neo*) from Tn*5* (Jorgenson *et al.* 1979). This was accomplished by digesting pGR1 with *Stu*I and *Nae*I, purifying a 4.4 kb fragment of pGR1 from the 1,497 bp fragment by 1% agarose gel electrophoresis, and ligating a 2.4 kb blunt-ended *Hinc*II restriction fragment containing the *neo* gene from Tn*5* (Jorgenson *et al.* 1979) to the 4.4 kb fragment. The resulting plasmid, carrying the substitution #1 allele, pPD15 (Figure 3.2), contains a single *Bam*HI site which was used to insert pPD15 into the *Bam*HI site of broad-host-range plasmid pRK310 (Ditta *et al.* 1985) to form pPD16.

We transformed pPD16 into the *A. tumefaciens* strain A348 which contains a wild-type Ti plasmid and used a marker exchange procedure (Garfinkel *et al.* 1981; Miranda *et al.* 1992) to identify a homogenote (WR5000) carrying the kanamycin resistant *virE2* substitution #1 allele in the Ti plasmid. In the marker exchange procedure, a plasmid (pPH1JI) (Beringer *et al.* 1978) incompatible with the broad-host-range plasmid pRK310, was transformed into A348 containing pPD16. The plasmid pPH1JI encodes gentamicin resistance. To select for a recombination event between the *virE*

operon on pPD16 and the *virE* operon on the Ti plasmid, we selected for kanamycin resistance (the *virE2* deletion), gentamicin resistance (pPH1JI), and screened for carbenicillin sensitivity (loss of pPD16). We refer to the resulting *A. tumefaciens* strain as WR5000. The structure of the Ti plasmid was verified by Southern blot analysis of genomic DNA after digestion with *Eco*R1 (Figures 3.2 and 3.3).

Construction of *A. tumefaciens* Strains for Virulence Assays

The mutagenized pGR1 derivatives, pDP1 through pPD10 (Table 2.1), were linearized at their single *Bam*HI site and inserted into the *Bam*HI site of the broad-host-range plasmid pRK310. The *virE* operon and the *lacZ* gene of pRK310 are transcribed in the same direction. This resulted in plasmids pPD101 through pPD110 (Table 2.1). These plasmids were then used to transform the *virE2* null strain WR5000, with selection for carbenicillin and kanamycin resistance, and also verification by Southern blot analysis (Figures 3.4 and 3.5).

Fusion of *virE* to an *E. coli* Promoter

In order to assess the binding activities of the wild-type and mutant VirE2 proteins in *E. coli* extracts, the *virE* operon was fused to the *trc* promoter in pTrc99A (Amann *et al.* 1988, this plasmid is available from Pharmacia). The *Sph*I restriction site that lies outside the multiple cloning region of pTrc99A was first removed by performing a limited digestion of pTrc99A with *Sph*I, isolating full-length linear plasmid DNA, and creating blunt ends by incubation with T4 DNA polymerase. The blunt-ended DNA was ligated into circular molecules, and transformed into *E. coli* (Hanahan 1983). From among these transformants, we isolated pBL17, a pTrc99A derivative with a single *Sph*I site that lies in the multiple cloning region. We cleaved pBL17 with *Nco*I and *Sph*I and ligated to it an annealed pair of DNA oligonucleotides with *Nco*I and *Sph*I cohesive ends to create pWR223 (Figure 3.6). The annealed oligonucleotides contain the first eight codons of *virE1*; the first codon (ATG) occupies the *Nco*I compatible end, and the sequence contains the only *Sph*I site within the *virE* operon. Plasmid pGR1 contains two *Sph*I sites, one in *virE1* and another in the multiple cloning region of pUC18, beyond the 3' end of *virE2*. By inserting the 2.5 kb *Sph*I

pUC18, beyond the 3' end of *virE2*. By inserting the 2.5 kb *Sph*I fragment into pWR223 (in the proper orientation), we reconstructed the *virE* operon downstream of a strong, lactose-inducible promoter, thereby creating pWR225. Plasmids that contain mutant *virE2* genes were made similarly (Table 2.1). The plasmids were transformed into *E. coli* strain JC10,289 (Table 2.1).

DNA Methods

Rubidium Chloride Transformation of *E. coli*

This transformation method is based on the work of Hanahan (1983). Cells (MM294, DH5α, SK1592) were grown to a density of 5 x 10^7 cells/ml (Klett 50-60) (5 ml per transformation). Cells were pelleted for 5 minutes at 13,000 x g at 25°C, resuspended in 0.2 volumes ice-cold RbCl buffer (100 mM RbCl, 45 mM $MnCl_2$, 10 mM $CaCl_2$, 35 mM KCH_2COOH, 15% sucrose, pH 6.0), incubated on ice for 5 minutes and resuspended in 0.04 volumes ice-cold RbCl buffer. DNA (50 ng) was mixed with 200 µl competent cells and placed on ice for 60 minutes. Cells were heat-shocked at 42°C for two minutes; then diluted to 2.0 ml with L broth and incubated for 45 minutes at 37°C.

Cells were then centrifuged at 2,000 x g for 5 minutes, plated on L agar containing appropriate antibiotics and incubated overnight at 37°C.

Calcium Chloride *A. tumefaciens* Transformation

This transformation method is based on the work of Holsters (1978). Overnight cultures were used to inoculate 40 ml of YEP and the cells were grown to a Klett reading of 100-150. Cells were then pelleted at 2,600 x g for 7 minutes and resuspended in 0.5 volumes of ice-cold 150 mM NaCl. The cells were pelleted again and resuspended in 0.01 volumes ice-cold 75 mM $CaCl_2$. DNA (10 µg) was added to 200 µl cells then the mixture was incubated for 30 minutes on ice and frozen in a dry ice/ethanol bath for three minutes. Cells were heat-shocked at 37°C for five minutes then diluted into 10 ml YEP and incubated at 28°C with shaking for two hours. Cells were again pelleted at 2,600 x g for 7 minutes, then plated on AB glucose agar plates (Garfinkel *et al.* 1981) containing the appropriate antibiotics and incubated 2-3 days at 28°C.

Plasmid DNA Miniprep (boiling method)

E. coli cells were grown overnight, pelleted (1.5 ml per miniprep) for 2 minutes in a microfuge at 13,000 x g and resuspended in 300 µl STET (8% sucrose, 0.5% Triton X-100, 50 mM EDTA, 10 mM Tris-HCl (pH 8.0)). Twenty-five µl of lysozyme solution (10 mg/ml in 10 mM Tris-HCl (pH 8.0)) was then added to each tube and the cells were incubated on ice for 10 minutes. Cells were boiled 40 seconds and centrifuged 7 minutes at 13,000 x g. The white, stringy pellets were discarded and 300 µl isopropanol was added to each tube. The supernatant was mixed with the isopropanol for 30 seconds by inverting several times. The DNA was pelleted for 15 minutes at 13,000 x g and resuspended in sterile water. To further purify the DNA, an equal volume of phenol/chloroform (1:1) was added and the mixture was vortexed briefly prior to centrifuging for 5 minutes at 13,000 x g. The top layer, containing the DNA, was removed to another microfuge tube and extracted with an equal volume of chloroform:isoamyl alcohol (24:1). The DNA was precipitated by adding 0.1 volume 8 M LiCl and 2 volumes 100% ethanol and incubating at -20°C for 20 minutes. The

DNA was pelleted by centrifugation at 13,000 x g, 15 minutes, and resuspended in sterile water.

Ligation in Low Melt Agarose

A 1% Sea Plaque (FMC Bioproducts) agarose gel in 1X TAE buffer (0.04 M Tris-acetate, 0.002 M EDTA (pH 8.1)) containing 0.5 μg/ml ethidium bromide was allowed to solidify at least one hour at 4°C. Digested DNA fragments (0.5-5 μg digested DNA per lane) were subjected to electrophoresis through the gel at 75 mV. The DNA was visualized using a long-wavelength UV transilluminator and the bands of interest were excised from the gel. The DNA-containing agarose was melted at 70°C for 5 minutes. For a 20 μl ligation reaction, 10 μl molten agarose containing DNA was used. The reaction was incubated overnight at room temperature, heated for 5 minutes at 70°C and 10 μl was used to transform *E. coli* as described previously.

Southern Blot

DNA (1-5 µg) was subjected to electrophoresis through an 0.8% agarose gel cast in 1X TBE buffer (0.045 M Tris-borate, 2 mM EDTA (pH 8.4)) containing 0.5 µg/ml ethidium bromide. The gel was placed in a plastic container, covered with 0.25 N HCl, and shaken gently for 15 minutes, and then shaken with 0.4 M NaOH for 10 minutes. A piece of Gene Screen Plus nylon membrane (NEN Research Products) was cut to the size of the gel, soaked in dH_2O for 5 minutes and then soaked in 0.4 M NaOH for 10 minutes. The DNA in the gel was then transferred to the filter by a downward blotting procedure for 2.5 hours using a transfer solution of 0.4 M NaOH (Koetsier *et al.* 1993).

The membrane was rinsed in 2X SSC (0.3 M NaCl, 0.03 M sodium citrate) then incubated for 10 minutes at 37°C to dry completely. The membrane was then placed in a hybridization tube containing 8 ml FBI solution (0.5 M sodium phosphate (pH 7.5), 7% SDS) and incubated at 65°C for one hour. The FBI solution was discarded and three ml fresh FBI solution was added.

DNA (1 µg) was labeled with [α-^{32}P]dCTP (50 µCi) by nick translation (Bethesda Research Laboratories nick translation system) (Ausubel *et al.* 1987). The unincorporated deoxynucleoside

triphosphates were removed using a spin column. A 0.9 ml column of G50 Superfine (Sephadex) was prepared in a 1 ml syringe containing a plug of siliconized glass wool at the bottom. The Sephadex was equilibrated in TE (10 mM Tris-HC1 (pH 8.0), 1 mm EDTA) prior to use. The syringe was filled with Sephadex to 1 ml volume and centrifuged at 2,900 RPM for 2.5 minutes in a Beckman GH-3.7 rotor. This process was repeated 2 or 3 times until a column volume of 0.9 ml was obtained after centrifugation. The nick translation reaction was applied to the top of the column and the centrifugation repeated as above. The unincorporated nucleotides remained in the column after centrifugation. Using this method typical specific activities of 3 x 10^6 cpm per µg of DNA were obtained and approximately 0.3 µg of probe DNA was added to 0.5 ml FBI solution. To denature the labeled DNA, the DNA/FBI solution was boiled for 3 minutes before being added to the membrane. The membrane was then incubated at 65°C overnight.

The membrane was rinsed briefly in 15 ml of 2X SSC plus SDS (0.3 M NaCl, 30 mM sodium citrate, 1% SDS) and then washed twice with 15 ml 0.2X SSC plus SDS (0.03 M NaCl, 3 mM sodium citrate, 1% SDS) at 65°C for 30 minutes. The membrane was allowed to air dry

and exposed to Kodak X-Omat AR film at -80°C with an intensifying screen.

DNA Fragment Purification from an Agarose Gel for Probe Synthesis

A 517 base pair (bp) DNA fragment was purified from a *Hinf*1 restriction digest of 8 μg of pUC18. Fifty ng of this DNA was end-labeled in 40 ul of buffer consisting of 0.25 mM dTTP, 0.25 mM dCTP, 0.25 mM dGTP, 2.5 units *E. coli* DNA polymerase I, Large fragment (New England Biolabs), 50 μCi of [α-^{32}P]dATP, 50 mM potassium phosphate (pH 7.5), 3 mM $MgCl_2$ and 1 mM 2-mercapto-ethanol. The reaction was incubated for five minutes at room temperature and the enzyme was inactivated by adding 1 μl of 0.5 M EDTA (pH 8.0) and heating to 75°C for 10 minutes. The unincorporated deoxynucleoside triphosphates were removed using a spin column as described previously. The DNA was precipitated by adding 0.5 volumes of 7.5 M ammonium acetate and 2 volumes of 100% ethanol, and placing at -20°C for 20 minutes. The DNA was pelleted at 13,000 x g for 30 minutes at 4°C and resuspended in TE (10 mM Tris-HCl (pH 8.0), 1 mM EDTA).

This 517 bp fragment was isolated from an agarose gel as described in the ligation in low melt agarose section (see DNA methods, section 2.3). The agarose gel was melted at 70°C for 5 minutes, three volumes of TE (10 mM Tris-HCl (pH 8), 1 mM EDTA (pH 8.0)) were added, and the mixture was incubated for 5 minutes at 70°C. The mixture was vortexed briefly, frozen at -80°C for 5 minutes and thawed at room temperature. After thawing, the tube was tapped vigorously against the lab bench a few times and centrifuged at 13,000 x g for 5 minutes. The supernatant was removed and the DNA precipitated by adding 0.1 volume of 8 M LiCl and 2 volumes of 100% ethanol, then incubating at -80°C for 20 minutes. The DNA was pelleted by centrifugation at 25°C (15 minutes, 13,000 x g). To precipitate fragments less than 1 kb, the DNA was incubated in LiCl plus ethanol overnight at -20°C, and centrifuged at 4°C for 30 minutes at 13,000 x g.

Virulence Assays

Potato Disc Assay

For quantitative virulence assays, potato tuber discs (7 mm diameter) were inoculated by the method of Shurvinton and Ream (1991). A brief description follows. Five ml cultures of *A. tumefaciens* strains in YEP broth with appropriate antibiotics were grown with shaking at 28°C, and 100 µl of each overnight culture was diluted with 900 µl phosphate buffered saline (3 mM sodium phosphate dibasic, 10 mM potassium phosphate monobasic, 12 mM sodium chloride pH 7.2). Red, organic potatoes were removed from the cold room and allowed to warm overnight to room temperature. Organic potatoes are more susceptible to infection by *A. tumefaciens* than potatoes treated with sprout-inhibiting chemicals. Potatoes were peeled and surface-sterilized for 10 minutes in a 20% bleach solution.

Using a laminar flow hood to prevent contamination, the potato was rinsed thoroughly with sterile water and placed on a sterile paper towel. Using a sterilized cork borer (7 mm diameter) and glass pipette (to push cores out of borer) the potatoes were cored

and sliced into discs 3-4 mm thick. A large potato yielded about 10 cores and 80 discs. The last 3-4 discs at the core ends were not used as they had been in contact with the bleach solution. The discs were placed on water agar plates (7.5 gm agar per 500 ml water) using sterile tweezers. Ten µl (2 x 10^7 cfu) of a diluted *A. tumefaciens* strain was placed on each separate disc. Parafilm was wrapped around the edge of each covered plate to prevent the agar from drying out, and the plates were incubated at 28°C for three weeks. The tumors appeared as white crystalline protrusions and were counted using a dissecting microscope.

Carrot Slice Assay

An assay similar to the potato assay was used for carrots. Organic carrots (grown without pesticides or herbicides) with green leafy tops gave the best results. After sterilization and rinsing, carrots were sliced and placed on water agar plates facing upwards on the agar in the direction they grew in the soil. The meristem surrounding the core of each slice was inoculated with 10 µl of PBS-diluted bacteria (2 x 10^7 cfu). Comparison between different *A.*

tumefaciens strains was made using discs from the same carrot. Tumors arose from the meristemmatic tissue surrounding the core of each slice as callous-like material; the individual tumors were indistinguishable and therefore only qualitative virulence results could be obtained. The tumors were scored after three weeks.

Kalanchoe daigremontiana and Tomato Assays

K. daigremontiana leaves and tomato stems (cv. Bonnie Best) were infected by wounding the tissue with a sterile toothpick and packing wounds with *A. tumefaciens* cells cultured on AB glucose agar plates (Garfinkel et al. 1981) containing appropriate antibiotics. The *K. daigremontiana* leaves and tomato stems were scored after four weeks.

Protein Methods

Preparation of VirE2 from *E. coli* Extracts

Twenty ml cultures of *E. coli*, harboring wild-type or mutant *virE2* in pBL17, were grown at 37°C with aeration in L-broth to an optical cell density (A_{595}) of 0.7. The *trc* promoter was induced by

the addition of IPTG (0.5 mM final concentration), and incubation continued for three hours. Cells were harvested by centrifugation (10,800 x g, 4°C), resuspended in 1.5 ml ice-cold Buffer A (10 mM Tris-HCl pH 8.0, 10% v/v glycerol, 25 mM sodium chloride, 1 mM phenyl methyl sulfonyl fluoride [PMSF], 1mM dithiothreitol), and lysed in a French press at 19,600 pounds per square inch (PSI). The lysates were centrifuged at 17,000 x g at 4°C for 6 minutes and 50 µl aliquots of the supernatant were frozen at -80°C. The soluble VirE2 protein in these supernatants was used to determine the DNA binding affinities of the wild-type and mutant VirE2 proteins. The insoluble VirE2 protein in the pellet was purified by electroelution from an SDS-polyacrylamide gel. This purification is described in the next section. The protein concentration in each extract was determined using the Bradford dye-binding procedure with a bovine serum albumin standard curve (Bradford 1976; Bio-Rad). The total protein concentrations obtained were between 4.0-6.5 mg/ml.

VirE2 Protein Purification

To prepare homogeneous VirE2 protein to estimate the VirE2 concentrations by immunoblot analysis, the insoluble VirE2 protein

in the pellet was purified by electroelution from a 10% SDS-polyacrylamide gel. This insoluble VirE2 protein was resistant to protease degradation in *E. coli* VirE2 protein was solubilized by resuspending the pellet in 1.5 ml ice-cold buffer containing urea (10 mM Tris-HCl (pH 8.0), 10% v/v glycerol, 1 M sodium chloride, 1 mM phenyl methyl sulfonyl fluoride [PMSF], 1 mM dithiothreitol, 4 M urea) and incubated on ice for 30 minutes. After centrifugation (17,000 x g, at 4°C for 6 minutes) the supernatant was dialyzed for 2 hours at 4°C against 2 liters of buffer A (10 mM Tris-HCl (pH 8.0), 10% (v/v) glycerol, 25 mM sodium chloride, 1 mM dithiothreitol) and then overnight at 4°C against 2 liters of fresh buffer A. After dialysis, the soluble protein was frozen at -80°C. The soluble protein was subjected to electrophoresis through a 10% SDS-polyacrylamide gel, the gel was stained with 0.05% Coomassie blue G250 in water, destained in water, and the VirE2 containing band was excised. The gel slice was chopped into smaller pieces and VirE2 was electroeluted in 1 liter tris/glycine buffer (2 liters dH_2O, 9.94 g tris base, 57.6 g glycine, 2 g SDS) using an Elutrap electroelution apparatus (Schleicher and Schuell) for 3 hours at 4°C and 150 mV. The concentration of VirE2 purified by electroelution

was determined by gel electrophoresis. A known volume (10 ul) of the electroeluted protein was subjected to electrophoresis through a 10% SDS polyacrylamide gel next to a known concentration range (0.23 ng/ul to 6.0 ng/ul) of bovine serum albumin (BSA). After silver staining, the band intensity of each protein was determined using a Molecular Dynamics densitometer coupled to ImageQuant software, which generated a standard curve for the concentration of BSA. This standard curve was used to estimate the concentration of the purified VirE2, which was determined to be 3.8 ng per μl. . The purified VirE2 protein did not retain ssDNA-binding activity.

Determination of VirE2 Concentration

The concentration of the overexpressed VirE2 protein in crude *E. coli* extracts was determined immunologically, similarly to the procedure described by Ausubel *et al.* 1987, using a standard curve of purified VirE2.

Varying amounts of purified VirE2 (ranging from 1.6 to 11.4 ng) were subjected to electrophoresis through a 10% polyacrylamide gel to generate a linear standard curve. Aliquots of cellular extracts were loaded on the same gel and proteins from the gel were

electrophoretically transferred to a nitrocellulose membrane (Schleicher and Schuell) for 75 minutes at 50 mAmps using a Hoefer semi-dry transfer apparatus (Ausubel *et al.* 1987). The transfer buffer consisted of 400 ml 10X Transfer Buffer Concentrate (1 liter dH_2O, 14.5 g tris base, 67 g glycine), 800 ml methanol and 2.8 liters dH_2O. The membrane was incubated for 30 minutes in 15 ml MTBS (20 mM Tris-HCl pH 7.5, 500 mM sodium chloride, 5% (w/v) Carnation nonfat dry milk) at room temperature with gentle agitation. A 1:80 dilution of *E. coli* extract (Promega) in 15 ml TTBS (20 mM Tris-HCl pH 7.5, 500 mM sodium chloride, 0.1% Tween 20) was incubated with a 1:4,000 dilution of polyclonal rabbit antiserum raised against VirE2 (Das 1988) for 30 minutes at 37°. The MTBS solution was discarded from the membrane and the VirE2 antiserum in the TTBS solution was added. After incubation for 45 minutes at room temperature with gentle agitation, the membrane was washed twice (5 minutes each) with 15 ml TTBS at room temperature with gentle agitation. The membrane was then incubated for 45 minutes with 15 ml of a 1:5000 dilution of goat anti-rabbit horseradish peroxidase (GAR-HRP) (Bio-Rad) in MTTBS (20 mM Tris-HCl pH 7.5, 500 mM sodium chloride, 0.1% Tween 20, 5% (w/v) Carnation nonfat dry milk)

at room temperature with gentle agitation. The membrane was washed twice in 30 ml TTBS at room temperature with gentle agitation (5 minutes each) and then washed twice in 30 ml TBS at room temperature with gentle agitation (10 minutes each). The HRP was detected with an ECL Western blot chemiluminescence development kit (Amersham). To quantitate light emissions, flashed X-ray film (the film was flashed from a distance of 9 feet) was exposed to the filters, and the resulting band intensity measured on a Molecular Dynamics densitometer interfaced to ImageQuant software. For each immunoblot, a standard curve was generated from the purified VirE2 data and the amount in each cellular extract was estimated.

DNA Binding Assays

To locate domains important for DNA binding, we assessed the ssDNA binding activity of each VirE2 mutant. A 517-bp *Hin*FI fragment from pUC18 was labeled using the Klenow fragment of DNA polymerase I (New England Biolabs) and [α -^{32}P]dATP; the labeled DNA was boiled prior to use to denature the double-stranded DNA.

E. coli extracts containing VirE2 extracts containing VirE2 (10-71 ng/ul) were mixed with 1 ng of ^{32}P-labeled ssDNA (10 µl total volume), and incubated for ten minutes on ice. Loading buffer (3 µl of 10% v/v glycerol 0.1% bromphenol blue) was added prior to electrophoresis on a 4% polyacrylamide gel, cast in low ionic-strength buffer (6.7 mM Tris-HCl (pH 7.5), 1 mM EDTA, 3.3 mM sodium acetate). A potential of 75 volts was applied to the gel for 15 minutes at 4° C prior to loading the samples and for 75 minutes after loading. The gel was dried and exposed to a phosphorimager screen. Signals were quantitated using a Molecular Dynamics phosphorimager with ImageQuant software.

CHAPTER 3. RESULTS

Construction of *virE2* Mutants

The results of the linker insertion mutagenesis of *virE2* and the location of the ten amino acid deletion are shown in Figure 3.1. The two nuclear localization sequences in *virE2* are also shown. Changes in the amino acid sequence as a consequence of the linker insertions are described in the legend to Figure 3.1. The 30 bp deletion was located between insertion 1 and 2 near the amino terminus.

Construction of the *virE2* Null *A. tumefaciens* Strain

The *virE2* null *A. tumefaciens* strain was constructed using marker exchange as described in Experimental Procedures and the final construct is shown in Figure 3.2. A 1.5 kb segment of *virE2* was replaced by a 2.4 kb fragment encoding the kanamycin resistance gene (*neo*). This resulted in a change in the *Eco*R1 restriction sites at this locus (Figure 3.2).

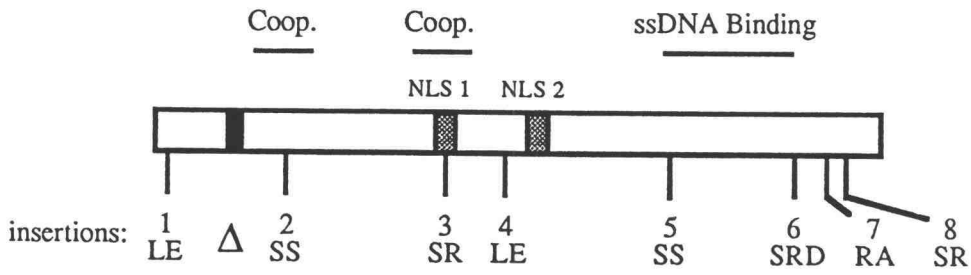

Figure 3.1. Map of mutations in *virE2*. NLS=nuclear localization signal, NLS 1= ^{205}-KLR PED RYV QTE RYG RR-^{226} NLS 2= ^{273}-KRR YGG ETE IKL KSK-^{287} The basic amino acids in the nuclear localization sequences are underlined. Δ =the deletion of residues 56-65 (SSSLY SGSEH) from *virE2* L=leucine, E=glutamic acid, S=serine, R=arginine, D=aspartic acid, A=alanine, P=proline, Y=tyrosine V=valine Q=glutamine, T=threonine, G=glycine, K=lysine. Insertion 1=LE; Insertion 2=SS; Insertion 3=SR; Insertion 4=LE; Insertion 5=SS; Insertion 6=the replacement of residue 472, a tyrosine by a serine and the insertion of an arginine and aspartic acid after residue 472; Insertion 7=RA; Insertion 8=SR. The deletion was created using site-directed mutagenesis as described in the experimental procedures chapter (see DNA methods in section 2.3). Linker insertion mutagenesis is also described in the chapter on experimental procedures (see DNA methods in section 2.3).

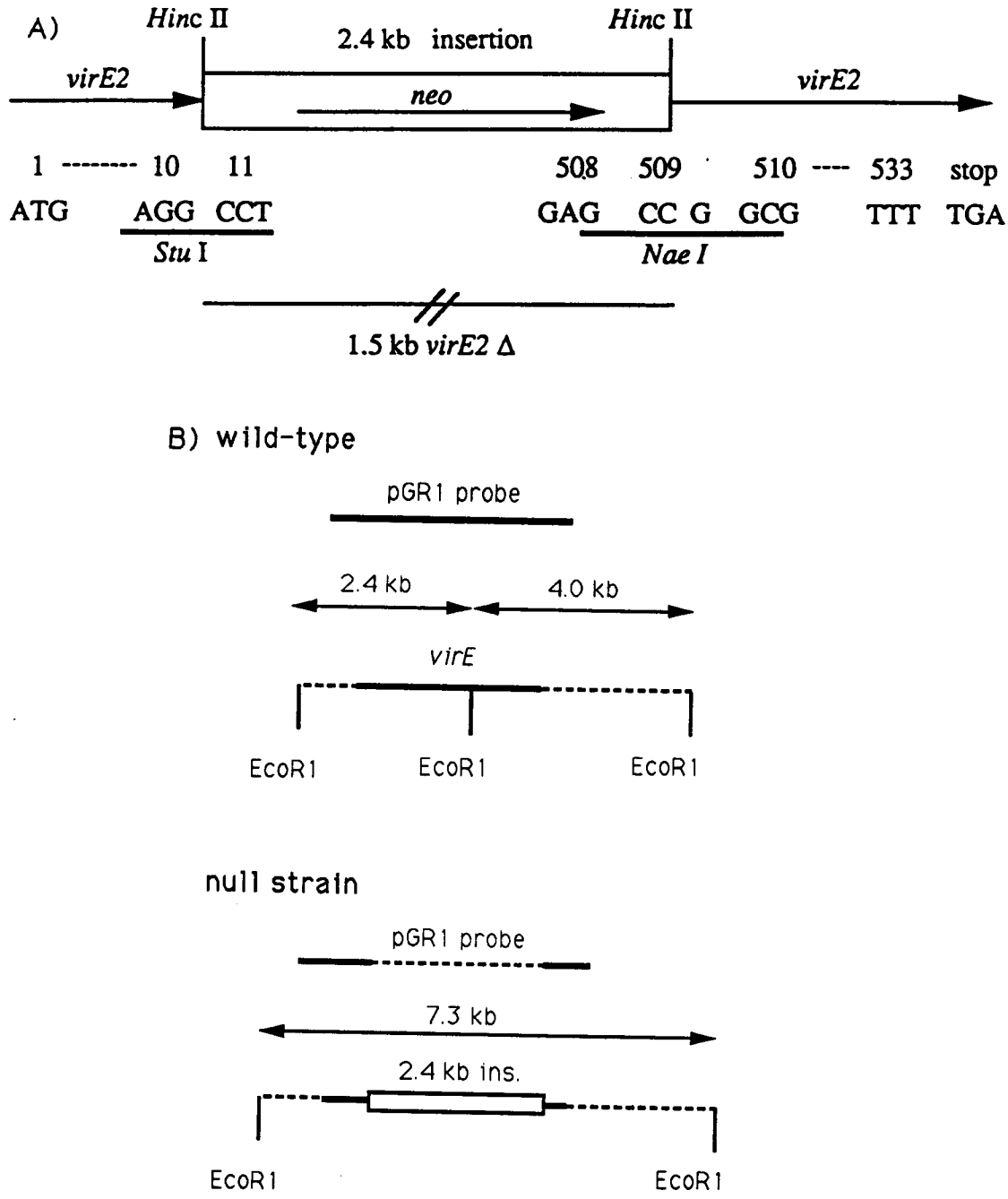

Figure 3.2. Replacement of *virE2* with *neo* from Tn*5* and a Map of the *virE2* null *A. tumefaciens* strain. A) Numbers indicate codons in the wild-type virE2 gene. Arrows indicate the direction of transcription. Restriction sites used in the construction of pPD15 are indicated B) Strain A348 has a wild-type Ti plasmid. In WR5000, the *virE2* gene on the Ti plasmid is replaced by the *neo* gene encoding resistance to kanamycin. The *EcoR1* restriction sites are shown.

The integrity of the Ti plasmid in the *A. tumefaciens virE2* null strain WR5000 was verified by Southern blot analysis (Figure 3.3). Genomic DNA from the *A. tumefaciens* transformants was digested with *Eco*R1 and probed with nick-translated pGR1 which contains the *virE* operon. This probe will hybridize to the regions flanking the *virE2* gene (Figure 3.2). The wild-type *virE2* gene has one *Eco*R1 restriction site which was removed by insertion of the kanamycin resistance gene. When digested with *Eco*R1, two fragments (2.4 kb and 4.0 kb) of the wild-type gene (bands B and C) hybridize to the probe, whereas the mutant has a single band of 7.3 kb (A) that hybridizes to the probe because the *neo* gene does not contain any *Eco*R1 sites.

Construction of the *A. tumefaciens* Strains Used For Virulence Assays

After verifying the absence of the *virE2* gene from the null strain WR5000 (Figure 3.3), this strain was transformed with plasmids encoding wild-type or mutant forms of *virE2*. Strain WR5000 was transformed with plasmids pPD100 through pPD110

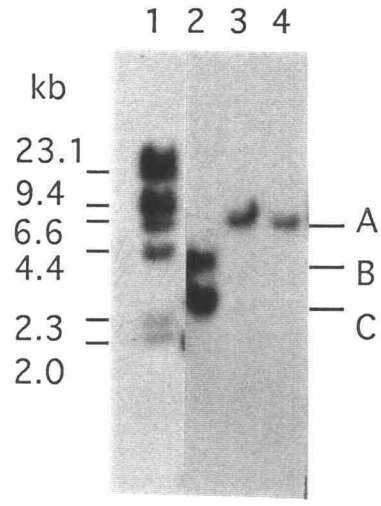

Figure 3.3. Southern blot analysis of *virE2* null *A. tumefaciens* strain WR5000.
Lane 1. λ *Hin*dIII ladder
Lane 2. strain A348 which harbors a wild-type Ti plasmid-pTiA6NC
Lanes 3-4. strain WR5000 isolates harboring a Ti plasmid with *neo* from Tn*5* replacing *virE2* on pTiA6NC
A. tumefaciens DNA was prepared, digested with *Eco*R1, and probed with pGR1. Note the disappearance of bands B and C (seen in lane 2) and the appearance of a larger band (A) in lanes 3 and 4. The *Eco*R1 site in *virE2* on the Ti plasmid was eliminated due to its replacement by *neo*.

(Table 2.1), yielding *A tumefaciens* strains designated WR5100 through WR5110 (Table 2.1).

To verify the integrity of these plasmids, Southern blot analysis was performed (Figure 3.4). Genomic DNA was digested with *Bam*H1 and *Xho*1 and probed with pGR1, which contains the *virE* operon. The mutagenized pGR1 derivatives, pPD1 through pPD10 (Table 2.1), were linearized at their single *Bam*H1 site and inserted into the *Bam*H1 site of the broad host range plasmid pRK310 to yield plasmids pPD101 through pPD110. Therefore, a *Bam*H1 digest will cut the plasmids pPD101 through pPD110 twice resulting in two fragments. One fragment (20.4 kb) will be pRK310 which does not hybridize to pGR1 and therefore will not be detected. The second fragment, containing the *virE* operon in pUC18 will be detected (Figure 3.5).

*Bam*H1 cuts once in the multiple cloning site in pUC18, 900 base pairs (bp) upstream from the start of the *virE2* gene *Xho*1 cuts only at the site of the linker insertion (Figure 3.5). An *Xho*1 and *Bam*H1 digest of a wild-type *virE2* gene results in the detection of a single fragment, whereas a similar digest of a linker insertion

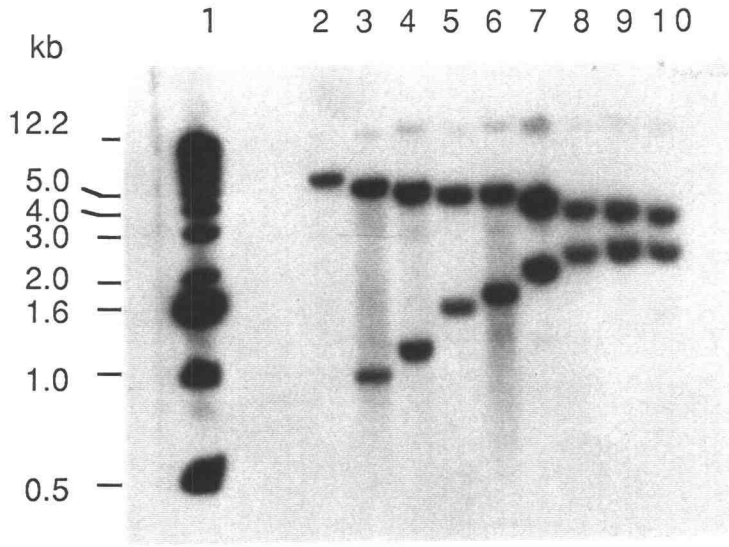

Figure 3.4. Southern blot analysis of *A. tumefaciens* strains with mutations in *virE2*. Total genomic *A. tumefaciens* DNA was prepared, digested with *Xho*I and *Bam*HI, and probed with pGR1. A second band appears in the strains containing an *Xho*I linker insertion in *virE2*.

Lane 1. 1 kb ladder

Lane 2. strain WR5100
strain WR100 = pPD100 (WT *virE2*) in WR5000

Lanes 3 -10. strains WR5101 - WR5108
strains WR5101 - WR5108 = pPD101- PPD108
(*virE2* linker insertion mutants) in WR5000

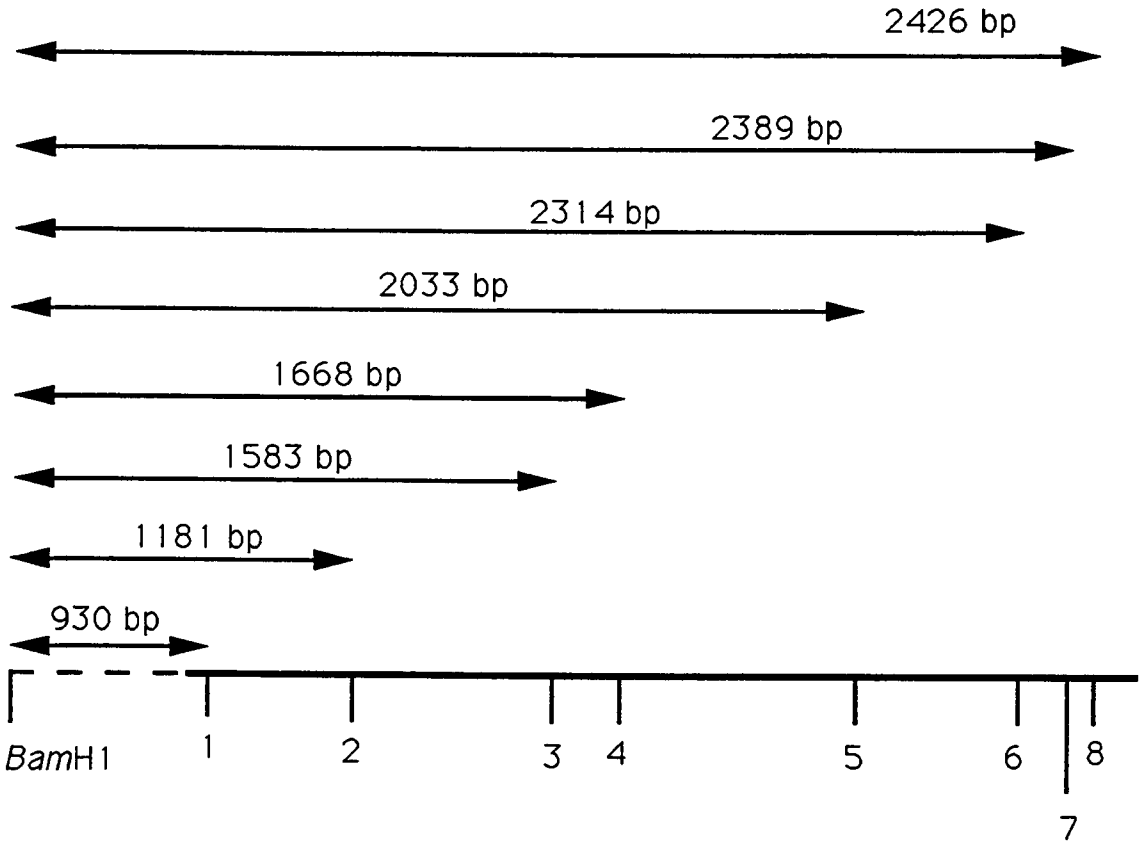

Figure 3.5. Map of the *virE* gene cloned into pUC18. Numbers 1-8 show the positions of the *Xho*1 linker insertions. The location of the unique *Bam*H1 site used for Southern analysis is shown.

mutant results in the detection of two fragments due to the presence of an *Xho*1 site in the linker insertion.

The sizes of the fragments expected from insertions 1 through 8 were confirmed in this analysis, thereby confirming the location of the insertions. Furthermore, the locations of the mutations were also confirmed by sequencing (Central Services Lab, Oregon State University).

Determination of VirE2 Protein Concentration in *E. coli* Extracts

To determine the binding activities of the wild-type and mutant VirE2 proteins, the *virE* operon was inserted into pTrc99A (Amann et al. 1988) which resulted in the expression of VirE2 in *E. coli*. As described in the chapter on Experimental Procedures, this cloning was facilitated by inserting a pair of oligonucleotide linkers into a derivative of pTrc99A (pBL17) as shown in Figure 3.6.

The VirE2 protein concentration in *E. coli* extracts was estimated using immunoblot analysis and purified VirE2 protein as described in Chapter 2 (see protein methods, section 2.5). The Immunoblots and the relationship between the amount of purified

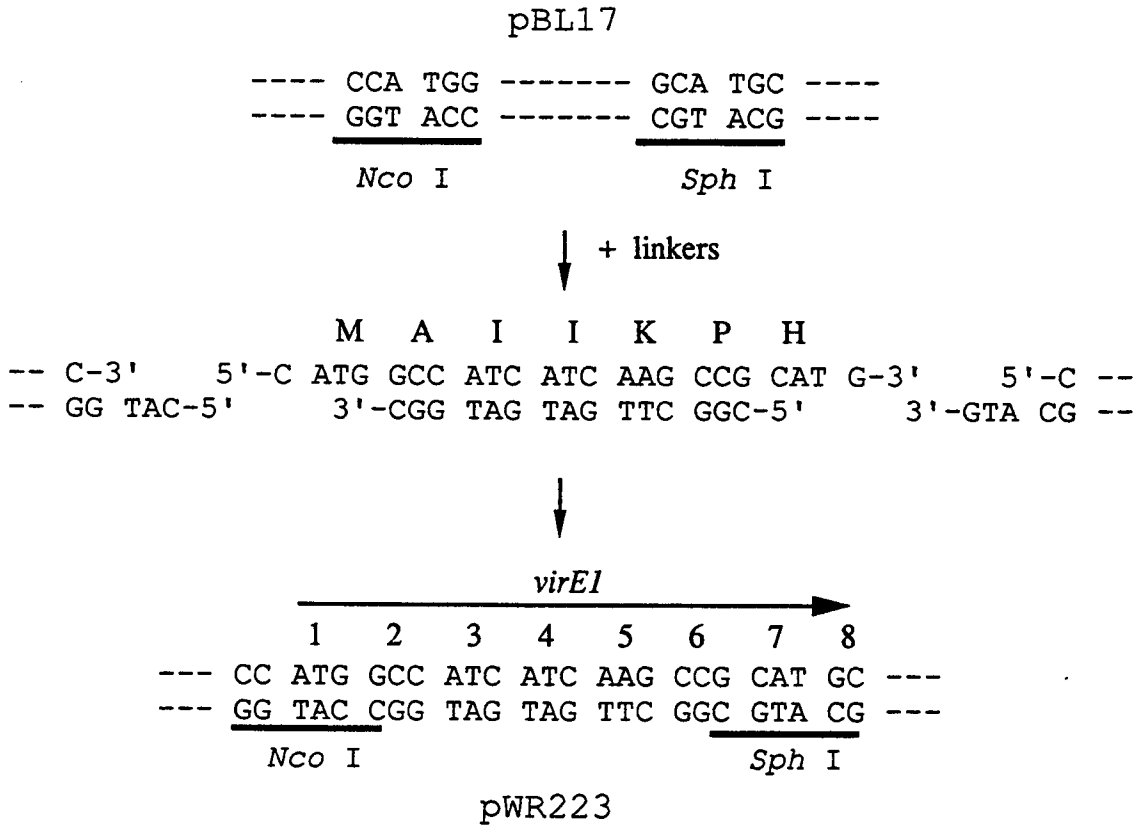

Figure 3.6. Construction of pWR223. Oligonucleotide linkers containing the first seven codons of *virE1* were ligated into a pTrc99A expression vector to facilitate the expression of *virE* in *E. coli*. M=methionine A=alanine I=isoleucine K=lysine P=proline H=histidine

VirE2 protein and the signal obtained from the densitometer are presented are shown in Figures 3.7 through 3.12. A fraction of the soluble VirE2 protein produced in *E. coli* was cleaved by a protease. Therefore, the antibody recognized two species: full length VirE2 (approximately 66 kDa on an SDS-PAGE gel) and a slightly smaller VirE2 species (approximately 64 kDa on an SDS-PAGE gel) which migrated as a separate band (Figures 3.7, 3.9 and 3.11).

The signals from both bands were used to estimate the amount of VirE2 protein. In most cases, approximately half of the VirE2 protein produced was cleaved, except for VirE2 mutants with insertions 2, 7, and 8. In the case of insertions 7 and 8, the majority of VirE2 protein produced was cleaved, whereas insertion 2 rendered VirE2 resistant to the protease.

Figure 3.7. Immunoblot analysis of protein extracts from *E. coli* with mutations in *virE2*. Purified VirE2 (lanes 1-3) or *E. coli* extracts overexpressing VirE2 were transferred to nitrocellulose and immunologically detected with antiVirE2 serum. The blot was developed using goat anti-rabbit horseradish peroxidase and an ECL chemiluminescence development kit (Amersham). A standard curve was generated from the signal emitted in lanes 1, 2, and 3. This standard curve is shown in Figure 3.8. This relationship was used to estimate the amounts of VirE2 protein in the *E. coli* extracts (lanes 4-8). Only uncleaved VirE2 protein is seen in the purified standards in lanes 1, 2, and 3. The cleaved VirE2 protein, VirE2', is seen in lanes 4, 5, 6, and 8. The signal from both bands was used to estimate the amount of VirE2 protein in each extract. Only the cleaved product, VirE2', is seen in lane 7. The signal in lane 4 is outside the linear range of the ECL system, and therefore this estimate was not used. A smaller volume of this extract was immunoblotted again so that the signal was within the linear range and this signal was used to estimate the amount of VirE2 protein in the Mutant 5 extract.
Lane 1. 3.8 ng purified VirE2
Lane 2. 7.6 ng purified VirE2
Lane 3. 11.4 ng purified VirE2
Lane 4. 13.5 ng Mutant 5
Lane 5. 6.5 ng Mutant 3
Lane 6. 6.5 ng Mutant 6
Lane 7. 4.6 ng Mutant 7
Lane 8. 5.3 ng Deletion

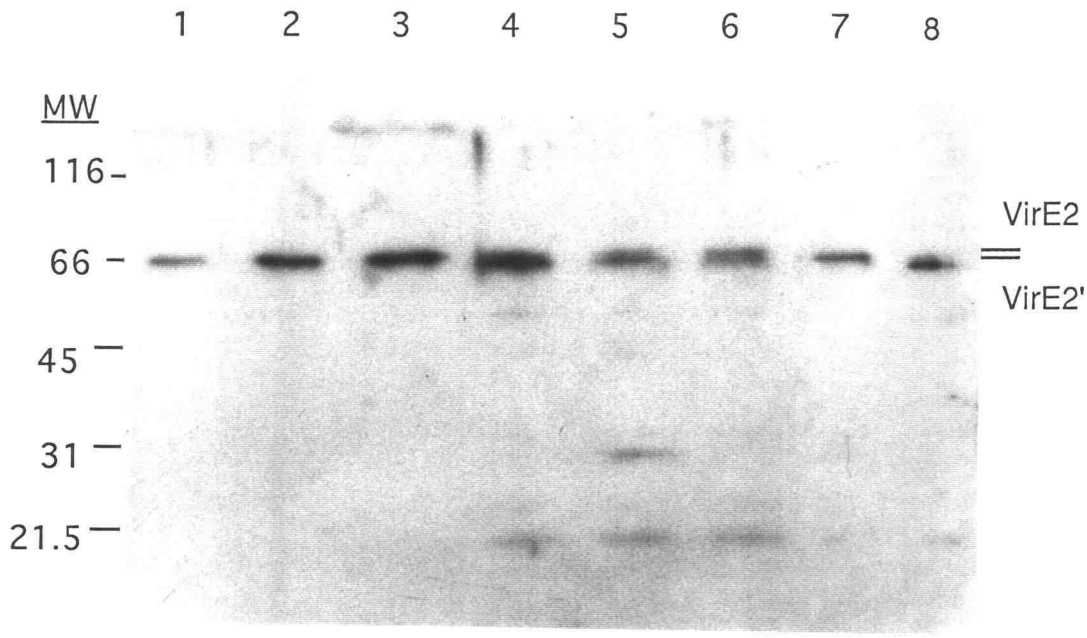

Figure 3.7

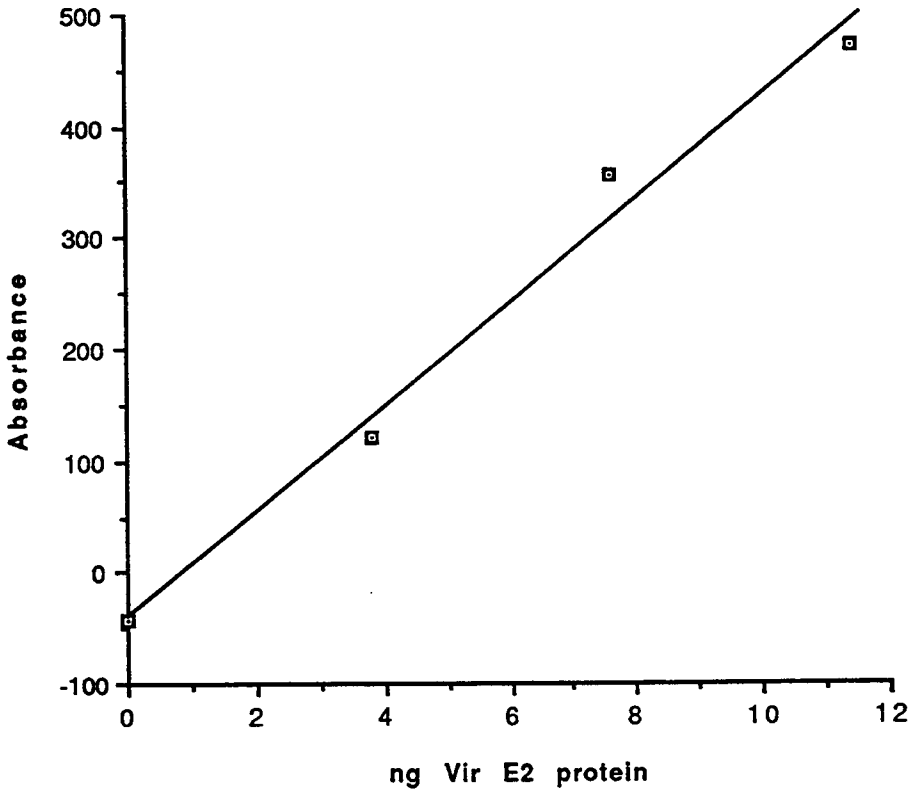

Figure 3.8. Absorbance of purified VirE2 standards in immunoblot analysis of *E. coli* extracts. The signal in lanes 1, 2, and 3 from Figure 3.7 was measured on a Molecular Dynamics densitometer interfaced with ImageQuant software. The signal obtained is plotted versus the amount of VirE2 protein loaded in each lane. This curve was used to determine the amount of VirE2 protein in the *E. coli* cell extracts (lanes 4-8 Figure 3.7).

Figure 3.9. Immunoblot analysis of protein extracts from *E. coli* with mutations in *virE2*. Purified VirE2 (lanes 1-3) or *E. coli* extracts overexpressing VirE2 were transferred to nitrocellulose and immunologically detected with antiVirE2 serum. The blot was developed using goat anti-rabbit horseradish peroxidase and an ECL chemiluminescence development kit (Amersham). A standard curve was generated from the signal emitted in lanes 1, 2, and 3. This standard curve is shown in Figure 3.10. This relationship was used to estimate the amounts of VirE2 protein in the *E. coli* extracts (lanes 4-8). Only uncleaved VirE2 protein is seen in the purified standards in lanes 1, 2, and 3. The cleaved VirE2 protein, VirE2', is seen in lane 7. The signal from both bands was used to estimate the amount of VirE2 protein in this extract. Only the cleaved product, VirE2', is seen in lanes 6 and 7.
Lane 1. 3.8 ng purified VirE2
Lane 2. 7.6 ng purified VirE2
Lane 3. 11.4 ng purified VirE2
Lane 4. 3.3 ng Mutant 5
Lane 5. 7.1 ng Mutant 8
Lane 6. 12.1 ng Mutant 8
Lane 7. 4.8 ng Mutant 4

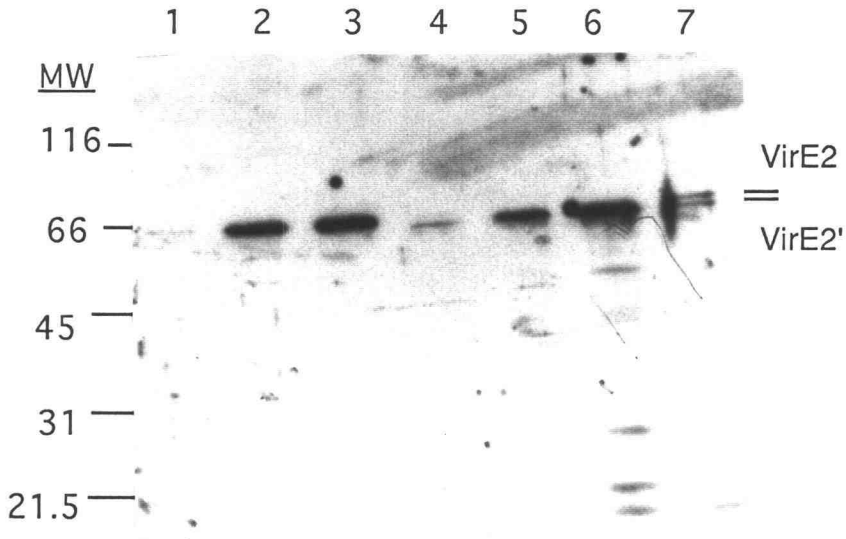

Figure 3.9

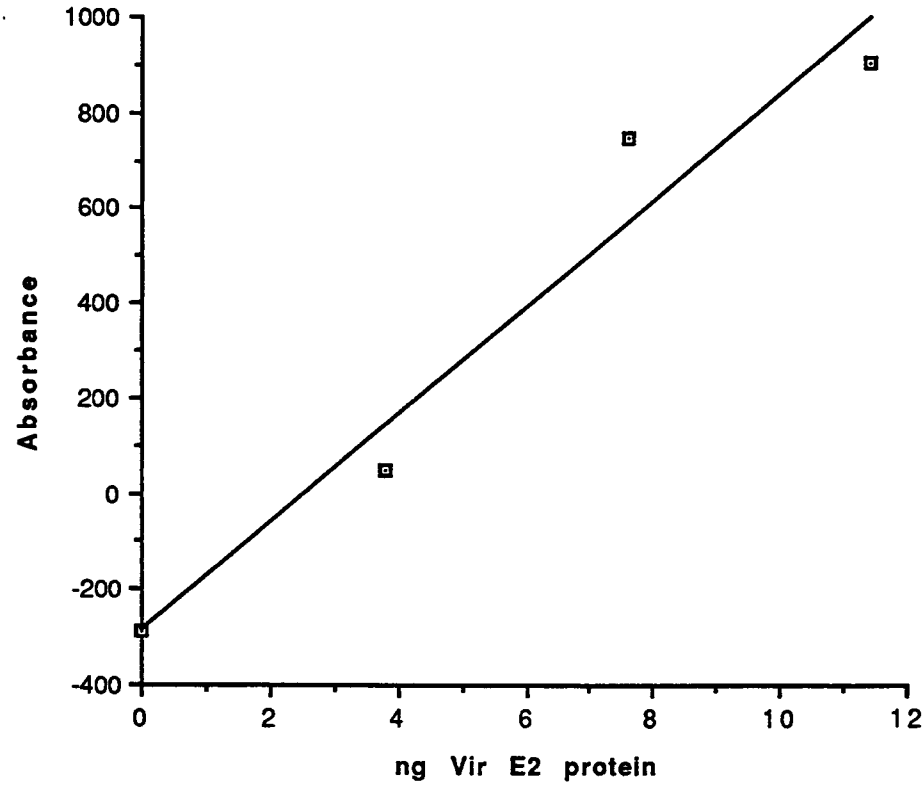

Figure 3.10. Absorbance of purified VirE2 standards in immunoblot analysis of *E. coli* extracts. The signal in lanes 1, 2, and 3 from Figure 3.9 was measured on a Molecular Dynamics densitometer interfaced with ImageQuant software. The signal obtained is plotted versus the amount of VirE2 protein loaded in each lane. This curve was used to determine the amount of VirE2 protein in the *E. coli* cell extracts (lanes 4-7 Figure 3.9).

Figure 3.11. Immunoblot analysis of protein extracts from *E. coli* with mutations in *virE2*. Purified VirE2 (lanes 1-3) or *E. coli* extracts overexpressing VirE2 were transferred to nitrocellulose and immunologically detected with antiVirE2 serum. The blot was developed using goat anti-rabbit horseradish peroxidase and an ECL chemiluminescence development kit (Amersham). A standard curve was generated from the signal emitted in lanes 1, 2, 3, and 4. This standard curve is shown in Figure 3.12. This relationship was used to estimate the amounts of VirE2 protein in the *E. coli* extracts (lanes 5-9). Only uncleaved VirE2 protein is seen in the purified standards in lanes 1, 2, 3, and 4. The cleaved VirE2 protein, VirE2', is seen in lanes 5-8. The signal from both bands was used to estimate the amount of VirE2 protein in each extract. Only uncleaved VirE2 is seen in lane 9.
Lane 1. 1.9 ng purified VirE2
Lane 2. 3.8 ng purified VirE2
Lane 3. 7.6 ng purified VirE2
Lane 4. 11.4 ng purified VirE2
Lane 5. 4.9 ng wild-type
Lane 6. 1.5 ng wild-type
Lane 7. 4.2 ng Mutant 1
Lane 8. 1.5 ng Mutant 1
Lane 9. 8.0 ng Mutant 2

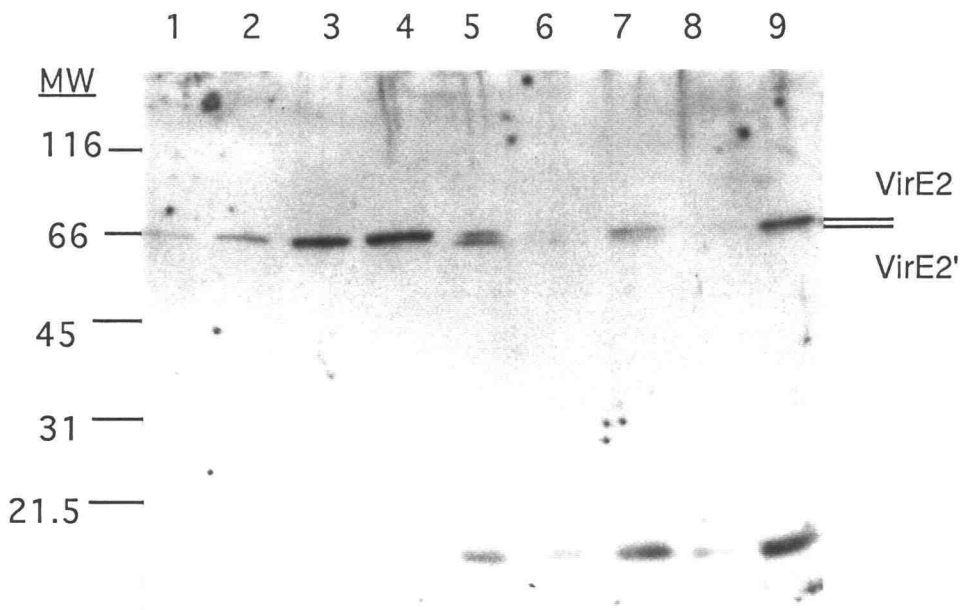

Figure 3.11

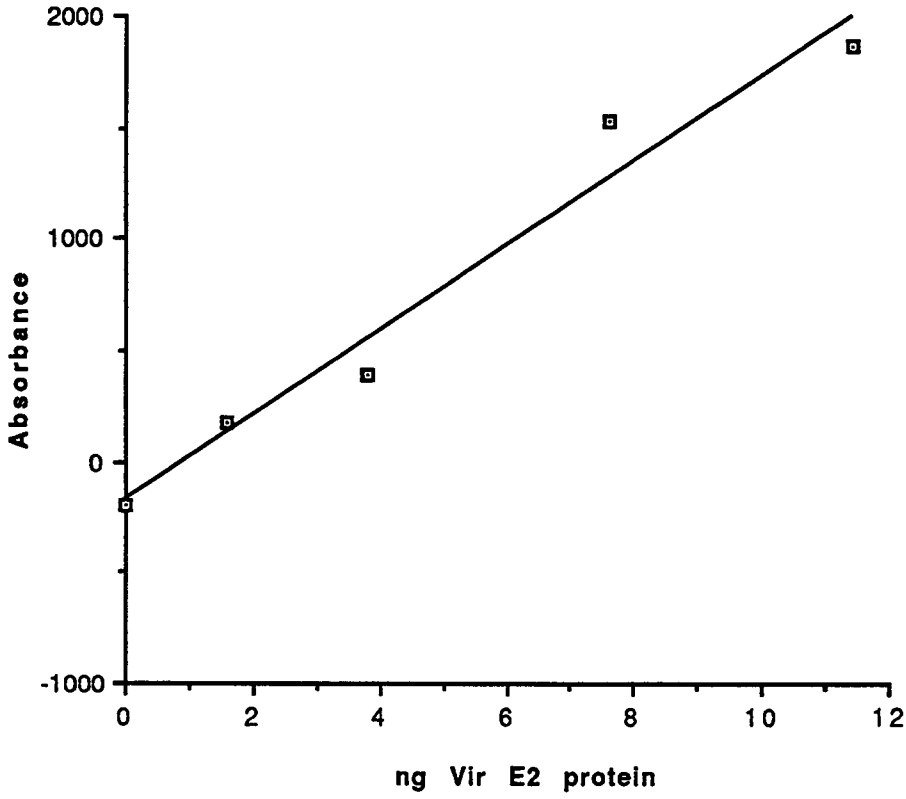

Figure 3.12. Absorbance of purified VirE2 standards in immunoblot analysis of *E. coli* extracts. The signal in lanes 1, 2, 3, and 4 from Figure 3.11 was measured on a Molecular Dynamics densitometer interfaced with ImageQuant software. The signal obtained is plotted versus the amount of VirE2 protein loaded in each lane. This curve was used to determine the amount of VirE2 protein in the *E. coli* cell extracts (lanes 5-9, Figure 3.11).

Virulence Data

Potato Inoculations

Potato discs were photographed three weeks after inoculation with *A. tumefaciens* (Figure 3.13). Disease incidence for each mutant is presented in Figure 3.14. For each mutant, the wild-type strain (WR5100) was used as a control to inoculate discs from the same potato. As depicted in Figure 3.14, five of the mutations resulted in a substantial decrease in virulence whereas four did not, determined by the number of tumors formed on the potato discs compared to wild-type. These data are summarized in Table 3.1. Insertions 1, 2, 4, 5 and 6 resulted in less than 5% of wild-type virulence (Figure 3.13). Insertions 3, 7 and 8 are similar in virulence phenotype and resulted in 37 to 47% wild-type virulence. The virulence of the deletion mutant most closely matched the virulence of the wild-type strain, with 67% wild-type virulence. A student's t-test (Langley 1971) indicated the relative virulence of each of the mutants was significantly different from wild-type ($P<0.01$).

Figure 3.13. Potato discs infected with *A. tumefaciens* mutants. Potato discs were infected with wild-type (WR5100) and mutant *A. tumefaciens* strains. After three weeks the tumors were counted using a light microscope. A)Virulence of mutant 1 (WR5101) and wild-type (WR5100) B)Virulence of mutant 2 (WR5102) and wild-type (WR5100) C)Virulence of mutant 5 (WR5105) and wild-type (WR5100) D)Virulence of mutant 3 (WR5103), wild-type (WR5100), mutant 8 (WR5108), and mutant 7 (WR5107) E)Virulence of mutant 6 (WR5106) and wild-type (WR5100) F)Virulence of wild-type (WR5100) and mutant 4 (WR5104) G)Virulence of wild-type (WR5100) and the deletion (WR5110).

A) mutant 1 wild-type

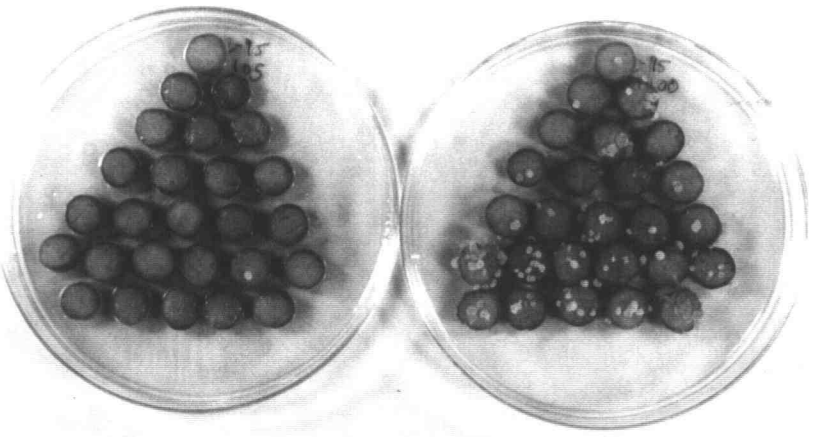

B) mutant 2 wild-type

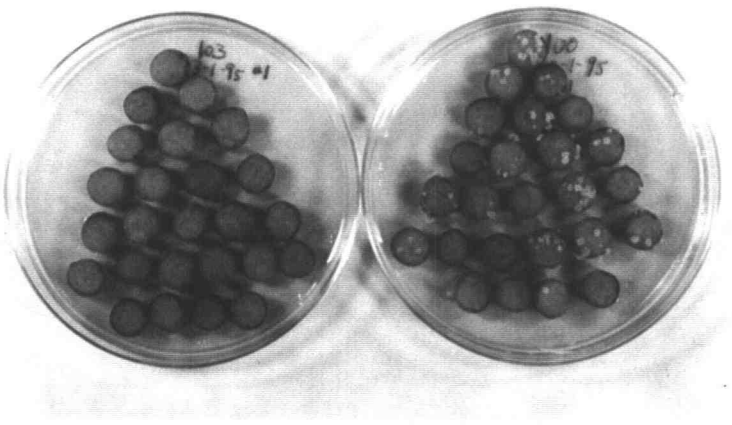

C) mutant 5 wild-type

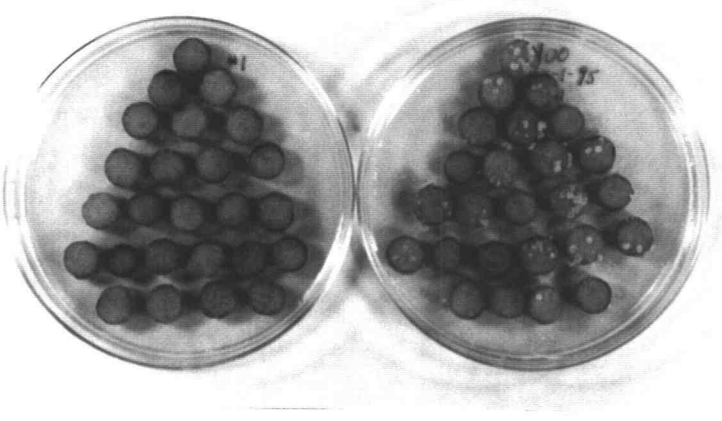

Figure 3.13

D)

mutant 3 wild-type

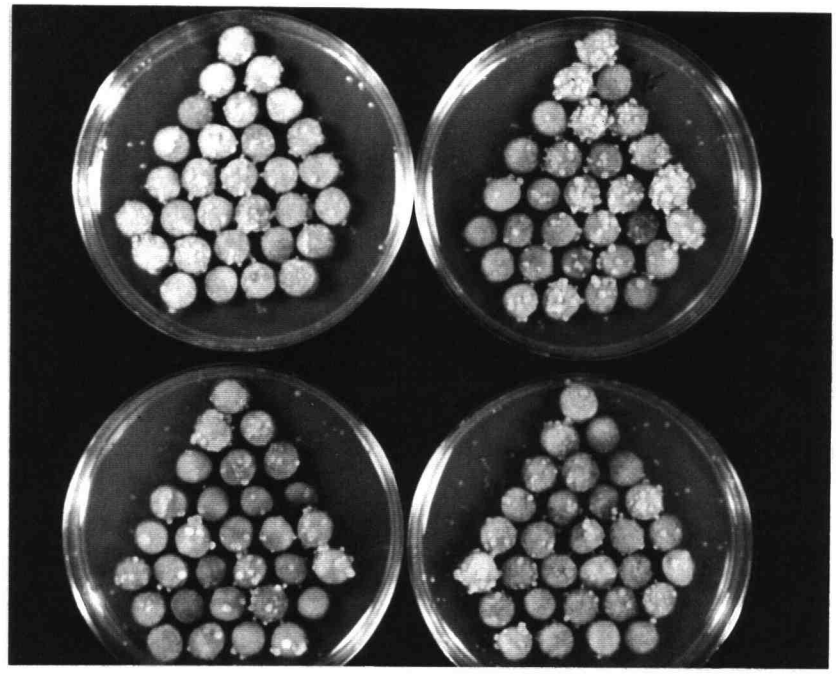

mutant 8 mutant 7

E)

mutant 6 wild-type

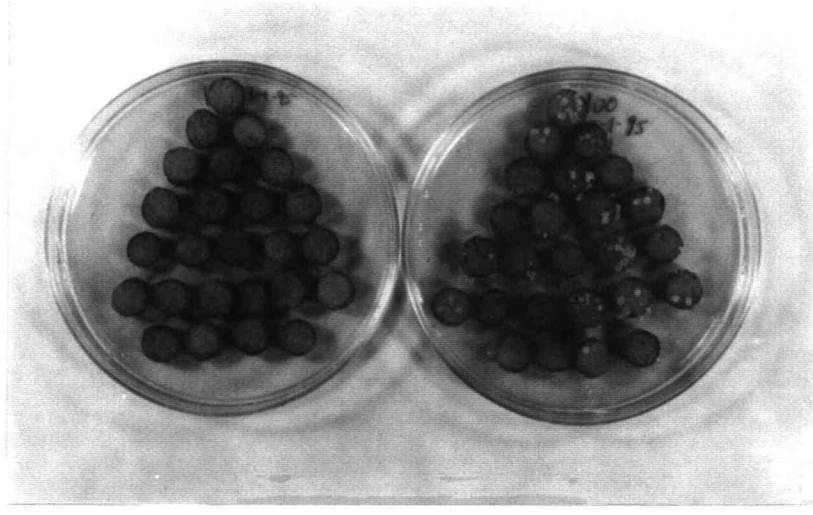

Figure 3.13 (continued)

F) wild-type (top) mutant 4 (bottom)

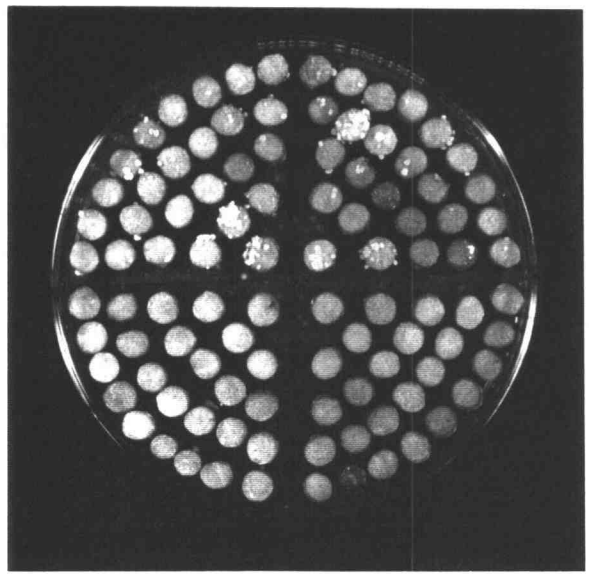

G) wild-type (top) deletion (bottom)

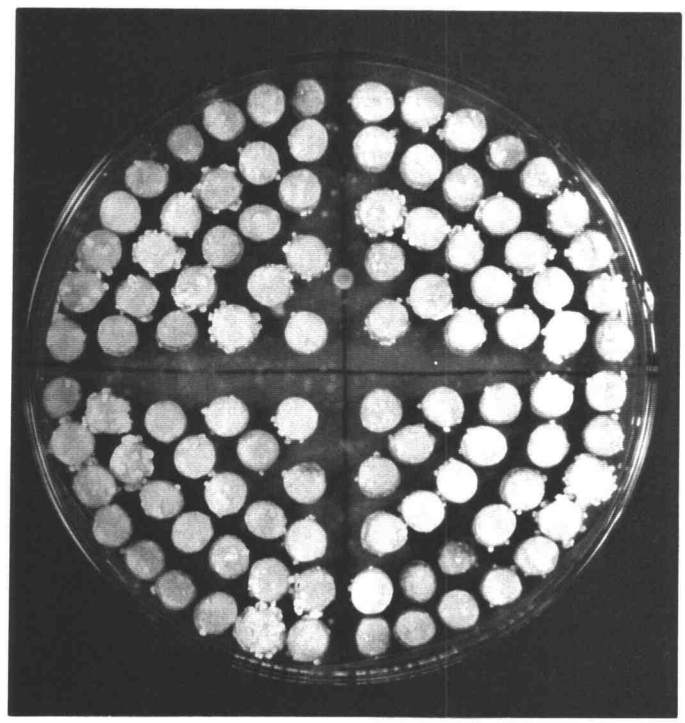

Figure 3.13 (continued)

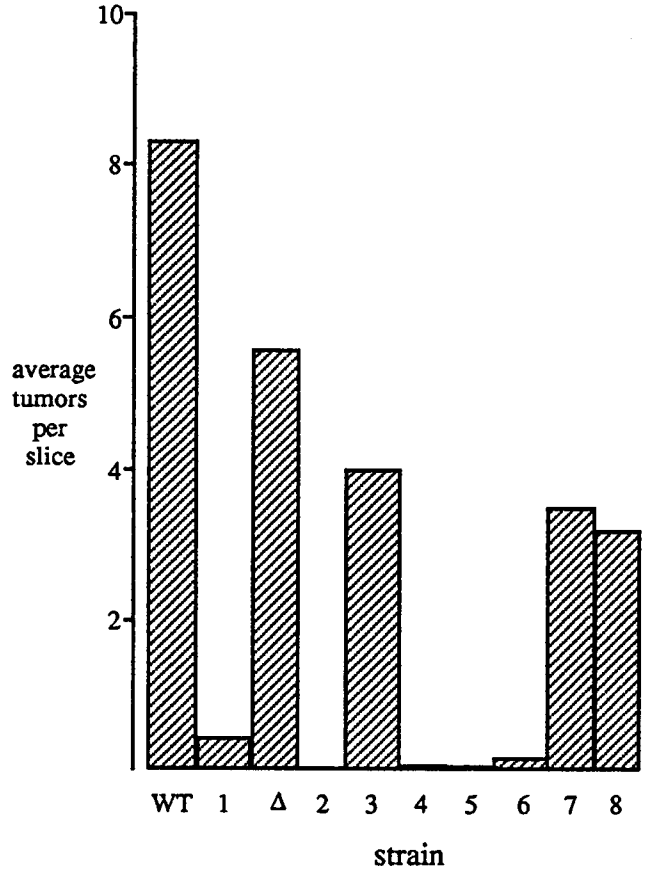

Fig. 3.14. Effect of mutations in *virE2* on the virulence of *A. tumefaciens* strains on potato discs. Potato discs were infected with *A. tumefaciens*. After three weeks, the tumors were counted using a light microscope.

Table 3.1. Virulence of strains with mutations in *virE2* on potato discs.

Strain	*virE2* allele	Disks	Average tumors per disk	Relative virulence
WR5100	+	548	8.3 ± 8.8	100
WR5101	ins. 1	125	0.37 ± 0.7	4.5
WR5102	ins. 2	123	0.02 ± 0.15	0.24
WR5103	ins. 3	174	3.9 ± 4.8	47
WR5104	ins. 4	273	0.05 ± 0.3	0.60
WR5105	ins. 5	79	0.04 ± 0.19	0.48
WR5106	ins. 6	88	0.13 ± 0.47	1.6
WR5107	ins. 7	133	3.5 ± 4.7	42
WR5108	ins. 8	140	3.1 ± 4.7	37
WR5110	del. 1	300	5.5 ± 6.7	66

Carrot Inoculations

Because a ring of tumor tissue arose at the meristem, the carrot assays yield only qualitative results, which are depicted in Figure 3.15. Carrot slices from the same carrot, infected with the wild-type strain (WR5100) are also shown for comparison. Strains with decreased virulence on the potato discs, also had reduced virulence on the carrot slices. Insertion mutants 1, 2, 4, 5, and 6 had severely reduced virulence on the carrot slices; very few or no tumors were seen. Insertion mutants 7 and 8 had reduced virulence compared to infection with the wild-type strain, while the deletion mutant and insertion mutant 3 had virulence phenotypes that were similar to wild-type.

Figure 3.15. Carrot slices infected with *A. tumefaciens* mutants. Carrot slices were infected with wild-type (WR5100) and mutant *A. tumefaciens* strains. After three weeks the tumors were scored.

A)Virulence of wild-type (WR5100) and mutant 1 (WR5101)
B)Virulence of wild-type (WR5100) and mutant 2 (WR5102)
C)Virulence of wild-type (WR5100) and mutant 3 (WR5103)
D)Virulence of wild-type (WR5100) and mutant 4 (WR5104)
E)Virulence of wild-type (WR5100) and mutant 5 (WR5105)
F)Virulence of wild-type (WR5100) and mutant 6 (WR5106)
G)Virulence of wild-type (WR5100) and mutant 7 (WR5107)
H)Virulence of wild-type (WR5100) and mutant 8 (WR5108)
I) Virulence of wild-type (WR5100) and deletion (WR5110)

A) wild-type

mutant 1

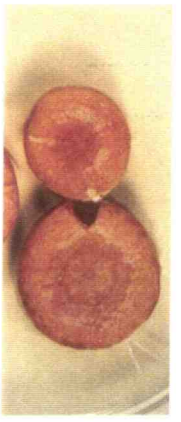

B) wild-type

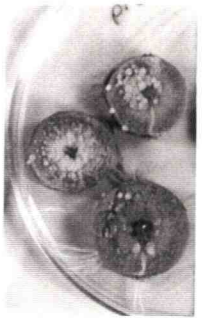

mutant 2

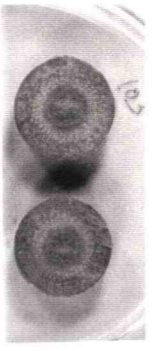

C) wild-type

mutant 3

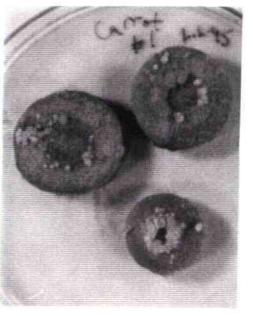

Figure 3.15

D) wild-type mutant 4

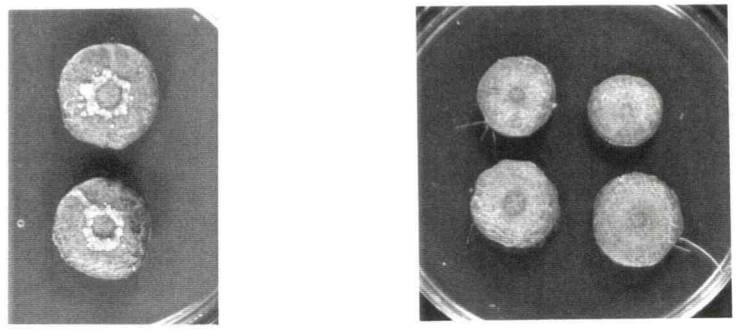

E) wild-type mutant 5

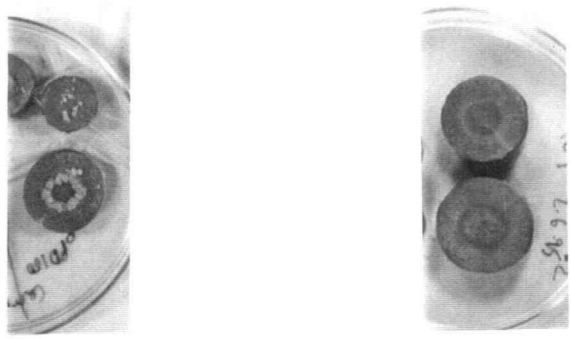

F) wild-type mutant 6

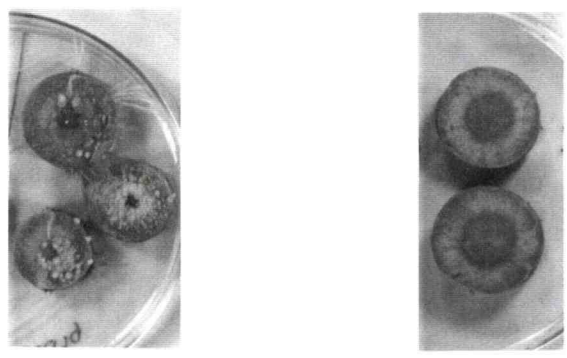

Figure 3.15 (continued)

G) wild-type mutant 7

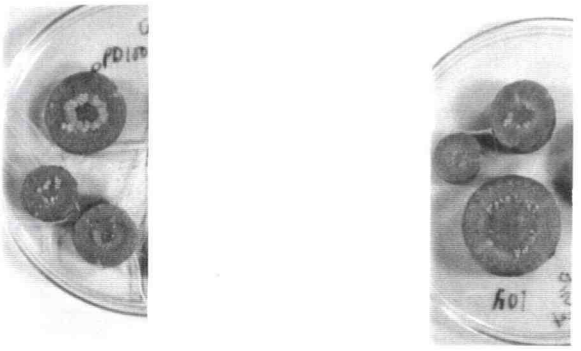

H) wild-type mutant 8

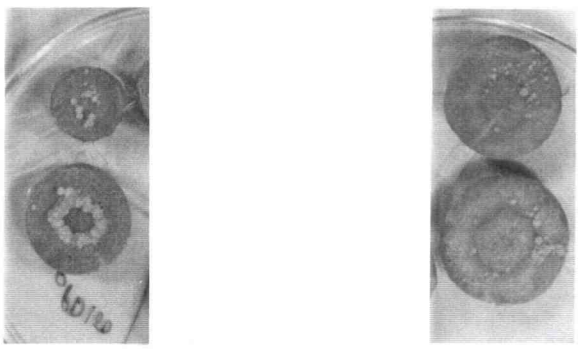

I) wild-type deletion

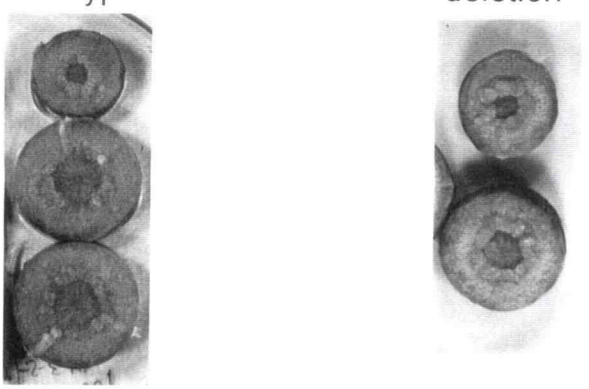

Figure 3.15 (continued)

Kalanchoe daigremontiana Inoculations

K. daigremontiana leaves were wounded, inoculated with wild-type or mutant *A. tumefaciens* strains and scored for tumors after four weeks. The positive control strains used were A348 and WR5100. Strain A348 has a wild-type Ti plasmid, whereas WR5100 has the *virE2* gene deleted from the Ti plasmid and replaced with the *neo* gene encoding kanamycin resistance. WR5100 also harbors a broad-host-range plasmid expressing a wild-type copy of *virE2*. *K. daigremontiana* leaves were also inoculated with the negative control strains WR5000 and WR3095. Strain WR3095 has both of the right border regions located next to the transferred DNA (T-DNA) regions deleted from the Ti plasmid. A wound-only uninoculated control was also included on each leaf.

Mutants 2, 5, and 6 had severely reduced virulence on *K. daigremontiana* as shown in Figure 3.16. Mutant 4 had reduced virulence and formed smaller tumors compared to wild-type. The virulence phenotype of mutant 1 was inconsistent and tumors that varied from smaller than wild-type to wild-type in size were formed. Mutants 3, 7, 8, and the deletion were fully virulent, and produced tumors similar in size to wild-type.

Figure 3.16. *Kalanchoe daigremontiana* leaves infected with *A. tumefaciens* mutants. *K. daigremontiana* leaves were wounded and infected with wild-type and mutant *A. tumefaciens* strains. Leaves were photographed after four weeks. Positive control strains included A348, with wild-type *virE2* on the Ti plasmid, and WR5100, containing a deletion of *virE2* from the Ti plasmid and a broad-host-range plasmid containing a wild-type copy of *virE2*. Negative controls included WR5000, containing a deletion of *virE2* on the Ti plasmid and WR3095, which has both of the right-border repeats of the T-DNA regions deleted from the Ti plasmid.
A) **top of leaf**: wild-type (WR5100), wild-type (A348), negative control (WR5000), negative control (WR3095), wound only
bottom of leaf: mutant 1 (WR5101), mutant 8 (WR5108), mutant 5 (WR5105), mutant 4 (WR5104), deletion (WR5110)
B) **top of leaf**: mutant 6 (WR5106), mutant 3 (WR5103), mutant 2 (WR5102), mutant 7(WR5107)
bottom of leaf: wild-type (WR5100), wild-type (A348), negative control (WR5000), negative control (WR3095), wound only

A) positive controls negative controls

WR5100 A348 WR5000 WR3095 wound only

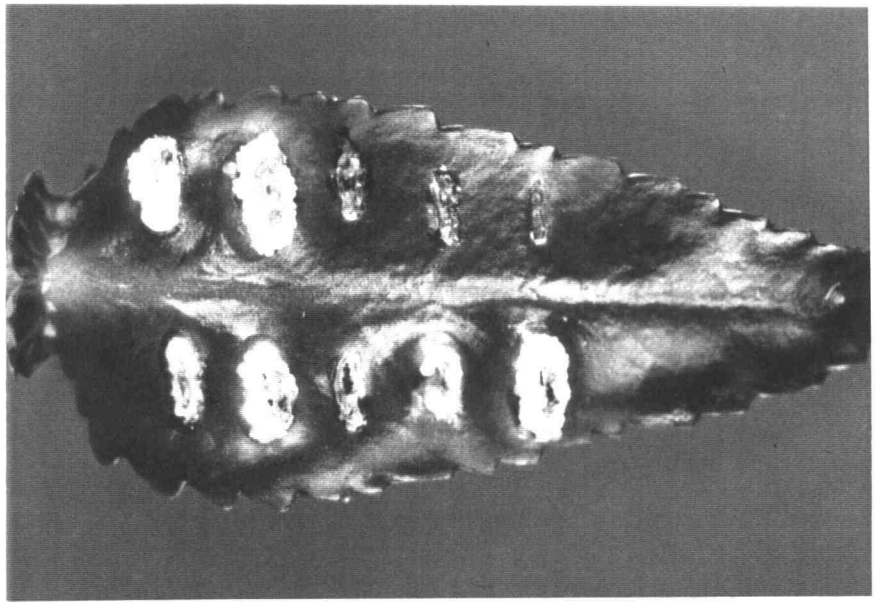

mutant 1 mutant 8 mutant 5 mutant 4 deletion

B) mutant 6 mutant 3 mutant 2 mutant 7

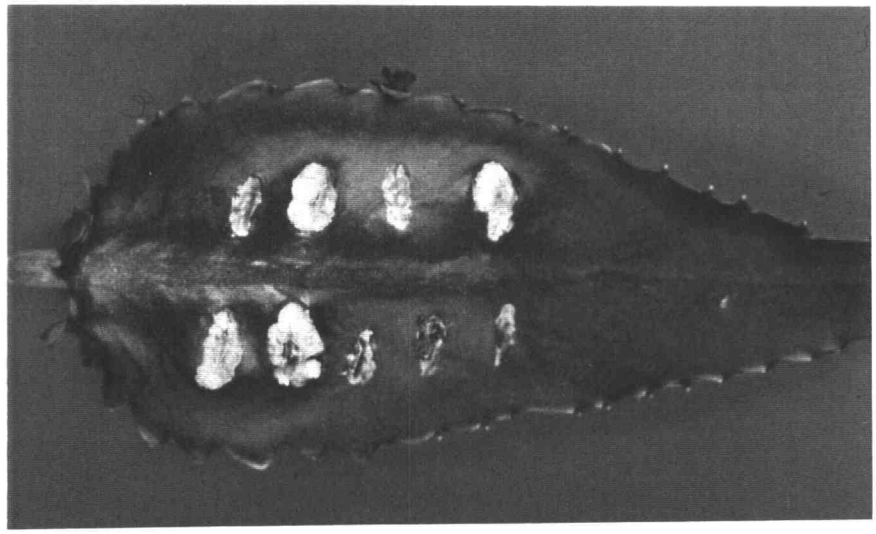

positive controls negative controls

WR5100 A348 WR5000 WR3095 wound only

Figure 3.16

Tomato Inoculations

Tomato stems were wounded and inoculated with wild-type or mutant *A. tumefaciens* strains and scored for tumors after four weeks. The stems were also infected with the negative control strains WR5000 and WR3095 for comparison. WR5000, the *virE2* null strain, formed a few tiny tumors on the tomato stems (Figure 3.17). WR5000 transformed with insertions 2, 5, and 6 were also nearly avirulent on tomato stems; their phenotypes were identical to WR5000. Insertion 4 formed tumors that were intermediate in size between tumors formed by the wild-type strains and tumors formed by WR5000. Insertions 1, 3, 7, 8, and the deletion were virulent and formed tumors that were similar in number and size to wild-type. The tumorigenesis studies are summarized in Table 3.2.

Figure 3.17. Tomato stems infected with *A. tumefaciens* mutants. Tomato stems were wounded and infected with wild-type or mutant *A. tumefaciens* strains. Positive control strains included A348, with wild-type *virE2* on the Ti plasmid and WR5100, containing a deletion of *virE2* from the Ti plasmid and a broad-host range plasmid containing a wild-type copy of *virE2*. Negative controls included WR5000, containing a deletion of *virE2* on the Ti plasmid and WR3095, which has both of the right-border repeats of the T-DNA regions deleted from the Ti plasmid.
A) **Left**-A348 (top), WR5100 (center), wound-only (bottom)
Right- WR5000 (top), WR3095 (bottom)
B) mutant 7 (WR5107), mutant 1 (WR5101), mutant 3 (WR5103)
D) mutant 6 (WR5106), mutant 3 (WR5103), mutant 2 (WR5102)
E) mutant 5 (WR5105), mutant 4 (WR5104), deletion (WR5110)

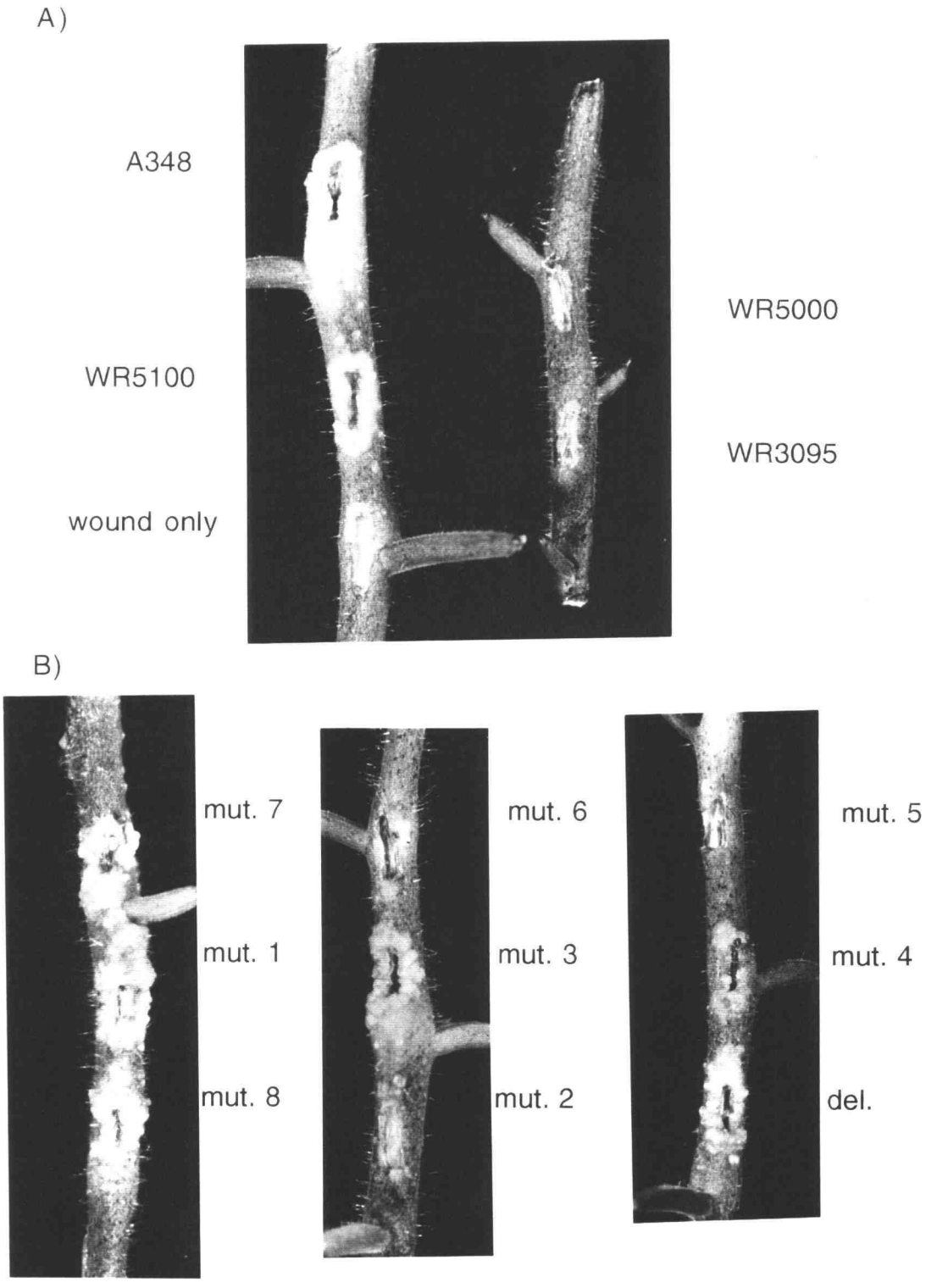
A)
A348
WR5100
wound only
WR5000
WR3095
B)
mut. 7
mut. 1
mut. 8
mut. 6
mut. 3
mut. 2
mut. 5
mut. 4
del.

Figure 3.17

Table 3.2. Virulence of strains with mutations in *virE2* on potato discs, carrot, *K. daigremontiana* and tomato.

virE2 allele	potato	carrot	*K. daigremontiana*	tomato
wild-type	100	wild-type	wild-type	wild-type
ins.1	4.5	-	variable: small to wild-type	wild-type
ins. 2	0.24	-	-	-
ins. 3	47	wild-type	wild-type	wild-type
ins. 4	0.60	-	reduced	intermed. size
ins. 5	0.48	-	-	-
ins. 6	1.6	-	-	-
ins. 7	42	+/-	wild-type	wild-type
ins. 8	37	+/-	wild-type	wild-type
del. 1	66	wild-type	wild-type	wild-type

Single-stranded DNA Binding

To locate domains important for DNA binding, we assessed the ssDNA binding activity of each mutant. *E. coli* extracts were prepared containing wild-type and mutant VirE2 proteins (see Protein methods section 2.5). These extracts were used to assay for ssDNA binding (see DNA methods section 2.3). The single-stranded DNA (ssDNA) binding data are shown in Figure 3.18. The signals were quantitated using a Molecular Dynamics phosphorimager with ImageQuant software.

To determine the percentage of probe bound, the signal that shifted to the top of the gel due to binding to VirE2 was divided by the total signal in each lane; this took into account small differences in the amount of probe loaded in each lane. To test for ssDNA binding by other proteins in the extract, labeled ssDNA was incubated with extract from a strain containing only pTrc99A; the amount of protein added, estimated by the Bradford dye-binding method (Bio-Rad) equaled the total protein in incubations containing the maximum amount of VirE2. These control extracts shifted only 3 to 6 percent of the probe to the top of the gel, indicating that the contribution by other SSB proteins was minimal. The percentage of

Figure 3.18. Single-stranded DNA binding assays of protein extracts from *E. coli* strains overexpressing mutant forms of VirE2. a) wild-type; b) mutant 1; c) mutant 2; a lane with 21 ng of mutant 1, which binds similarly to wild-type, was also included as a positive control d) mutant 3; e) mutant 4; f) deletion; e) mutants 5 and 6; a lane with 21 ng of Deletion 1, which binds similarly to wild-type, was also included as a positive control.
Lane 1. 22 ng mutant 5 VirE2
Lane 2. Protein extract from *E. coli* containing plasmid pTrc99A (vector control)
Lane 3. 22 ng mutant 6 VirE2
Lane 4. Protein extract from *E. coli* containing plasmid pTrc99A (vector control)
Lane 5. 21 ng Deletion 1

a). Wild Type

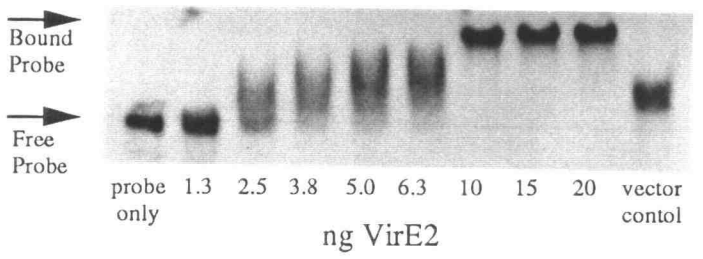

b). Mutant 1

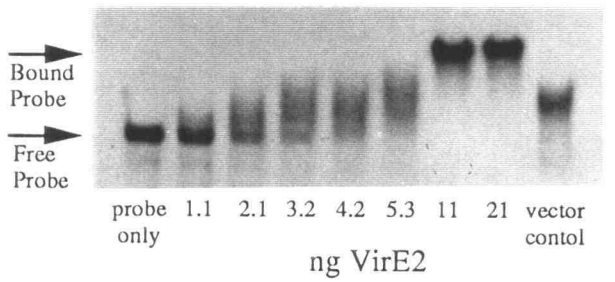

c). Mutant 2

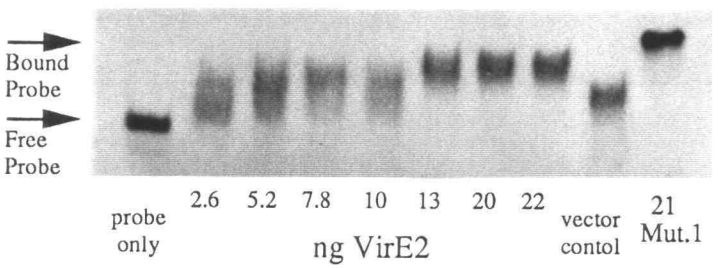

d). Mutant 3

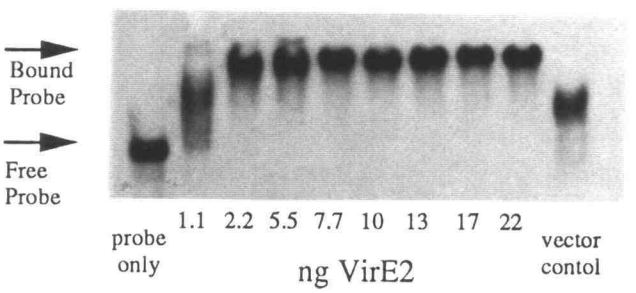

Figure 3.18

e). Mutant 4

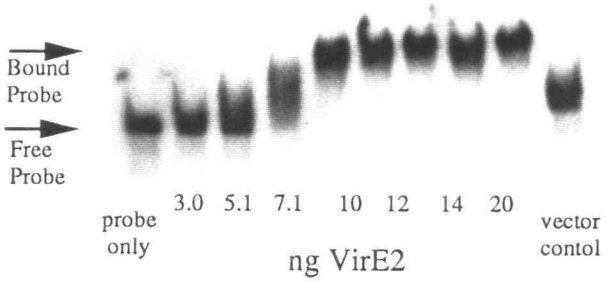

f). Deletion

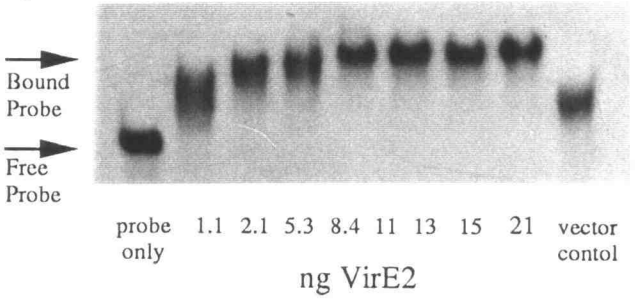

g). Mutants 5 and 6

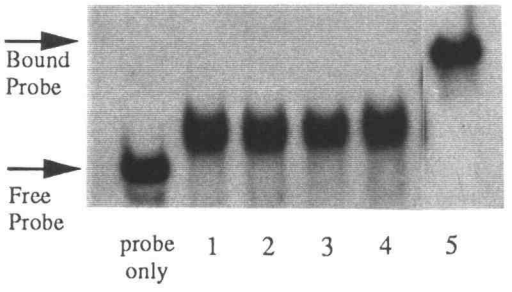

Figure 3.18 (continued)

probe shifted by the VirE2 protein in the *E. coli* cell extracts as determined using the phosphorimager, is plotted versus the amount VirE2 protein in each extract in Figure 3.19.

Insertion mutant 2 showed decreased cooperative binding; less of the probe is shifted to the bound region of the gel compared to wild-type VirE2. Mutant 3 showed increased cooperative binding, visualized as a more rapid transition from unbound to fully bound probe when compared to wild-type VirE2. Mutants one and four and the deletion mutant showed binding similar to wild-type VirE2. Mutants 5 and 6 did not bind ssDNA; neither shifted any of the probe to the top of the gel.

Accumulation of VirE2 in *A. tumefaciens*

The accumulation of mutant VirE2 proteins produced in *A. tumefaciens* was determined by immunoblot analysis of *A. tumefaciens* cell extracts and compared with the accumulation of wild-type VirE2 protein (Figure 3.20). Mutant proteins 1, 2, 5 and 6 did not accumulate VirE2 to wild-type levels in *A. tumefaciens*. Insertion mutants 3, 4, 7, 8 and the deletion mutant accumulated VirE2 to levels similar to wild-type.

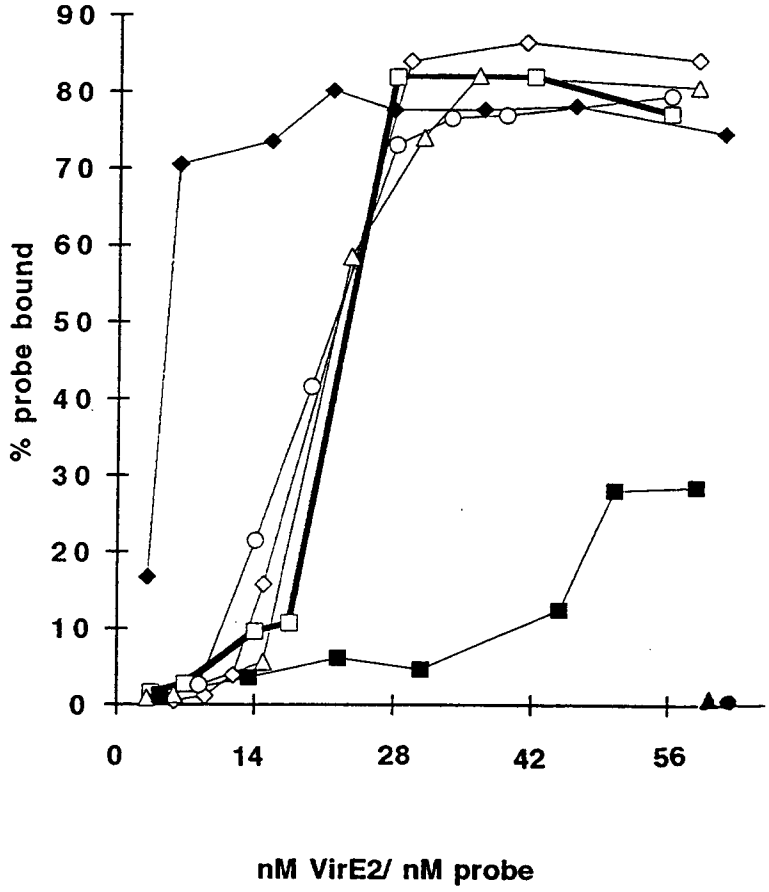

Figure 3.19. Single-stranded DNA binding affinities of wild-type and mutant VirE2 proteins. wild-type ⊡ mutant 1 ◇ deletion △ mutant 2 ■ mutant 3 ◆ mutant 4 ○ mutant 5 ▲ mutant 6 ● Mutant 2 shows decreased cooperative DNA binding compared to wild-type. Mutant 3 shows increased cooperative DNA binding compared to wild-type.

Figure 3.20. Immunoblots of protein extracts from *A. tumefaciens* strains with mutations in *virE2*, without(-) and with(+) *vir* gene induction by acetosyringone. a) wild-type (WR5100), mutant 1 (WR5101), mutant 2 (WR5102), mutant 3 (WR5103), mutant 4 (WR5104); b) wild-type (WR5100), mutant 5 (WR5105), mutant 6 (WR5106), mutant 7 (WR5107), mutant 8 (WR5108); c) wild-type (WR5100), deletion 1 (WR5110).
a.s. = acetosyringone

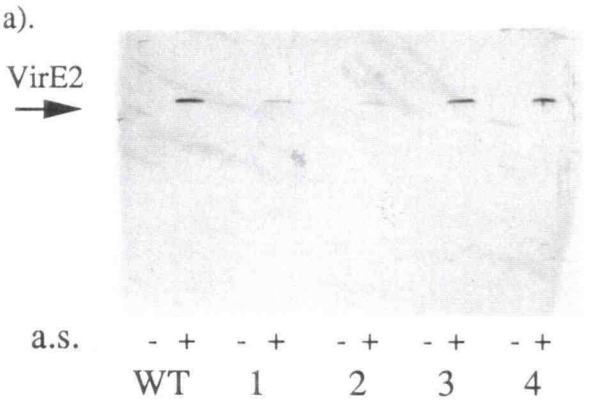

Figure 3.20

Summary of Mutant Phenotypes

Abolition of Single-stranded DNA Binding and Virulence

Insertion mutations 5 and 6, which lie in the C-terminal half of VirE2 (Figure 3.1), eliminated single-stranded DNA binding (Figures 3.18 and 3.19) and severely reduced tumorigenesis on potato discs (Table 3.1, Figures 3.13 and 3.14). Both mutants also severely reduced virulence on *K. daigremontiana* leaves (Figure 3.16), tomato (Figure 3.17), and carrot (Figure 3.15). These insertions also prevent the accumulation of VirE2 to wild-type levels in *A. tumefaciens* (Figure 3.20).

Changes in Cooperativity

Insertions 2 and 3, located in the N-terminal half of VirE2 (Figure 3.1), influenced the cooperative binding of VirE2 to ssDNA. Insertion 2 decreased the ability of VirE2 to bind cooperatively; less of the probe was shifted to the bound region of the gel when compared to wild-type VirE2 (Figure 3.18).

This decreased the sigmoidal nature of the ssDNA binding curve (Figure 3.19). Insertion 2 also reduced VirE2 accumulation in *A. tumefaciens* (Figure 3.20) and nearly abolished tumorigenesis on all plants tested. Therefore, the severe decrease in tumorigenesis may be attributed to the instability of VirE2 with this insertion in *A. tumefaciens*. Insertion 3 increased cooperative ssDNA binding, causing an extremely rapid transition from unbound probe to fully-shifted probe (Figures 3.18 and 3.19). This mutation decreased tumorigenesis on potato discs by half compared to wild-type VirE2 (Table 3.1, Figures 3.13 and 3.14). A students t-test (Langley 1971) indicated that this difference was significant ($P<0.01$). However, this strain appeared fully virulent on *K. daigremontiana* (Figure 3.16), tomato (Figure 3.17), and carrot (Figure 3.15). Insertion 3 did not decrease the accumulation of VirE2 protein in *A. tumefaciens* cells (Figure 3.20).

Wild-type Single-stranded DNA Binding and Virulence

A deletion of ten amino acids from the N-terminus of VirE2 (Figure 3.1) had little effect on its ability to bind ssDNA (Figures 3.18 and 3.19) or on tumorigenesis on potato discs (Table 3.1,

Figures 3.13 and 3.14). This mutant was fully virulent on *K. daigremontiana* (Figure 3.16), carrot (Figure 3.15), and tomato (Figure 3.17); this mutant VirE2 protein was stable in *A. tumefaciens* (Figure 3.20).

Wild-type Single-stranded DNA Binding and Decreased Virulence

Insertion 1 (in the N-terminal half of VirE2) and insertion 4 (in the central region of VirE2) significantly reduced tumorigenesis without affecting its ability to bind ssDNA (Figures 3.18 and 3.19). The virulence of insertion mutant 1 was severely decreased on potato discs (4.4% of wild-type, Table 3.1, Figure 3.14) and carrot (Figure 3.15). Insertion 1 was tumorigenic on tomato (Figure 3.17) and had variable virulence on *K. daigremontiana* (Figure 3.16), forming small- to normal-sized tumors. Insertion 1 decreased the accumulation of VirE2 in *A. tumefaciens* cells (Figure 3.20), which probably accounts for the reduction in tumorigenesis caused by this mutation. Insertion mutant 4 decreased virulence on potato discs to less than 4) and also severely reduced virulence on carrot slices (Figure 3.15). Mutant 4 formed fewer tumors on tomato (Figure 3.17)

and smaller tumors on *K. daigremontiana* (Figure 3.16) compared to wild-type *A. tumefaciens,* and this mutant VirE2 protein was stable in *A. tumefaciens* (Figure 3.20), indicating that this mutation affects another property of VirE2 other than ssDNA binding or VirE2 accumulation in *A. tumefaciens.*

C-terminal Insertions

Insertions 7 and 8 destabilized VirE2 in *E. coli*, which prevented an accurate estimate of their binding to ssDNA. Both mutations lie near the C-terminus of VirE2 (Figure 3.1), and each slightly reduced tumorigenesis, to about 40% of wild-type, on potato discs (Table 3.1, Figures 3.13 and 3.14), and these mutations also reduced virulence on carrot (Figure 3.15). Both strains exhibited full virulence on *K. daigremontiana* (Figure 3.16) and tomato (Figure 3.17). VirE2 protein with either insertion accumulated to wild-type levels in *A. tumefaciens* cells (Figure 3.20).

Summary

A genetic map of the mutations in *virE2* with a summary of the results tabulated beneath each mutation is presented in Figure 3.21. Insertions 5 and 6 did not bind to ssDNA. Insertions 2 and 3 influenced cooperative binding to ssDNA. Insertions 1, 4 and the deletion mutant all bound to ssDNA similarly to wild-type VirE2 protein. However, insertions 1 and 4 decreased virulence on the host plants. Insertion 1 destabilized VirE2 in *A. tumefaciens*, and probably as a result, its virulence is decreased.

Figure 3.21. Map of mutations in *virE2* with summary of results. NLS=nuclear localization signal, NLS 1= ^{205}-KLR PED RYV QTE RYG RR-^{226} NLS 2= ^{273}-KRR YGG ETE IKL KSK-^{287} The basic amino acids in the nuclear localization sequences are underlined. Δ =the deletion of residues 56-65 (SSSLY SGSEH) from *virE2* ; L=leucine; E=glutamic acid; S=serine; R=arginine; D=aspartic acid; A=alanine; P=proline; Y=tyrosine; V=valine; Q=glutamine; T=threonine; G=glycine; K=lysine. Insertion 1=LE; Insertion 2=SS; Insertion 3=SR; Insertion 4=LE; Insertion 5=SS; Insertion 6=the replacement of residue 472, a tyrosine by a serine and the insertion of an arginine and aspartic acid after residue 472; Insertion 7=RA; Insertion 8=SR. Binding: ng of wild-type or mutant VirE2 needed to bind 50% of the ssDNA probe fully. ND=not determined. Virulence: percentage of wild-type virulence on potato discs. Stability: accumulation of wild-type or mutant VirE2 in acetosyringone-induced *A. tumefaciens* cells.

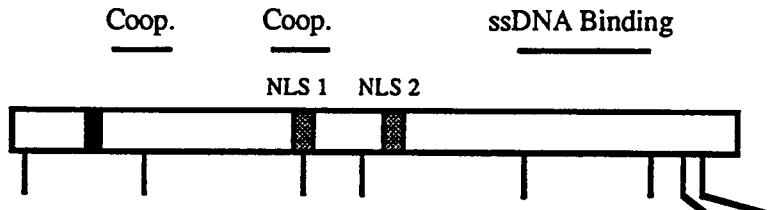

insertions:	1 LE	Δ	2 SS	3 SR	4 LE	5 SS	6 SRD	7 RA	8 SR	wild type
binding: (ng/50%)	8	8	>22	2	8	no binding	no binding	ND	ND	8
virulence: (% WT)	4.5	66	0.2	47	0.6	0.5	1.6	42	37	100
stability: (in Agro.)	-	+	-	+	+	-	-	+	+	+

Figure 3.21

CHAPTER 4. DISCUSSION

Introduction to the Chou and Fasman Method of Secondary Structure Prediction

One goal of this research was to identify domains required for ssDNNA binding and cooperativity using insertional mutagenesis. The changes in VirE2 protein structure as a result of this mutagenesis were predicted using the method of Chou and Fasman (1978). The prediction of protein secondary and tertiary structure can be determined only by high resolution X-ray crystallography or nuclear magnetic resonance (NMR). Over twenty methods have been proposed to predict secondary structure based on the assumption that the amino acid sequence of a short region determines its local structure (Branden and Tooze 1991).

An accepted method of predicting secondary structure is that of Chou and Fasman (Branden and Tooze 1991). Their research involved the statistical analysis of 15 proteins with known X-ray structure, establishing alpha helix and beta sheet conformation potentials for all 20 amino acids (Chou and Fasman 1973). Short

regular turns were also predicted. The preferences for different amino acids at the first, second, third and fourth position of a bend are also taken into account (Branden and Tooze 1991).

In a Chou-Fasman prediction the amino acid sequence is first analyzed for the formation of alpha helices and beta sheets which are extended at both ends until a residue occurs with a high probability of turns or a low probability of both alpha helix and beta strand formation (Branden and Tooze 1991).

Often protein regions contain residues with a high probability of both alpha helix and beta strand formation, therefore the following rules are useful (Branden and Tooze 1991). One, alpha helices usually contain a greater number of residues than beta strands and there is almost always a turn between regions of alpha helix and beta sheet. Two, there is also a high probability that when there are one or two alpha helices among many beta strands that they all should be beta strands.

The Chou and Fasman method had an overall accuracy of 50% based upon the analysis of a large number of X-ray structures consisting of over 10,000 residues (Branden and Tooze 1991). Many of the errors occurred at the ends of alpha helices and beta sheets,

whereas their central regions were correctly predicted, and some errors occurred because of the difficulty in differentiating between helix and strand.

The secondary structure predictions were generated by the program, MacVector, using the Chou-Fasman method of secondary structure prediction.

Insertions 5 and 6 Identified a Single-stranded DNA Binding Domain

VirE2 has two nuclear localization sequences (NLSs) (Figure 4.1, Citovsky *et al.* 1992), and conversion of two lysine residues to glycine in the C-terminal NLS decreases the efficiency of nuclear localization and abolishes ssDNA binding (Citovsky *et al.* 1994). Insertions 5 and 6, in the C-terminal half of VirE2, also eliminated ssDNA binding.

This suggests that the ssDNA binding domain may extend from the lysine residues of this NLS (residues 285 and 287) through insertion 5 (after residue 378) and to insertion 6 (after residue 471, Figure 4.1). The secondary structure of this DNA binding region

Figure 4.1. Secondary Structure Prediction of VirE2. VirE2 is shown schematically above the secondary structure prediction. NLS=nuclear localization signal, NLS 1= ^{205}-KLR PED RYV QTE RYG RR-^{226} NLS 2= ^{273}-KRR YGG ETE IKL KSK-^{287} The basic amino acids in the nuclear localization sequences are underlined. Δ =the deletion of residues 56-65 (SSSLY SGSEH) from *virE2* Numbers 1-8 indicate positions of linker insertions. The boxes indicate: top - alpha helix, middle - beta strand, bottom - turn (by the method of Chou and Fasman 1978).

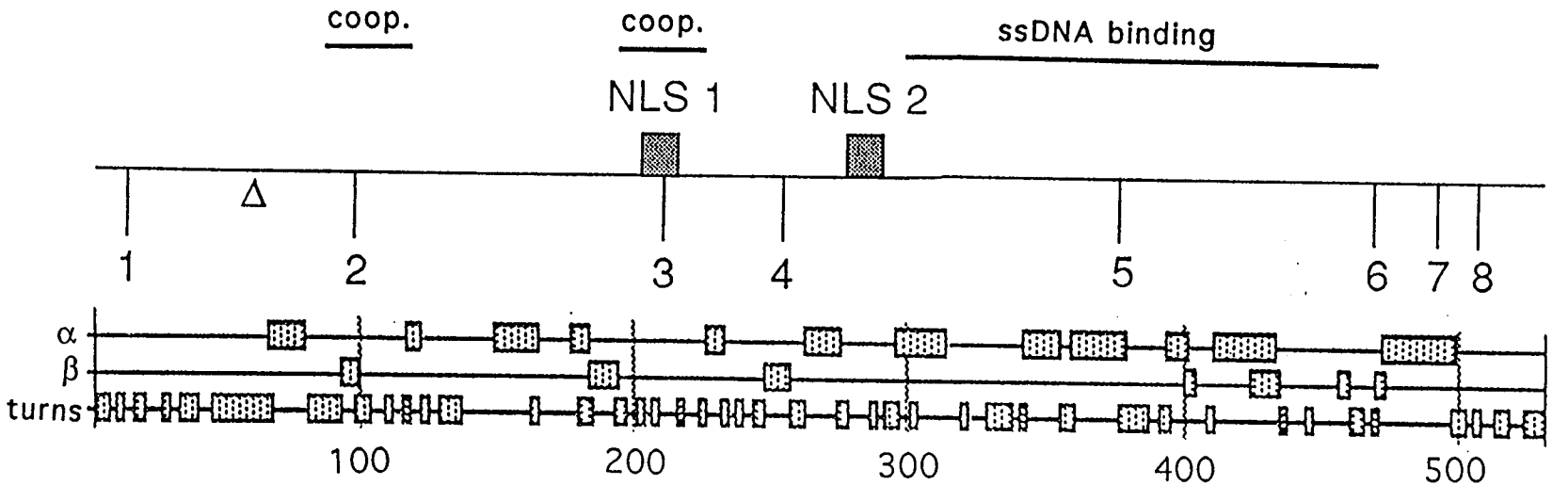
coop.
coop.
ssDNA binding
NLS 1
NLS 2
Δ
1
2
3
4
5
6
7
8
α
β
turns
100
200
300
400
500

Figure 4.1

(from residues 285 through 471) is predicted to be primarily alpha helix and turn (Figure 4.1). Insertion 5 inserts two serines which slightly extends a predicted alpha helix (Figure 4.2). Presumably, this change in secondary structure brought about by the insertion most likely perturbs a region of VirE2 critical for DNA binding.

Insertion 6 similarly results in localized changes of predicted secondary structure (Figure 4.3). This insertion adds arginine and aspartic acid after residue 472, which is changed from a tyrosine to a serine. Thus, this linker insertion adds two charged amino acids, one basic and one acidic. Tyrosine and serine are both polar amino acids, although tyrosine is also an aromatic residue and therefore may interact with the DNA bases during binding (Prasad and Chiu 1987).

Insertion 6 also extends a putative region of turn that begins near amino acid 460 and continues for about 7 amino acids, eliminating a region of beta strand and extending a region of turn. This change may also occur in, or near the ssDNA binding domain, since this mutation completely eliminates binding to ssDNA. Conversion of the two lysine residues to glycines (in the NLS, Citovsky et al. 1994) also results in only localized changes in

Figure 4.2. Secondary Structure Prediction of VirE2 Mutated by Linker Insertion 5. A) wild-type VirE2, B) insertion 5, two serines were inserted after residue. The boxes indicate: top - alpha helix, middle - beta strand, bottom - turn.

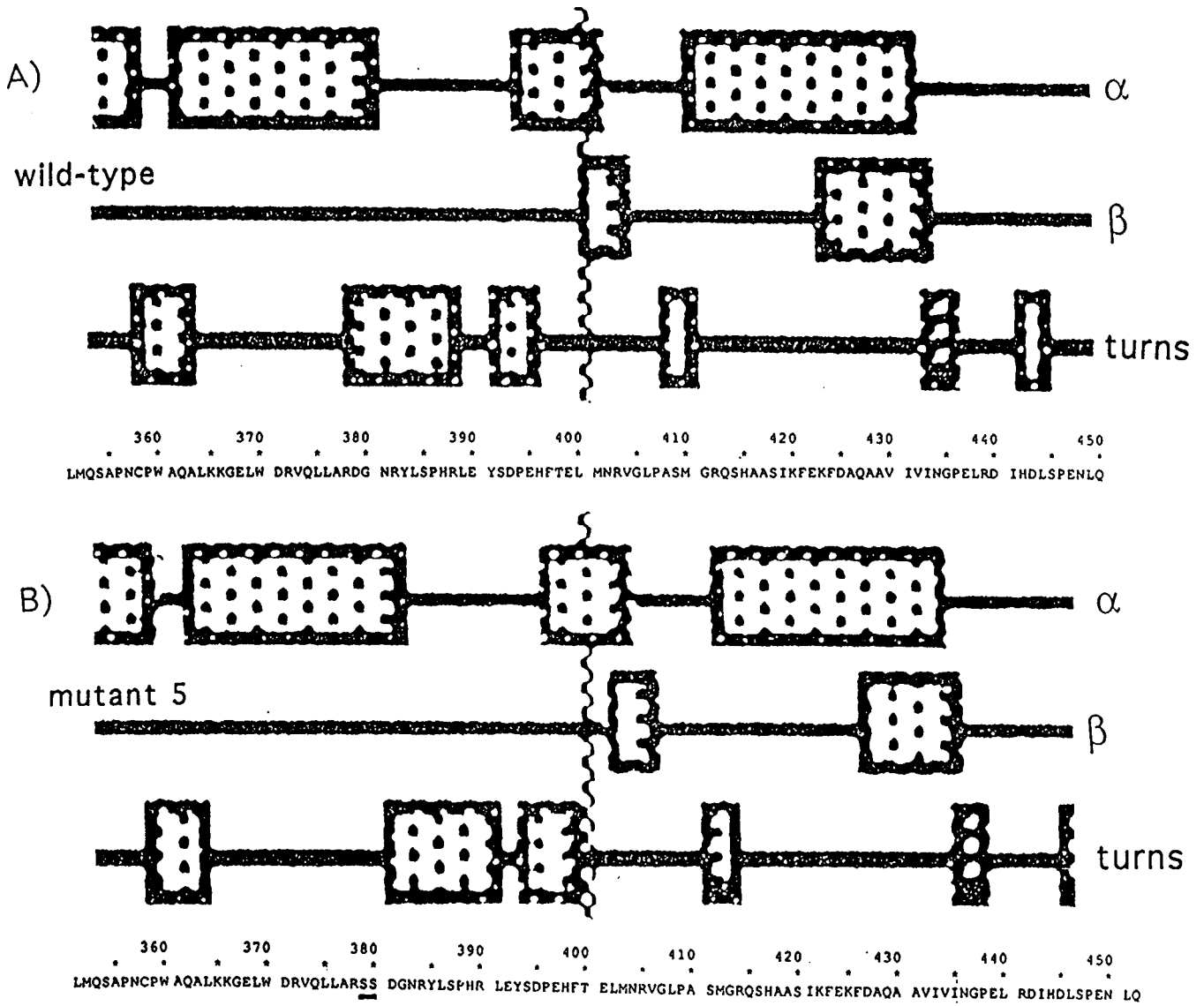
A)
wild-type
α
β
turns
360 370 380 390 400 410 420 430 440 450
LMQSAPNCPW AQALKKGELW DRVQLLARDG NRYLSPHRLE YSDPEHFTEL MNRVGLPASM GRQSHAASIKFEKFDAQAAV IVINGPELRD IHDLSPENLQ
B)
mutant 5
α
β
turns
360 370 380 390 400 410 420 430 440 450
LMQSAPNCPW AQALKKGELW DRVQLLARSS DGNRYLSPHR LEYSDPEHFT ELMNRVGLPA SMGRQSHAAS IKFEKFDAQA AVIVINGPEL RDIHDLSPEN LQ

Figure 4.2

Figure 4.3. Secondary Structure Prediction of VirE2 Mutated by Linker Insertion 6. A) wild-type VirE2, B) insertion 6, an arginine and an aspartic acid were inserted after residue 472, residue 472 was also changed from a tyrosine to a serine. The boxes indicate: top - alpha helix, middle - beta strand, bottom - turn.

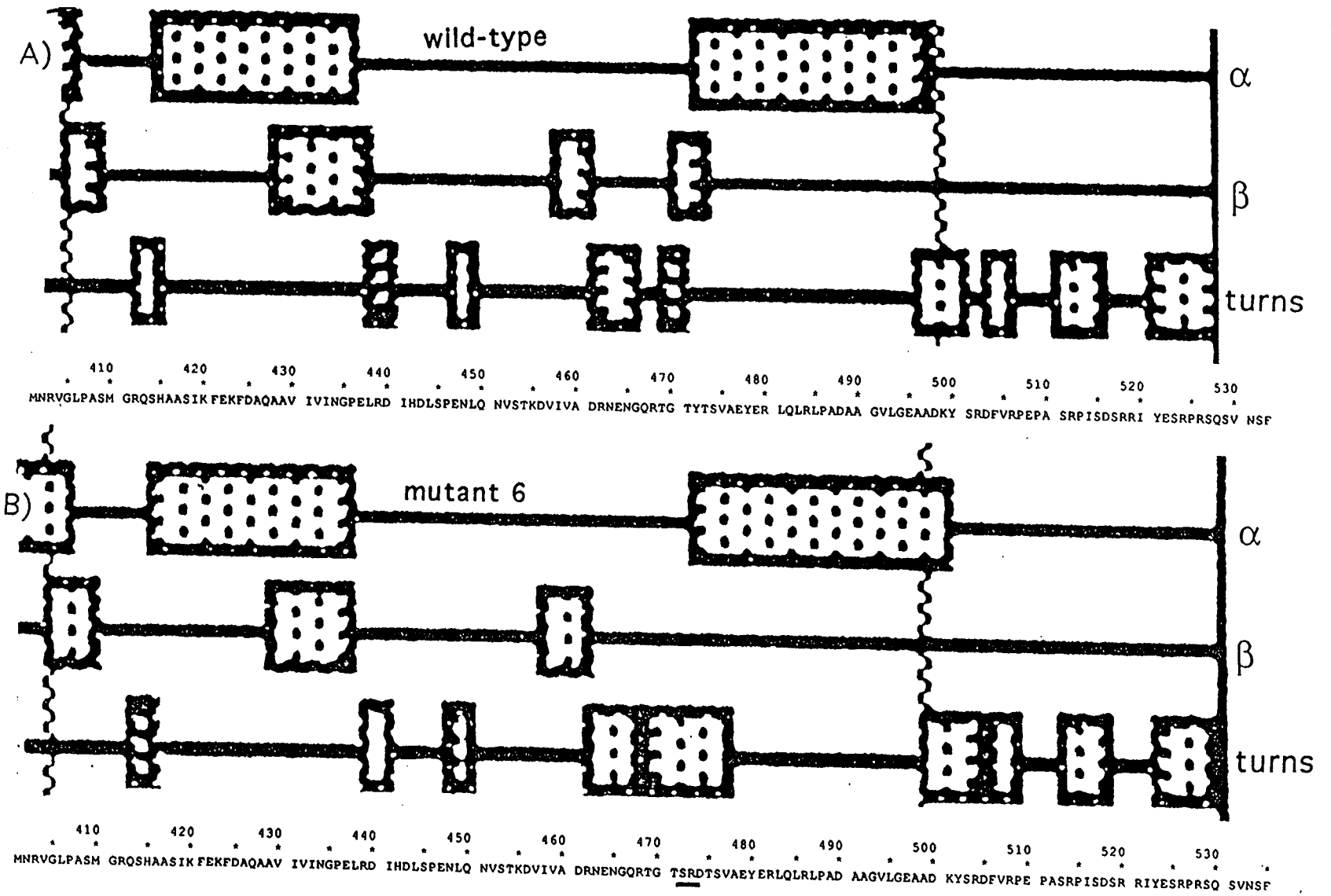
A)
wild-type
α
β
turns
410 420 430 440 450 460 470 480 490 500 510 520 530
MNRVGLPASM GRQSHAASIK FEKFDAQAAV IVINGPELRD IHDLSPENLQ NVSTKDVIVA DRNENGQRTG TYTSVAEYER LQLRLPADAA GVLGEAADKY SRDFVRPEPA SRPISDSRRI YESRPRSQSV NSF
B)
mutant 6
α
β
turns
410 420 430 440 450 460 470 480 490 500 510 520 530
MNRVGLPASM GRQSHAASIK FEKFDAQAAV IVINGPELRD IHDLSPENLQ NVSTKDVIVA DRNENGQRTG TSRDTSVAEY ERLQLRLPAD AAGVLGEAAD KYSRDFVRPE PASRPISDSR RIYESRPRSQ SVNSF

Figure 4.3

predicted secondary structure (Figure 4.4). Therefore, these three mutations are likely to define the ssDNA binding domains of VirE2.

Insertions 2 and 3 Result in Changes in Cooperative DNA Binding

Insertion 2 decreased the stability of VirE2 in *A. tumefaciens*, almost abolished tumorigenesis, and decreased cooperative DNA binding to ssDNA. Because this mutation decreased the stability of VirE2 in *A. tumefaciens*, the influence of decreased cooperativity on tumorigenesis could not be determined. To determine whether tumorigenesis depends upon cooperative ssDNA binding by VirE2, a mutation that specifically eliminates cooperativity without destabilizing the protein or affecting NLS activity should be constructed and analyzed.

In this mutant VirE2, two serine residues were inserted after residue 94, extending a putative turn region that begins near residue 80 (Figure 4.5). It is unlikely that this localized change disrupts the overall protein conformation. However, the mutant protein was destabilized in *A. tumefaciens*, possibly by increased susceptibility to proteases, or by decreased protein-protein

Figure 4.4. Secondary Structure Prediction of VirE2 Mutated by Changing Residues 285 and 287 from Lysines to Glycines.

A) Wild-type VirE2, B) VirE2 with residues 285 and 287 changed from leucines to glycines (Citovsky *et al.* 1994), these residues are part of one of the nuclear localization signals. The boxes indicate: top - alpha helix, middle - beta strand, bottom - turn.

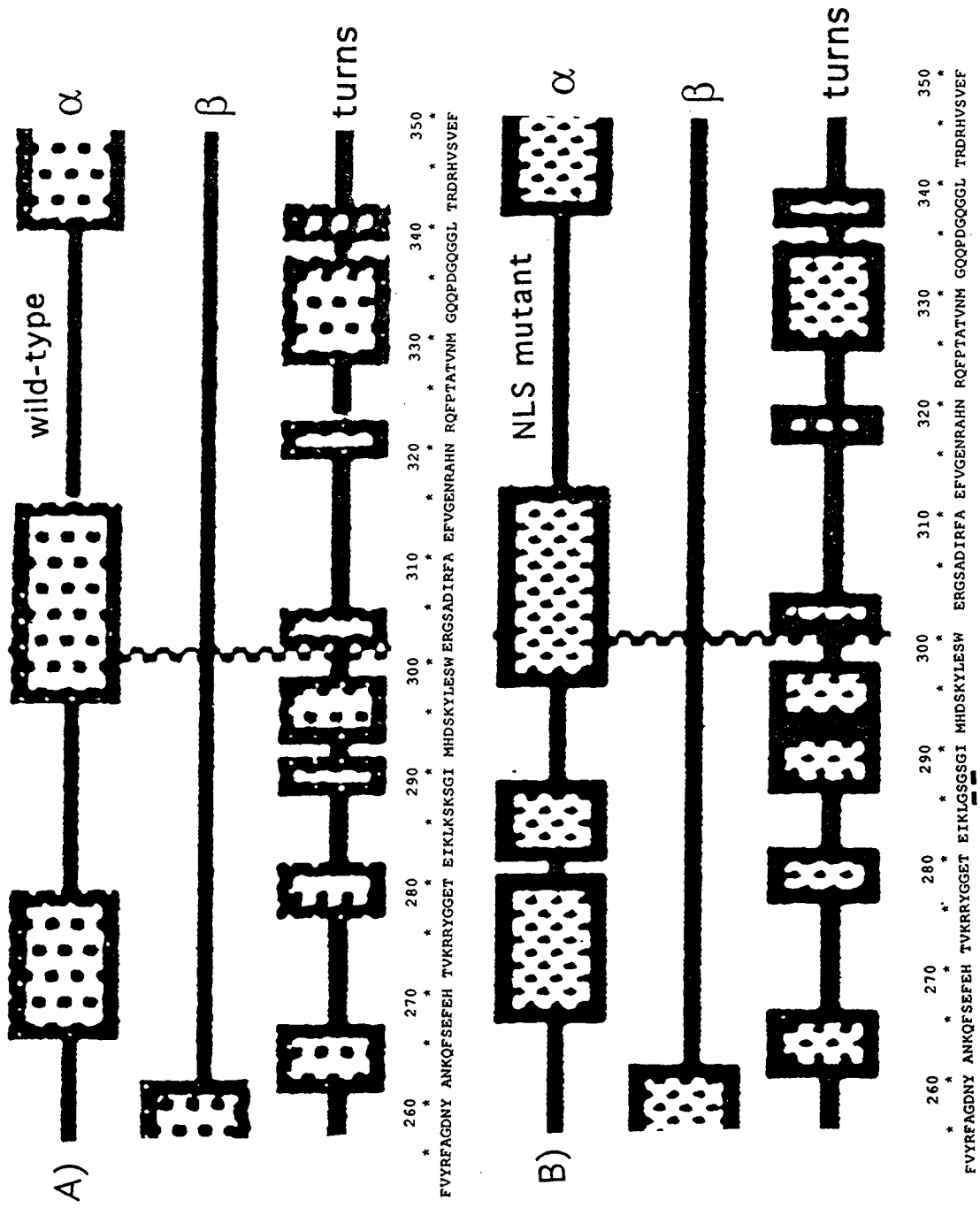
A)
wild-type
α
β
turns
260 270 280 290 300 310 320 330 340 350
FVYRFAGDNY ANKQFSEFEH TVKRRYGGET EIKLKSKSGI MHDSKYLESW ERGSADIRFA EFVGENRAHN RQFPTATVNM GQQPDGQGGL TRDRHVSVEF
B)
NLS mutant
α
β
turns
260 270 280 290 300 310 320 330 340 350
FVYRFAGDNY ANKQFSEFEH TVKRRYGGET EIKLGSGSGI MHDSKYLESW ERGSADIRFA EFVGENRAHN RQFPTATVNM GQQPDGQGGL TRDRHVSVEF

Figure 4.4

Figure 4.5. Secondary Structure Prediction of VirE2 Mutated by Linker Insertion 2. A) wild-type, B) insertion 2, two serines were inserted after residue 94. The boxes indicate: top - alpha helix, middle - beta strand, bottom - turn.

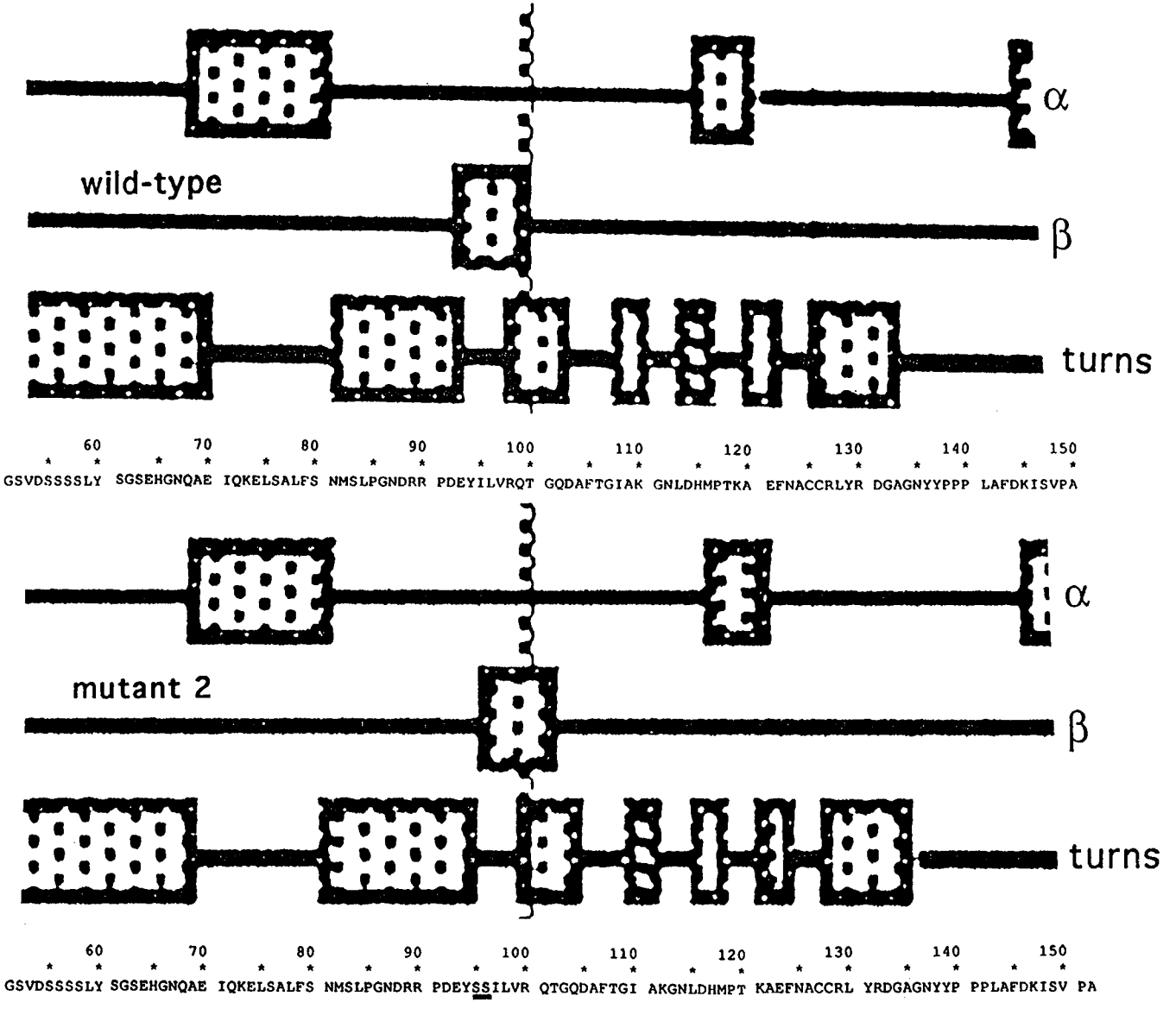
α
wild-type
β
turns
60 70 80 90 100 110 120 130 140 150
GSVDSSSSLY SGSEHGNQAE IQKELSALFS NMSLPGNDRR PDEYILVRQT GQDAFTGIAK GNLDHMPTKA EFNACCRLYR DGAGNYYPPP LAFDKISVPA
α
mutant 2
β
turns
60 70 80 90 100 110 120 130 140 150
GSVDSSSSLY SGSEHGNQAE IQKELSALFS NMSLPGNDRR PDEYSSILVR QTGQDAFTGI AKGNLDHMPT KAEFNACCRL YRDGAGNYYP PPLAFDKISV PA

Figure 4.5

interactions, either with itself or with other proteins necessary for the accumulation of VirE2 in *A. tumefaciens*.

Insertion 3 (after residue 213) did not destabilize VirE2 in *A. tumefaciens*, and it affected tumorigenesis only slightly. Insertion 3 adds a serine and an arginine after residue 213 which increased the cooperativity of ssDNA binding, in contrast to another mutation in this region that reduced cooperativity (Citovsky *et al.* 1994). The new arginine residue could interact ionically with negatively charged oxygens on the DNA backbone, increasing the affinity of this mutant protein for ssDNA (Prasad and Chiu 1978). This insertion also slightly enlarges a region of putative random coil, as no helix, sheet or turn regions are predicted in this area and the secondary structure predictions outside this immediate area are unchanged (Figure 4.6). Therefore, the addition of a charged amino acid, rather than a structural change, probably results in the increased cooperativity of this mutant.

Figure 4.6. Secondary Structure Prediction of VirE2 Mutated by Linker Insertion 3. A) wild-type VirE2, B) insertion 3, a serine and an arginine were inserted after residue 213. The boxes indicate: top - alpha helix, middle - beta strand, bottom - turn.

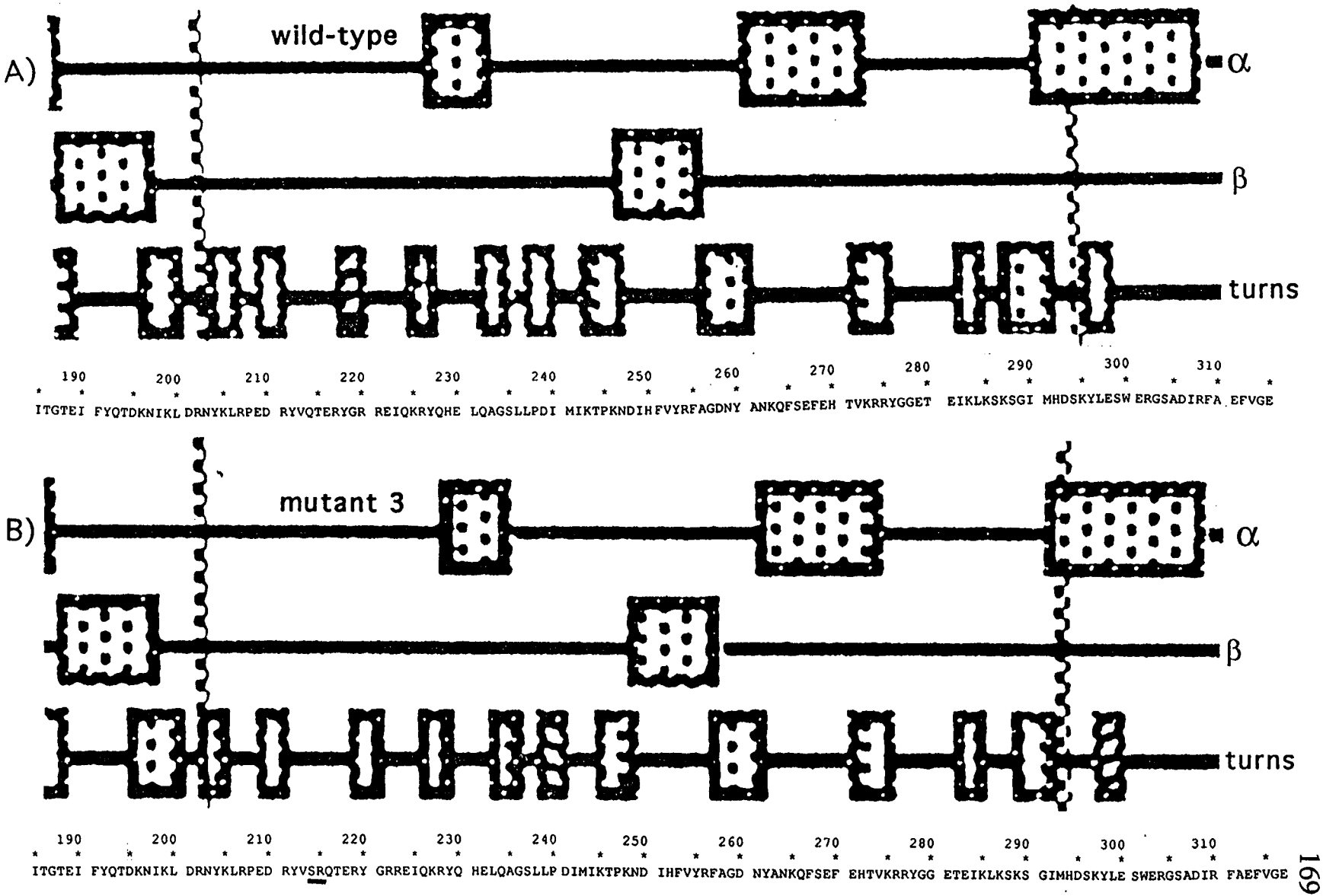
A)
wild-type
α
β
turns
190 200 210 220 230 240 250 260 270 280 290 300 310
ITGTEI FYQTDKNIKL DRNYKLRPED RYVQTERYGR REIQKRYQHE LQAGSLLPDI MIKTPKNDIH FVYRFAGDNY ANKQFSEFEH TVKRRYGGET EIKLKSKSGI MHDSKYLESW ERGSADIRFA EFVGE
B)
mutant 3
α
β
turns
190 200 210 220 230 240 250 260 270 280 290 300 310
ITGTEI FYQTDKNIKL DRNYKLRPED RYVSRQTERY GRREIQKRYQ HELQAGSLLP DIMIKTPKND IHFVYRFAGD NYANKQFSEF EHTVKRRYGG ETEIKLKSKS GIMHDSKYLE SWERGSADIR FAEFVGE

Figure 4.6

The VirE2 Deletion Resulted in Wild-type Single-stranded DNA Binding and Virulence

The serine-rich region (SSSLYSGS) deleted from VirE2 shows sequence similarity to another non-specific single-stranded DNA binding protein encoded by gene 32 of bacteriophage T4 (gp32) (SSSGSSSS) (Hurley *et al.* 1993; Krassa *et al.* 1991). This region of gp32 interacts with other proteins during T4 DNA replication (Hurley *et al.* 1993; Krassa *et al.* 1991). Interestingly, deletion of this region from VirE2 had no effect on tumorigenesis or its ssDNA binding ability; this serine-rich region is apparently unimportant for VirE2 function. This deletion of residues 55 to 65 shortened a predicted turn region that begins near residue 45, but it did not change the predicted secondary structure outside this region (Figure 4.7). This turn is not in a functionally important region of VirE2 because its length is unimportant for VirE2 function.

Figure 4.7. Secondary Structure Prediction of VirE2 Mutated by a Deletion of Residues 55-65. A) wild-type VirE2, B) deletion of residues 55-65. The boxes indicate: top - alpha helix, middle - beta strand, bottom - turn.

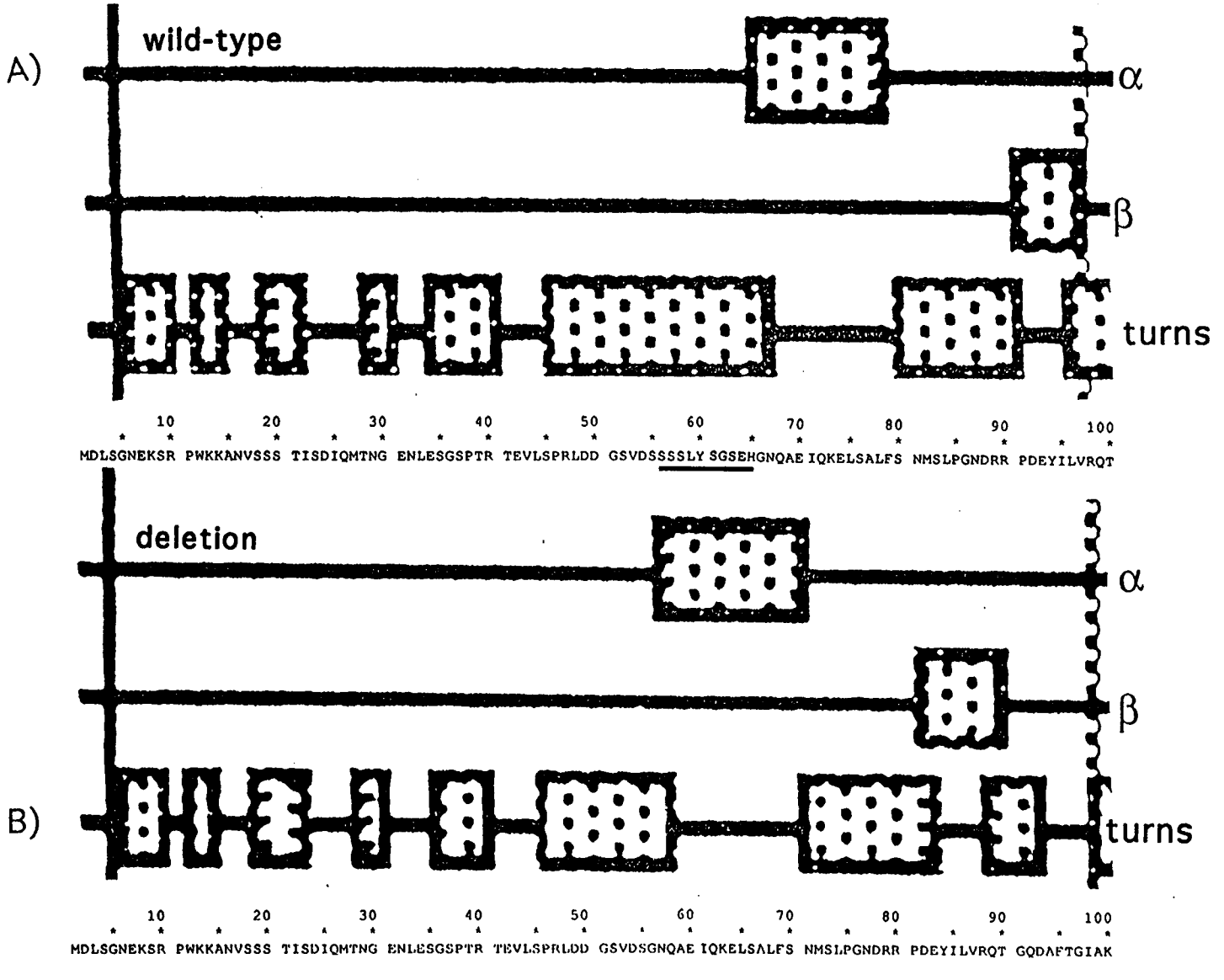
A)
wild-type
α
β
turns
10 20 30 40 50 60 70 80 90 100
MDLSGNEKSR PWKKANVSSS TISDIQMTNG ENLESGSPTR TEVLSPRLDD GSVDSSSSLY SGSEHGNQAE IQKELSALFS NMSLPGNDRR PDEYILVRQT
B)
deletion
α
β
turns
10 20 30 40 50 60 70 80 90 100
MDLSGNEKSR PWKKANVSSS TISDIQMTNG ENLESGSPTR TEVLSPRLDD GSVDSGNQAE IQKELSALFS NMSLPGNDRR PDEYILVRQT GQDAFTGIAK

Figure 4.7

Insertions 1 and 4: Wild-type Single-stranded DNA Binding and Reduced Tumorigenesis

Two linker insertions (1 and 4) reduced tumorigenesis without affecting ssDNA binding. Mutations that cause this phenotype may have influenced a function of VirE2 (other than ssDNA binding) that is important for T-DNA transmission or, alternatively, cause a destabilization of VirE2 in *A. tumefaciens.*

Immunoblots showed that insertion 1 reduced tumorigenesis by preventing normal accumulation of VirE2 in *A. tumefaciens.* Insertion 1 adds leucine and glutamic acid after residue 10 of VirE2. Leucine has a hydrophobic side chain while the side chain of glutamic acid is negatively charged. Both of these amino acids are strong helix formers according to the Chou and Fasman method of secondary structure prediction (1978). Consequently, insertion 1 is predicted to add an alpha helix of about seven amino acids in length to a region of turns (Figure 4.8). Although this change does not affect the ssDNA binding ability of VirE2, and would not be predicted to (because it is located near the N-terminus), it does decrease the

Figure 4.8. Secondary Structure Prediction of VirE2 Mutated by Linker Insertion 1. A) wild-type VirE2, B) insertion 1, a leucine and a glutamic acid were inserted after residue 10. The boxes indicate: top - alpha helix, middle - beta strand, bottom - turn.

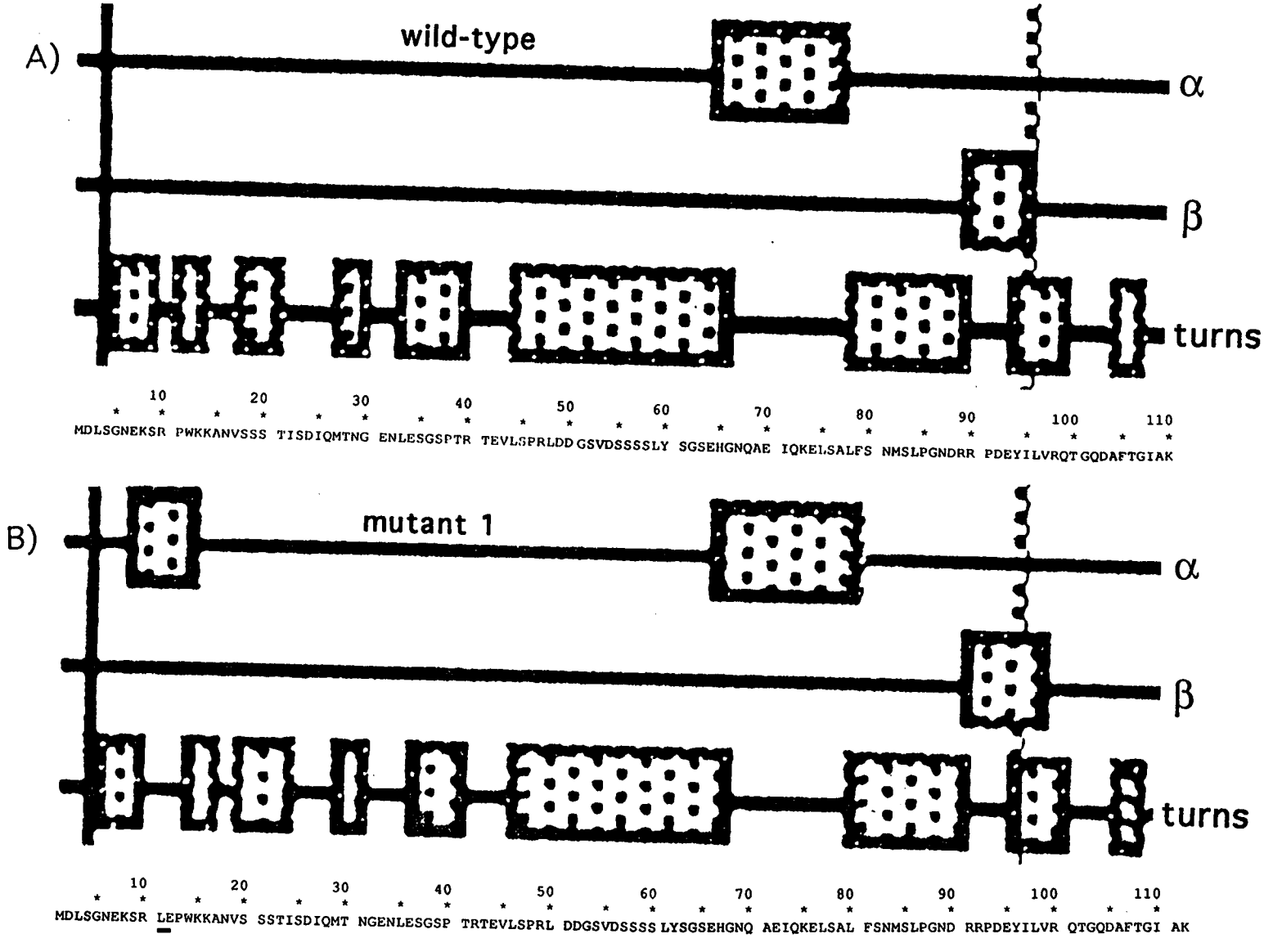
A)
wild-type
α
β
turns
10 20 30 40 50 60 70 80 90 100 110
MDLSGNEKSR PWKKANVSSS TISDIQMTNG ENLESGSPTR TEVLSPRLDD GSVDSSSSLY SGSEHGNQAE IQKELSALFS NMSLPGNDRR PDEYILVRQT GQDAFTGIAK
B)
mutant 1
α
β
turns
10 20 30 40 50 60 70 80 90 100 110
MDLSGNEKSR LEPWKKANVS SSTISDIQMT NGENLESGSP TRTEVLSPRL DDGSVDSSSS LYSGSEHGNQ AEIQKELSAL FSNMSLPGND RRPDEYILVR QTGQDAFTGI AK

Figure 4.8

stability in *A. tumefaciens.* The decreased stability of this VirE2 mutation leads to reduced virulence.

In contrast, insertion 4 appears to alter an important property of VirE2 other than ssDNA binding or protein stability. As with insertion 1, insertion 4 also adds leucine and glutamic acid residues, again resulting in the predicted formation of an alpha helix of roughly 7 amino acids in length (Figure 4.9). This insertion is located between the 2 NLS regions of wild-type VirE2. Because insertion 4 VirE2 and wild-type VirE2 bind ssDNA similarly (Figures 3.13 and 3.14), this insertion probably does not result in large changes in tertiary structure. Insertion 4 may therefore define a domain required for T-DNA integration inside the plant cell, or VirE2 export from the *A. tumefaciens* cell.

Figure 4.9. Secondary Structure Prediction of VirE2 Mutated by Linker Insertion 4. A) wild-type VirE2, B) insertion 4, a leucine and a glutamic acid were inserted after residue 256. The boxes indicate: top - alpha helix, middle - beta strand, bottom - turn.

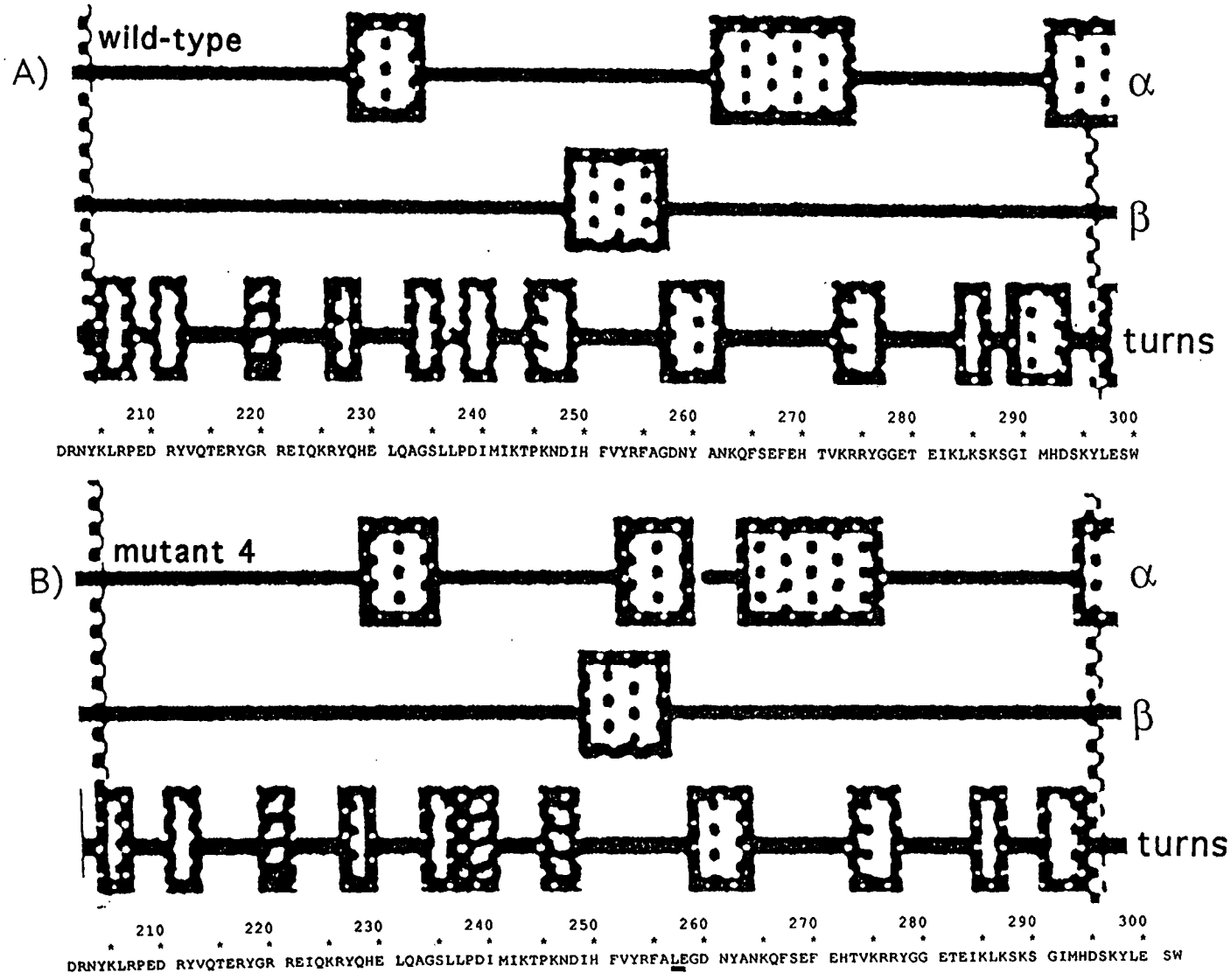
A)
wild-type
α
β
turns
210 220 230 240 250 260 270 280 290 300
DRNYKLRPED RYVQTERYGR REIQKRYQHE LQAGSLLPDIMIKTPKNDIH FVYRFAGDNY ANKQFSEFEH TVKRRYGGET EIKLKSKSGI MHDSKYLESW
B)
mutant 4
α
β
turns
210 220 230 240 250 260 270 280 290 300
DRNYKLRPED RYVQTERYGR REIQKRYQHE LQAGSLLPDI MIKTPKNDIH FVYRFALEGD NYANKQFSEF EHTVKRRYGG ETEIKLKSKS GIMHDSKYLE SW

Figure 4.9

Secondary Structure Comparison of VirE2 with RecA, SSB and gp32

The secondary structure of VirE2 was compared with those of three other proteins, all of which have been shown to bind cooperatively to ssDNA in a non-specific fashion (Figure 4.10). The proteins chosen were RecA, the single-stranded DNA binding protein (SSB) from *E. coli,* and gp32 from bacteriophage T4. SSB and gp32 function primarily by melting out secondary structure in ssDNA to facilitate DNA replication and repair (Chase and Williams 1986). Both proteins also protect exposed ssDNA from nucleases. RecA, on the other hand, has a more active role in DNA recombination and repair (Cox and Lehman 1987; Egelman 1993; Roca and Cox 1990). RecA promotes a strand exchange reaction between single-stranded and double-stranded DNA, hydrolyzes ATP and facilitates the cleavage of the LexA repressor, UmuD, and the λ repressor (Cox and Lehman 1987; Egelman 1993; Roca and Cox 1990). The crystal structures of both RecA and gp32 have been reported (Egelman and Stasiak 1986; Shamoo *et al.* 1995).

Figure 4.10. Secondary Structure Predictions of VirE2, RecA, gp32 and SSB. A) VirE2, B) RecA, C) SSB, D) gp32. The boxes indicate: top - alpha helix, middle - beta strand, bottom - turn.

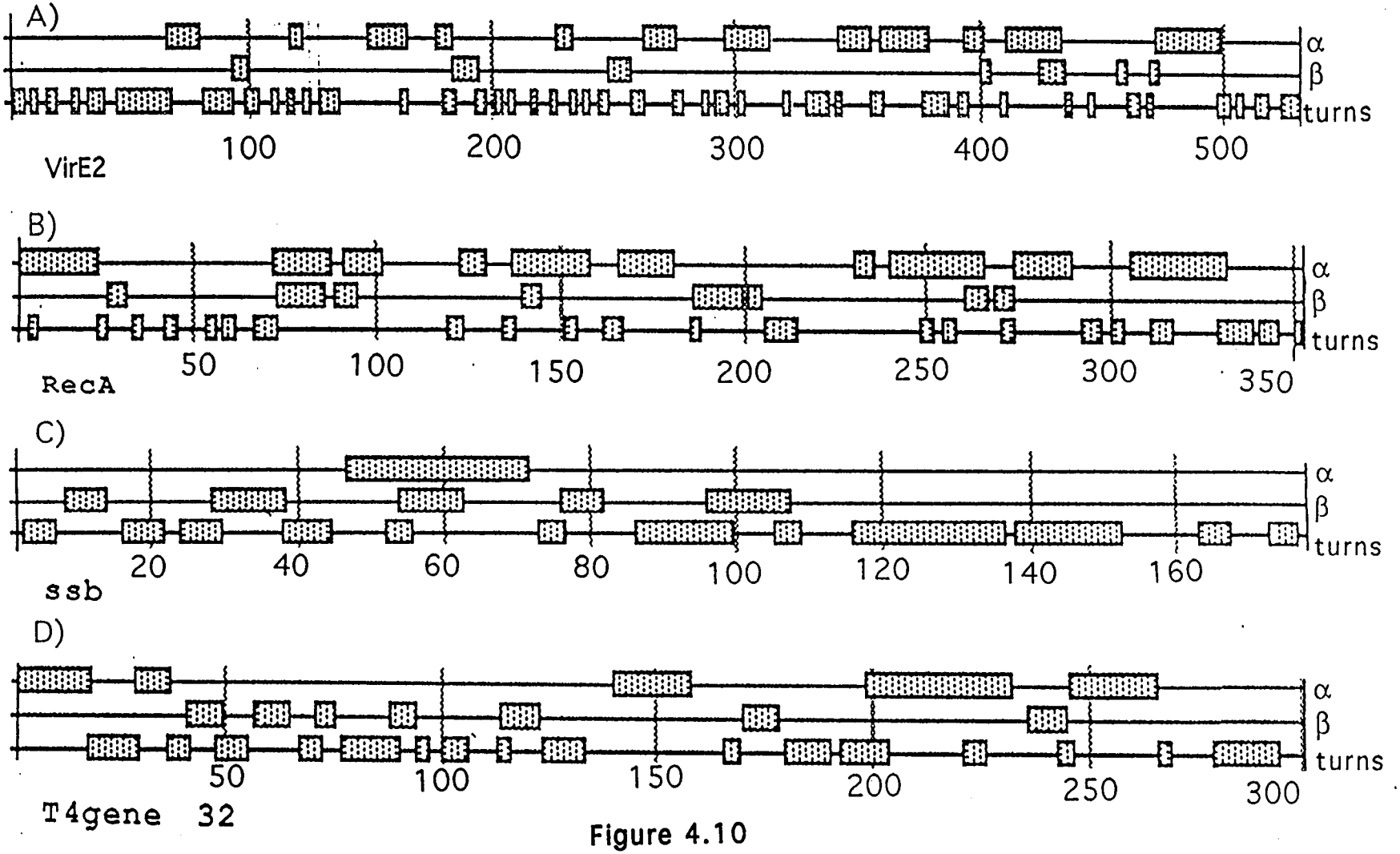
A)
α
β
turns
100
200
300
400
500
VirE2
B)
α
β
turns
50
100
150
200
250
300
350
RecA
C)
α
β
turns
20
40
60
80
100
120
140
160
ssb
D)
α
β
turns
50
100
150
200
250
300
T4gene 32

Figure 4.10

The DNA Binding and Strand-exchange Domain of RecA: Similarities to VirE2

The crystal structure of RecA without DNA suggests that the paired DNA strands reside in the center of a protein helix (Story *et al.* 1992). Two disordered loops line this helix and studies of RecA binding implicate one of these loops in DNA binding (Egelman and Stasiak 1986; Story *et al.* 1993; Mayerboeuf *et al.* 1995). This DNA binding loop includes a central phenylalanine that contacts the DNA. A 20 amino acid peptide, corresponding to residues 193-212, lies within this binding loop and can bind cooperatively to ssDNA (Gardner *et al.* 1995). This 20 amino acid peptide is also able to promote homologous DNA pairing and strand exchange (Voloshin *et al.* 1996); ten to twenty percent as many joint molecules are formed compared to full-length (353 amino acids) RecA. In this 20 amino acid peptide, a central phenylalanine at position 203 is highly conserved among both prokaryotic and eukaryotic RecA homologs (Story *et al.* 1993). If tryptophan replaces this phenylalanine the cooperativity of ssDNA binding by this peptide is increased and this altered peptide is still able to promote strand exchange (Voloshin *et al.* 1996). Other substitutions for this phenylalanine decrease

cooperativity or eliminate ssDNA binding and are not able to form joint molecules. In addition to the central phenylalanine residue, the two amino acids at either end of this region are highly conserved. VirE2 has no sequence homology to the peptide or to the highly conserved amino acids.

The 20 amino acid RecA peptide undergoes a change from random coil to beta strand and turn upon binding ssDNA (Voloshin *et al.* 1996). Chou-Fasman predicts this region (residues from 193-212), to form both beta stand and turn. Two regions in VirE2, beginning at amino acids 190 and 250 are most similar in predicted secondary structure to this region in RecA, although both the strand and turn regions in VirE2 are considerably shorter. Insertion 4 (after residue 260), which does not affect ssDNA binding but may be required for T-DNA integration lies close to one of these regions. Because VirE2 can mediate genetic recombination, it is tempting to speculate that one of these regions in VirE2 is needed for T-DNA integration. Because there is little secondary structural and sequence similarity between VirE2 and this region of RecA, it is unlikely that VirE2 mediates strand exchange in the same manner as RecA.

The DNA Binding Domain of gp32: Similarities to VirE2

The crystal structure of gp32 complexed to ssDNA has recently been determined (Shamoo *et al.* 1995). This crystal structure confirms the importance of electrostatic interactions between the lysine and arginine residues of gp32 and the phosphate oxygens of the DNA backbone (Prasad and Chiu, 1987). However, intercalation of the aromatic side chains into the DNA does not occur as predicted (Prasad and Chiu, 1987). Instead the bases lie near pockets of hydrophobic residues that surround a DNA binding groove. The groove is narrow, allowing gp32 to differentiate between ssDNA and dsDNA.

The DNA binding region of gp32 (residues 21-254) is predominantly sheet and turn (Shamoo *et al.* 1995), agreeing with the Chou-Fasman secondary structure prediction (Figure 4.10). However, the putative ssDNA binding domain in VirE2 (residues 285-472) is predicted to be predominantly alpha-helix (Figure 4.10). Therefore, VirE2 may not bind to single-stranded DNA in the same way gp32 binds.

In gp32, the serine-rich region (residues 281-288) which interacts with other T4 DNA replication proteins, is in a region of

beta turn (Figure 4.10). The corresponding region in VirE2 (residues 55-65), is also in a region of turn, although it is not surrounded by acidic residues as it is in gp32. Since deletion of these residues from VirE2 had little effect on either ssDNA binding or tumorigenesis, this region is not critical for those functions of VirE2.

The DNA Binding Domain of SSB: Similarities to VirE2

SSB differs from other ssDNA binding proteins because depending on the ratio of SSB protein to ssDNA and the salt concentration, SSB tetramers can bind to ssDNA in several modes (Lohman and Overman 1985). In one mode, the ssDNA wraps around one or two SSB tetramers and the DNA/SSB complex has a beaded appearance. At higher protein concentrations, the DNA does not wrap around the SSB protein and a smooth filament is formed instead. The amino terminal end (residues 1-105) binds to ssDNA, as well as to the full length protein. This domain is predicted to be beta strand and turn like the ssDNA binding domain of gp32 and therefore, differs from VirE2. The carboxy terminus of SSB and gp32 contains an acidic region, suggesting that this SSB domain might interact

with other replication proteins as has been demonstrated for gp32 (Chase and Williams 1986).

Cooperative Binding of VirE2, RecA, gp32 and SSB

VirE2, gp32, RecA, and SSB all exhibit cooperative binding to ssDNA, and studies with gp32 provide the most information. In dilute solution gp32 exists as a monomer, but at higher concentration it undergoes self-association (Alberts and Frey 1970). Removal of the first 9 residues from gp32 (Met-Phe-Lys-Arg-Lys-Ser-Thr-Ala-Glu) results in a protein that binds non-cooperatively and it fails to aggregate in solution (Hosoda *et al.* 1980). Since removal of these amino acids eliminates both cooperative DNA binding and self-association in solution, both processes are thought to be related (Chase and Williams 1986). Residues 3-7 in gp32 are identical to residues 110-114, and both regions have been designated as LAST (Lys-Arg-Lys-Ser-Thr) motifs (Casas-Finet *et al.* 1992). The LAST motif has several basic amino acids (underlined). A model has been proposed to explain cooperative ssDNA binding in gp32 (Casas-Finet *et al.* 1992). When gp32 is not bound to ssDNA, the central LAST motif interacts with a negatively

charged region of the protein. This negatively charged region is displaced when gp32 binds ssDNA freeing this region to interact with the N-terminal LAST motif in an adjoining gp32 molecule, and thus nucleate cooperative binding. The N-terminal LAST motif is in an alpha helical region of predicted secondary structure (Figure 4.10).

VirE2 has no similar LAST motif, although VirE2 bearing either insertions 2 or 3 caused a change in cooperative DNA binding. However, only insertion 3 is surrounded by basic amino acids, because it interrupts a NLS. Therefore, VirE2 cooperativity probably does not fit the model proposed for gp32. VirE2 does form a tetramer in solution (Das 1988), suggesting that protein-protein interactions are responsible for the cooperative binding of VirE2 to ssDNA. It would be of interest to purify VirE2 bearing insertions 2 or 3 and determine whether the mutant VirE2 proteins could form a tetramer. Insertion 2 may not form a tetramer in solution and may instead exist predominantly as a monomer or dimer since this insertion decreased cooperativity. Insertion 3, on the other hand, may form tetramers or larger complexes of VirE2 protein since this insertion resulted in increased cooperativity. Insertion 2 decreased

the cooperative binding of VirE2 and does not shift as much ssDNA to the top of the gel as when wild-type VirE2 protein is added (Figures 3.14 and 3.15). Several explanations for this observation are possible. If protein-protein interactions are involved in cooperative binding to DNA, the conformational change as a result of the insertion may result in weaker bond formation between adjacent VirE2 monomers so that they are not packed as closely together. Alternatively, this insertion might cause VirE2 monomers to aggregate, preventing additional monomers from binding. Gp32 has a DNA binding groove and is postulated to slide along the ssDNA (Voloshin *et al.* 1996). Therefore, if VirE2 binds to ssDNA similarly, this insertion may prevent VirE2 from easily sliding on the ssDNA, resulting in fewer bound molecules. This change in VirE2 could also limit the ability of VirE2 to induce a conformational change in the ssDNA that allows other VirE2 molecules to bind more easily.

As described for gp32 and VirE2, RecA forms aggregates in solution due to a protein-protein interaction (Brenner *et al.* 1988). Removal of the N-terminal 33 amino acids of RecA decreases both aggregation and ssDNA binding (Mikawa *et al.* 1995). The authors speculate that the defective protein-protein interaction leads to

defective DNA binding. This truncated protein interacts with full-length RecA in a 1:1 ratio, presumably by an interaction between the N-terminal site in full-length RecA and an internal site in the truncated protein (Mikawa *et al.* 1995). In RecA, as in gp32, the N-terminal cooperativity domain is in a putative alpha helical region of secondary structure based on Chou-Fasman predictions (Figure 4.10) and crystal structure analysis has shown residues 3-21 form an alpha helix (Story *et al.* 1992).

Insertions 2 and 3 in VirE2 are both near putative alpha helical regions of secondary structure. These regions may interact directly with charged regions in adjacent VirE2 monomers. Point mutations of the charged residues in these adjacent alpha helical regions could pinpoint the residues involved in cooperative binding. The protein-protein interactions between the mutant proteins should be characterized along with the ssDNA binding to more fully understand the nature of VirE2 cooperativity.

Variability in Virulence Data

Potato Inoculations

Quantitative virulence data were obtained using potato discs. However, large standard deviations were observed when these data were statistically analyzed. For example, the average number of tumors per disc for the wild-type strain WR5100 was 8.3 +/-8.8. In the potato inoculations, a potato disc with 8 or more tumors was sometimes located next to a disc with no tumors. However, tumor formation was consistent between potatoes: a strain that was virulent or almost avirulent on one potato was also virulent or almost avirulent on another potato. The high standard deviation was not decreased by compiling the results from the potatoes which had a higher-than-average number of tumors when infected with WR5100, the wild-type strain. Large standard deviations using this assay have been previously noted by others (Shurvinton *et al.* 1992). This suggests the variability in the data lies within the individual potatoes. Several reasons may explain this variability.

Slices from the center of the potato where the tissue is youngest, may be the most susceptible to infection. Another possibility could be the variable length of time that elapses between the cutting of a potato disc and inoculation. The discs from a single potato are inoculated at the same time to minimize this variability. However, a large potato may yield over 80 discs, and therefore the time required to inoculate each disc can vary from 10 to 45 minutes. A combination of these possibilities could account for the variability in the data.

Host Range

The *A. tumefaciens* strain WR5000, with a *virE2* deletion on the Ti plasmid, was avirulent on *K. daigremontiana* leaves, carrot slices and potato slices. However, on tomato stems, a few very small tumors formed. This indicates that VirE2 is critical for virulence on most plants, but that infection with a strain containing deletion in *virE2* can occur on very sensitive hosts. This variability in sensitivity to infection was also noticed when different hosts were infected by strains with insertions in *virE2*. For example, insertion 4 exhibited less than 1% of wild-type tumors on potato

discs and was almost avirulent on carrot slices. Insertion 4 also formed smaller tumors on *K. daigremontiana* leaves and fewer tumors on tomato stems compared to a wild-type strain. Insertion 1 formed 4.4% of wild-type tumors on potato discs and was also almost avirulent on carrot slices. However, the tumors on *K. daigremontiana* leaves were smaller to wild-type in size, and it was virulent on tomato stems.

Tomato stems are therefore the most sensitive host tissues of the plants tested. We used cultivar Bonnie Best because of low natural disease resistance and high sensitivity to *A. tumefaciens* infection (M. Canfield and L. Moore, personal communication). Potato discs and carrot slices are the least sensitive, and *K. daigremontiana* leaves are intermediate in sensitivity.

Differences in *A. tumefaciens* infection between host plants has been noticed previously. For example, removal of the NLS of VirD2 severely reduced virulence on tobacco stems, but only slightly reduced virulence on potato discs (Shurvinton *et al.* 1992). *A. tumefaciens* strains in nature have shown wide variability in the range of plants they are able to infect (Knauf *et al.* 1982). The strains with a narrow host range have a defective T-DNA cytokinin

biosynthetic gene or changes in *virA* or *virC* and, therefore, are not as effective as other strains at infecting plants (Yanofsky *et al.* 1985). These authors speculate that susceptible host plants may require T-DNA integration into only a few cells at the site of inoculation for tumors to appear, while less susceptible plants require T-DNA integration into many cells. Therefore, the frequency of T-DNA transfer is the critical host range determinant.

In *virE2* mutants, the frequency of T-DNA transfer is severely reduced. For example, a *virE2* deletion strain transferred T-DNA into tobacco at a frequency 2,500X less than a wild-type strain (Rossi *et al.* 1996). This may explain the virulence phenotype observed for WR5000, containing the *virE2* deletion. *virE2* mutants can infect petunia leaf discs, a very sensitive host, at a low frequency but not petunia stems (Horsch *et al.* 1986). When petunia leaf discs were infected by a *virE2* mutant, only one or two tumors formed on one-third to one-half of the discs, and often no tumors were visible for the first two weeks after infection (Horsch *et al.* 1986). On the other hand, mutations in *virA, B, D* and *G* completely eliminate virulence on the petunia leaf discs (Horsch *et al.* 1986). This is not surprising as these mutations would completely eliminate T-DNA

export. Therefore, the variability in virulence on different host plants reported here when infected with the *virE2* insertion mutants or the *virE2* deletion strain may be related to the number of T-DNA molecules transferred.

To summarize the results: the C-terminal half of VirE2 contains a domain critical for ssDNA binding as insertions 5 and 6 resulted in the loss of ssDNA binding ability. Insertions 2 and 3, in the N-terminal half of VirE2, identified cooperativity domains, because they either increased (insertion 3) or decreased (insertion 2) cooperative binding to ssDNA. Insertions 1 and 4 bind to ssDNA similarly to wild-type VirE2, nonetheless they reduce virulence. Insertion 1 did not accumulate to wild-type levels in *A. tumefaciens*, which accounts for its virulence phenotype. Insertions 2, 5 and 6 also severely reduced the accumulation of VirE2 in *A. tumefaciens* and reduced tumorigenesis. Insertion 4, in the central region of VirE2, did not affect the stability of VirE2 in *A. tumefaciens*. This mutation could therefore define another functional domain.

BIBLIOGRAPHY

Aiba, H., F. Nakasai, S. Mizushima, and T. Mizuno. 1989. Phosphorylation of a bacterial activator protein, OmpR, by a protein kinase, EnvZ, results in stimulation of its DNA-binding ability. J. Biochem. 106:5-7.

Akiyoshi, D. E., H. Klee, R. M. Amasino, E. W. Nester, M. P. Gordon. 1984. T-DNA of *Agrobacterium tumefaciens* encodes an enzyme of cytokinin biosynthesis. Proc. Natl. Acad. Sci. USA 81:5994-5998.

Alberts, B. M. and L. Frey. 1970. T4 bacteriophage gene 32: a structural protein in the replication and recombination of DNA. Nature 227:1313-1318.

Albright, L. M., M. F. Yanofsky, B. Leroux, D. Ma, and E. W. Nester. 1987. Processing of the T-DNA of *Agrobacterium tumefaciens* generates border nicks and linear, single-stranded T-DNA. J. Bacteriol. 169:1046-1055.

Amann, E., B. Ochs, and K. Abel. 1988. Tightly regulated *tac* promoter vectors useful for the expression of unfused and fused proteins in *Escherichia coli*. Gene 69:301-315.

Andrews, B. J., G. A. Proteau, L. G. Beatty, and P. D. Sadowski. 1985. The FLP recombinase of the 2 μ circle DNA of yeast: Interaction with its target sequences. Cell 40:795-803.

Ankenbauer, R. G., and E. W. Nester. 1990. Sugar-mediated induction of *Agrobacterium tumefaciens* virulence genes: structural specificity and activities of monosaccharides. J. Bacteriol. 172:6442-6446.

Argos, P., A. Landy, K. Abremski, J. B. Egan, E. Haggard-Ljungquist, R. H. Hoess, M. L. Kahn, B. Kalionis, S. V. L. Narayana, L. S. Pierson III, N. Sternberg and J. M. Leong. 1986. The integrase family of site-specific recombinases: regional similarities and global diversity. EMBO J. 5:433-440.

Austin, S., M. Ziese, and N. Sternberg. 1981. A novel role for site-specific recombination in maintenance of bacterial replicons. Cell 25:729-736.

Ausubel, F. M., R. Brent, R. E. Kingston, D. D. Moore, J. G. Seidman, J. A. Smith, and K. Struhl. 1987. Current protocols in molecular biology. Wiley, New York.

Bachmann, B. J. 1987. p. 1190-1219. *In* F. C. Neidhardt et al. (ed.), *Escherichia coli* and *Salmonella typhimurium*, cellular and molecular biology. ASM Press.

Bakkeren, G., Z. Koukolikova-Nicola, N. Grimsley, and B. Hohn. 1989. Recovery of *Agrobacterium tumefaciens* T-DNA molecules from whole plants early after transfer. Cell 57:847-857.

Bally, M., A. Filloux, M. Akrim, G. Ball, A. Lazdunski, and J. Tommason. 1992. Protein secretion in *Psuedomonas aeruginosa*: characterization of the seven *xcp* genes and processing of secretory protein apparatus components by pre-pilin peptidase. Mol. Microbiol. 6:1121-1131.

Barker, R., K. Idler, D. Thompson, and J. Kemp. 1983. Nucleotide sequence of the T-DNA region of the *Agrobacterium tumefaciens* octopine Ti plasmid pTi15955. Plant Mol. Biol. 2:335-350.

Barry, G. F., S. G. Rogers, R. T. Fraley, and L. Brand. 1984. Identification of a cloned cytokinin biosynthetic gene. Proc. Natl. Acad. Sci. USA 81:4776-4780.

Beijersbergen, A., S. J. Smith, and P. J. J. Hooykaas. 1994. Location and topology of VirB proteins of *Agrobacterium tumefaciens*. Plasmid 32:212-218.

Berger, B. R., and P. J. Christie. 1994. Genetic complementation analysis of the *Agrobacterium tumefaciens virB* operon: *virB2* through *virB11* are essential virulence genes. J. Bacteriol. 176:3646-3660.

Beringer, J. E., J. L. Beynon, A. V. Buchanan-Wollaston, and A. W. B. Johnston. 1978. Transfer of the drug-resistance transposon Tn*5* to *Rhizobium.* Nature (London) 276:633-634.

Binns, A. N., C. E. Beaupre, and E. M. Dale. 1995. Inhibition of VirB-mediated transfer of diverse substrates from *Agrobacterium tumefaciens* by the IncQ plasmid RSF1010. J. Bacteriol. 177:4890-4899.

Bradford, M. 1976. A rapid and sensitive method for the quantitation of microgram quantities of proteins utilizing the principle of protein-dye binding. Anal. Biochem. 72:248-254.

Branden, C. and J. Tooze. 1991. Introduction to protein structure. Garland Pub. Inc. New York.

Braun, A. C., 1947. Thermal studies on the factors responsible for tumor initiation in crown gall. Am. J. Bot. 34:234-240.

Brenner, S. L., A. Zlotnick, and J. D. Griffith. 1988. RecA protein self-assembly: multiple discrete aggregation states. J. Mol. Biol. 204:959-972.

Brock, T. D., M. T. Madigan, J. M. Martinko, and J. Parker. 1994. p. 266-271. *In* Biology of microorganisms. Seventh edition. Prentice Hall, Englewood Cliffs.

Buchanan-Wollaston, V., J. E. Passiatore, and F. Cannon. 1987. The *mob* and *oriT* mobilization functions of a bacterial plasmid promote its transfer to plants. Nature (London) 328:172-175.

Buchanan-Wollaston, V., J. E. Passiatore, and F. Cannon. 1988. The effect of *vir* mutations on plasmid transfer into plants. p.281-282. *In* R. Palichios and D. P. S. Varma (ed.), Molecular genetics of plant-microbe interactions. APS Press, St. Paul.

Cangelosi, G. A., R. G. Ankenbauer, and E. W. Nester. 1990. Sugars induce the *Agrobacterium* virulence genes through a periplasmic binding protein and a transmembrane signal protein. Proc. Natl. Acad. Sci. USA 87:6708-6712.

Casas-Finet, J. R., K. R. Fisher, and R. L. Karpel. 1992. Structural basis for the nucleic acid binding cooperativity of bacteriophage T4 gene 32 protein: the $(Lys/Arg)_3$ $(Ser/Thr)_2$ LAST motif. Proc. Natl. Acad. Sci. USA 89:1050-1054.

Charles, T. C. and E. W. Nester. 1993. A chromosomally encoded two-component sensory transduction system is required for virulence of *Agrobacterium tumefaciens*. J. Bacteriol. 175:6614-6625.

Chase, J. W. and K. R. Williams. 1986. Single-stranded DNA binding proteins required for DNA replication. Ann. Rev. Biochem. 55:103-136.

Chilton, M. D., M. H. Drummond, D. J. Merlo, D. Sciaky, A. L. Montoya, M. P. Gordon, and E. W. Nester. 1977. Stable incorporation of plasmid DNA into higher plant cells: the molecular basis of crown gall tumorigenesis. Cell 11:263-271.

Chilton, M. D., R. K. Saiki, N. Yadav, M. P. Gordon, and F. Quetier. 1980. T-DNA from *Agrobacterium* Ti plasmid is in the nuclear DNA fraction of crown gall tumor cells. Proc. Natl. Acad. Sci. USA 77:4060-4064.

Chou, P. Y. and G. D. Fasman. 1973. Structural and functional role of leucine residues in proteins. J. Mol. Biol. 74:251-276.

Chou, P. Y. and G. D. Fasman. 1978. Empirical predictions of protein conformation. Ann. Rev. Biochem. 47:251-276.

Christie, P. J., J. E. Ward, S. C. Winans, and E. W. Nester. 1988. The *Agrobacterium tumefaciens virE2* gene product is a single-stranded-DNA-binding protein that associates with T-DNA. J. Bacteriol. 170:2659-2663.

Citovsky, V., G. DeVos, and P. Zambryski. 1988. Single-stranded DNA binding protein encoded by the *virE* locus of *Agrobacterium tumefaciens*. Science 240:501-504.

Citovsky, V., D. Warnick, and P. Zambryski. 1994. Nuclear import of *Agrobacterium* VirD2 and VirE2 proteins in maize and tobacco. Proc. Natl. Acad. Sci. USA 91:3210-3214.

Citovsky, V., M. L. Wong, and P. Zambryski. 1989. Cooperative interactions of *Agrobacterium* VirE2 protein with single-stranded DNA: implications for the T-DNA transfer process. Proc. Natl. Acad. Sci. USA 86:1193-1197.

Citovsky, V., J. Zupan, D. Warnick, and P. Zambryski. 1992. Nuclear localization of *Agrobacterium tumefaciens* VirE2 protein in plant cells. Science 256:1802-1805.

Close, T. J., R. C. Tait, and C. I. Kado. 1985. Regulation of Ti plasmid virulence genes by a chromosomal locus of *Agrobacterium tumefaciens* J. Bacteriol. 164:774-781.

Cooley, M. B., M. R. D'Souza, and C. I. Kado. 1994. The *virC* and *virD* operons of the *Agrobacterium* Ti plasmid are regulated by the *ros* chromosomal gene: analysis of the cloned *ros* gene. J. Bacteriol. 173: 2608-2616.

Cox, M. M. and I. R. Lehman. 1987. Enzymes of general recombination. Ann. Rev. Biochem. 56:229-262.

Csonka, L. N., and A. J. Clark. 1979. Deletions generated by the transposon Tn*10* in the *srl recA* region of the *Escherichia coli* chromosome. Genetics 93:321-343.

Dale, E. M., A. N. Binns, and J. E. Ward, 1993. Construction and characterization of Tn*5* *virB*, a transposon that generates non-polar mutations and its use to define *virB8* as an essential virulence gene in *Agrobacterium tumefaciens*. J. Bacteriol. 175:887-891.

Das, A. 1988. *Agrobacterium tumefaciens virE* operon encodes a single-stranded DNA-binding protein. Proc. Natl. Acad. Sci. USA 85:2909-2913.

DeCleene, M., and J. DeLey. 1976. The host range of crown gall. Bot. Rev. 42:389-466.

Dessaux, Y., A. Petit, and J. Tempe'. 1993. Chemistry and biochemistry of opines: chemical mediators in parasitism. Phytochem. 34:31-38.

DeVos, G., and P. Zambryski. 1989. Expression of *Agrobacterium* nopaline specific VirD1, VirD2 and VirC1 proteins and their requirement for T-strand production in *E. coli.* Molec. Plant-Microbe Inter. 2:42-52.

Ditta, G., T. Schmidhauser, E. Yakobson, P. Lu, X. Liang, D. R. Finley, D. Guiney, and D. R. Helinski. 1985. Plasmids related to the broad-host-range vector, pRK290, useful for gene cloning and for monitoring gene expression. Plasmid 13:149-153.

D'Souza-Ault, M. R., M. B. Cooley, and C. I. Kado. 1993. Analysis of the Ros repressor of *Agrobacterium virC* and *virD* operons: molecular intercommunication between plasmid and chromosomal genes. J. Bacteriol. 175: 3486-3490.

Durrenberger, F., A. Crameri, B. Hohn, and Z. Koukolikova-Nicola. 1986. Covalently bound VirD2 protein of *Agrobacterium tumefaciens* protects the T-DNA from exonucleolytic degradation. Proc. Natl. Acad. Sci. USA 86:9154-9158.

Egelman, E. H. 1993. What do X-ray crystallographic and electron microscope structural studies of the RecA protein tell us about recombination? Curr. Opin. Struct. Biol. 3:189-197.

Egelman, E. H. and A. Stasiak. 1986. Structure of helical RecA-DNA complexes formed in the presence of ATP-gamma-S or ATP. J. Mol. Biol. 191:677-697.

Ellis, J. G., M. H. Ryder, and M. E. Tate. 1984. *Agrobacterium tumefaciens* TR-DNA encodes a pathway for agropine biosynthesis. Mol. Gen. Genet. 195:466-473.

Fernandez, D., T. A. T. Dang, G. M. Spudich, X. Zhou, B R. Berger, and P. J. Christie. 1996a. The *Agro. tum. virB7* gene product, a proposed component of the T-complex transport apparatus, is a membrane-

associated lipoprotein exposed at the periplasmic surface. J. Bacteriol. 178:3156-3167.

Fernandez, D., G. M. Spudich, X. Zhou, and P. J. Christie. 1996b. The *Agrobacterium tumefaciens* VirB7 lipoprotein is required for stabilization of VirB proteins during assembly of the T-complex transport apparatus. J. Bacteriol. 178:3168-3176.

Filichkin, S. A., and S. B. Gelvin. 1993. Formation of a putative relaxation intermediate during T-DNA processing directed by the *Agrobacterium tumefaciens* VirD1, VirD2 endonuclease. Molec. Microbiol. 8:915-926.

Finberg, K. E., T. R. Muth, S. P. Young, J. B. Maken, S. M. Heitritter, A. N. Binns, and L. M. Banta. 1995. Interactions of VirB9, -10, and -11 with the membrane fraction of *Agrobacterium tumefaciens*: solubility studies provide evidence for tight associations. J. Bacteriol. 177:4881-4889.

Frost, L. S., W. Paranchych, and N. S. Willetts. 1984. DNA sequence of the F *tra* ALE region that includes the gene for F. pilin. J. Bacteriol. 160:395-401.

Fullner, K. J., K. M. Stephens, and E. W. Nester. 1994. An essential virulence protein of *Agrobacterium tumefaciens*, VirB4, requires an intact mononucleotide binding domain to function in transfer of T-DNA. Mol. Gen. Genet. 245:704-715.

Gardner, R. C., and V. C. Knauf. 1986. Transfer of *Agrobacterium* DNA to plants requires a T-DNA border but not the *virE* locus. Science 231:725-727.

Gardner, R. V., O. N. Voloshin, and R. D. Cremerini-Otero. 1995. The identification of the single-stranded DNA-binding domain of the *E. coli* RecA protein. Eur. J. Biochem. 233:419-425.

Garfinkel, D. J., and E. W. Nester. 1980. *Agrobacterium tumefaciens* mutants affected in crown gall tumorigenesis and octopine catabolism. J. Bacteriol. 144:732-743.

Garfinkel, D. J., R. B. Simpson, L. W. Ream, F. F. White, M. P. Gordon and E. W. Nester. 1981. Genetic analysis of crown gall: a fine structure map of the T-DNA by site-directed mutagenesis. Cell 27:143-153.

Ghai, J., and A. Das. 1989. The *virD* operon of *Agrobacterium tumefaciens* Ti plasmid encodes a DNA-relaxing enzyme. Proc. Natl. Acad. Sci. USA 86:3109-3113.

Gheysen, G., R. Villarroel, M. Van Montagu. 1991. Illegitimate recombination in plants: a model for T-DNA integration. Genes Dev. 5:287-297.

Gietl, C., Z. Koukolikova-Nicola, and B. Hohn. 1987. Mobilization of T-DNA from *Agrobacterium* to plant cells involves a protein that binds single-stranded DNA. Proc. Natl. Acad. Sci. USA 84:9006-9010.

Goff, S. P. and V. R. Prasad. 1991. Linker insertion mutagenesis as a probe of structure-function relationships. p. 586-603. *In* Methods in Enzymology. R. Sauer (ed). Vol. 208 Academic Press, San Diego.

Gray, J., J. Wang, and S. B. Gelvin. 1992. Mutation of the *miaA* gene of *Agrobacterium tumefaciens* results in reduced *vir* gene expression. J. Bacteriol. 174:1086-1098.

Grevelding, C., V. Fantes, E. Kemper, J. Schell, and R. Masterson. 1993. Single-copy T-DNA insertions in *Arabidopsis* are the predominant form of integration in root-derived transgenics, whereas multiple insertions are found in leaf discs. Plant. Mol. Biol. 23:847-860.

Han, D. C. and S. C. Winans. 1994. A mutation in the receiver domain of the *Agrobacterium tumefaciens* transcriptional activator VirG increases its affinity for operator DNA. Molec. Microbiol. 12:23-30.

Hanahan, D. 1983. Studies on transformation of *Escherichia coli* with plasmids. J. Mol. Biol. 166:557-580.

Herrera-Estrella, A., Z. Chen, M. Van Montagu, and K. Wang. 1988. VirD proteins of *Agrobacterium tumefaciens* are required for the

formation of a covalent DNA-protein complex at the 5' terminus of T-strand molecules. EMBO J. 1:4055-4062.

Hino, O., K. Ohtake, and C. E. Rogler. 1989. Features of two hepatitis B virus (HBV) DNA integrations suggest mechanisms of HBV integration. J. Virol. 63:2638-2643.

Hirooka, T. and C. I. Kado. 1986. Location of the right-boundary of the virulence region on *Agrobacterium tumefaciens* plasmid pTiC58 and a host-specifying gene next to the boundary. J. Bacteriol. 168:237-243.

Hirooka, T., P. M. Rogowsky, and C. I. Kado. 1987. Characterization of the *virE* locus of *Agrobacterium tumefaciens* plasmid pTiC58. J. Bacteriol. 169:1529-1536.

Hoess, R. H. and K. Abremski. 1985. Mechanism of strand cleavage and exchange in the Cre-*lox* site-specific recombination system. J. Mol. Biol. 181:351-362.

Holsters, M., D. deWaele, A. Depicker, E. Messens, M. Van Montagu, and J. Schell. 1978. Transfection and transformation of *Agrobacterium tumefaciens*. Mol. Gen. Genet. 163: 181-187.

Hooykaas, P. J. J., and A. G. M. Beijersbergen. 1994. The virulence system of *Agrobacterium tumefaciens.* Ann. Rev. Phytopathol. 32:157-179.

Horsch, R. B., H. J. Klee, S. Stachel, S. C. Winans, E. W. Nester, S. G. Rogers, and R. T. Fraley. 1986. Analysis of *Agrobacterium tumefaciens* virulence mutants on leaf discs. Proc. Natl. Acad. Sci. USA 83:2571-2575.

Hosada, J., R. L. Burke, H. Moise, I. Kubota, and A. Tsugita. 1980. Mechanistic studies on DNA replication and genetic recombination. ICN-UCLA Symp. Mol. Cell. Biol. 19:505-513.

Howard, E. A., B. A. Winsor, G. DeVos, and P. Zambryski. 1989. Activation of the T-DNA transfer process in *Agrobacterium* results in the generation of a T-strand-protein complex: tight association of

VirD2 with the 5' ends of T-strands. Proc. Natl. Acad. Sci. USA 86:4017-4021.

Howard, E. A., J. R. Zupan, V. Citovsky, and P. C. Zambryski. 1992. The VirD2 protein of *Agrobacterium tumefaciens* contains a bipartite nuclear localization signal: implication for nuclear uptake in plant cells. Cell 68:109-118.

Hurley, J. M., S. Chervitz, T. C. Jarvis, B. S. Singer, and L. Gold. 1993. Assembly of bacteriophage T4 replication machine requires the acidic carboxy terminus of gene 32 protein. J. Mol. Biol. 229:398-418.

Inze, D., A. Follin, M. Van Lijsebettens, C. Simoens, C. Genetello, M. Van Montagu, and J. Schell. 1984. Genetic analysis of the individual T-DNA genes of *Agrobacterium tumefaciens*; further evidence that two genes are involved in indole-3-acetic acid synthesis. Mol. Gen. Genet. 194:265-274.

Jasper, F., C. Koncz, J. Schell, and H. H. Steinbiss. 1994. *Agrobacterium* T-strand production *in vitro*: sequence-specific cleavage and 5' protection of single-stranded DNA templates by purified VirD2 protein. Proc. Natl. Acad. Sci. USA 91:694-698.

Jayaswal, R. K., K. Veluthambi, S. B. Gelvin, and J. L. Slightom. 1987. Double-stranded cleavage of T-DNA and the generation of single-stranded T-DNA molecules in *E. coli* by a *virD* encoded border specific endonuclease from *Agrobacterium tumefaciens*. J. Bacteriol. 169:5035-5045.

Ji, J. M., A. Martinez, M. Dabrowski, K. Veluthambi, S. B. Gelvin, and W. Ream. 1988. The *overdrive* enhancer sequence stimulates production of T-strands from the*Agrobacterium tumefaciens* tumor-inducing plasmid. *In* B. Staskawicz, P. Ahlquist, and O. Yoder (ed.), Molecular biology of plant pathogen interactions. UCLA Symposium Mol. Cell. Biol. Alan R. Liss, New York.

Ji, M. J., K. Veluthambi, S. B. Gelvin, and W. Ream. 1988. The *Agrobacterium* transmission enhancer, *overdrive*, stimulates T-strand accumulation. p. 11-18. *In* N. T. Keen, T. Kosuge, L. L. Walling

(ed.). Physiology and Biochemistry of Plant-Microbial Interactions. Amer. Soc. of Plant Physiol., Washington, D. C.

Jin, S., R. K. Prusti, T. Roitsch, R. G. Ankenbauer, and E. W. Nester. 1990a. Phosphorylation of the VirG protein of *Agrobacterium tumefaciens* by the autophosphorylated VirA protein: essential role in biological activity of VirG. J. Bacteriol. 172:4945-4950.

Jin, S., T. Roitsch, P. J. Christie, and E. W. Nester. 1990b. The regulatory VirG protein specifically binds to a *cis*-acting regulatory sequence involved in transcriptional activation of *Agrobacterium tumefaciens* virulence genes. J. Bacteriol. 172:531-537.

Jin, S., Y. N. Song, W. Deng, M.P. Gordon, and E. W. Nester. 1993a. The regulatory VirA protein of *Agrobacterium tumefaciens* does not function at elevated temperatures. J. Bacteriol. 175:6830-6835.

Jin, S., Y. N. Song, S. Q. Pan, and E. W. Nester. 1993b. Characterization of a *virG* mutation that confers constitutive virulence gene expression in *Agrobacterium*. Molec. Microbiol. 7:555-562.

Jorgensen, R. A., S. J. Rothstein, and W.S. Reznikoff. 1979. A restriction enzyme cleavage map of Tn*5* and location of a region encoding neomycin resistance. Mol. Gen. Genet. 177:65-72.

Joyce, C. M., and N. D. T. Grindley. 1984. Method for determining whether a gene of *Escherichia coli* is essential: application to the *polA* gene. J. Bacteriol. 158:636-643.

Kado, C. I. 1994. Promiscuous DNA transfer system of *Agrobacterium tumefaciens*: role of the *virB* operon in sex pilus assembly and synthesis. Molec. Microbiol. 12:17-22.

Kahl, G. 1982. Molecular biology of wound healing: the conditioning phenomenon. p. 211-267. *In* Molecular biology of plant tumors. ed. G. Kahl and J. Schell. Academic Press, New York.

Kemp, J. D. 1982. Enzymes in octopine and nopaline metabolism. p. 461-471. *In* Molecular biology of plant tumors. ed. G. Kahl and J. Schell. Academic Press, New York.

Kerr, A. and J. G. Ellis. 1982. Conjugation and transfer of Ti plasmids in *Agrobacterium tumefaciens.* p.321-344. *In* Molecular biology of plant tumors. ed. G. Kahl and J. Schell. Academic Press, New York.

Knauf, V. C., C. G. Panagopoulos, and E. W. Nester. 1982. Genetic factors controlling host range of *Agrobacterium tumefaciens.* Phytopathol. 72:1545-1549.

Koestsier, P., A. J. Schorr, and W. Doerfler. 1993. A rapid optimized procedure of downward alkaline southern blotting of DNA. Biotechniques 15:260-261.

Koncz, C., N. Martini, R. Mayerhofer, Z. Koncz-Kalman, H. Korber, G. P. Redei, and J. Schell. 1989. High-frequency T-DNA-mediated gene tagging in plants. Proc. Natl. Acad. Sci. USA 86:8467-8471.

Krassa, K. B., L. S. Green, and L. Gold. 1991. Protein-protein interactions with the acidic COOH terminus of the single-stranded DNA-binding protein of the bacteriophage T4. Proc. Natl. Acad. Sci. USA 88:4010-4014.

Langley, R. 1971. Practical statistics simply explained. Dover Pub., New York.

Lee, K., M. W. Dudley, K. M. Hess, D. G. Lynn, R. D. Joeger, and A. N. Binns. 1992. Mechanism of activation of *Agrobacterium* virulence genes: identification of phenol-binding proteins. Proc. Natl. Acad. Sci. USA 89:8666-8670.

Leroux, B., M. F. Yanofsky, S. C. Winans, J. E. Ward, S. F. Zeigler, and E. W. Nester. 1987. Characterization of the *virA* locus of *Agrobacterium tumefaciens*: a transcriptional regulator and host range determinant. EMBO J. 6:84999-856.

Lessl, M., D. Balzer, K. Weyrauch, and E. Lanka. 1993. The mating pair formation system of plasmid RP4 defined by RSF1010 mobilization and donor-specific phage propagation. J. Bacteriol. 175:6415-6425.

Lessl, M., and E. Lanka. 1994. Common mechanisms in bacterial conjugation and Ti-mediated T-DNA transfer to plant cells. Cell 77:321-324.

Lessl, M., W. Pansegrau, and E. Lanka. 1992. Relationship of DNA-transfer-systems: essential transfer factors of plasmids RP4, Ti and F share common sequences. Nucleic Acids Res. 20:6099-6100.

Lin, T., and C. I. Kado. 1993. The *virD4* gene is required for virulence while *virD3* and *orf5* are not required for virulence of *Agrobacterium tumefaciens*. Mol. Microbiol. 9:803-812.

Lohman, T. M. and L. B. Overman. 1985. Two binding modes in *E. coli* single strand binding protein-single stranded DNA complexes: modulation by NaCl concentration. J. Biol. Chem. 260:3595-3603.

Maneewannakul, K., S. Maneewannakul, and K. Ippen-Ihler. 1993. Synthesis of F pilin. Bacteriol. 175:1384-1391.

Maniatis, T., E. F. Fritsch, and J. Sambrook. 1982. Molecular cloning: a laboratory manual. Cold Spring Harbor Laboratory, Cold Spring Harbor.

Manoil, C., J. J. Mekalanos, and J. Beckwith. 1990. Alkaline phosphatase fusions: sensors of subcellular location. J. Bacteriol. 172:515-518.

Mantis, N. J., and S. C. Winans. 1993. The chromosomal response regulatory gene *chvI* of *Agrobacterium tumefaciens* complements an *Escherichia coli phoB* mutation and is required for virulence. J. Bacteriol. 175:6626-6636.

Mayerboeuf, F., O. N. Voloshin, R. D. Camerini-Otero, and M. Takahashi. 1995. The central aromatic residue in loop L2 of RecA interacts with DNA. J. Biol. Chem. 270:30927-30932.

Mayerhofer, R., Z. Koncz-Kalman, C. Nawrath, G. Bakkeren, A. Crameri, K. Angelis, G. P. Redei, J. Schell, B. Hohn, and C. Koncz. 1991. T-DNA integration: a mode of illegitimate recombination in plants. EMBO J. 10:697-704.

McBride, K. E., and V. C. Knauf. 1988. Genetic analysis of the *virE* operon of the *Agrobacterium* Ti plasmid pTiA6. J. Bacteriol. 170:1430-1437.

McLeod, M., F. Volkert, and J. Broach. 1984. Components of the site-specific recombination system encoded by the yeast plasmid 2-micron circle. Cold Spring Harbor Symp. Quant. Biol. 49:779-787.

Melchers, L. S., A. J. G. Regensburg-Tuink, R. B. Bourret, N. J. A. Sedee, R. A. Schilperoort, and P. J. J. Hooykaas. 1989. Membrane topology and functional analysis of the sensory protein VirA of *Agrobacterium tumefaciens.* EMBO J. 8:1919-1925.

Messens, E., A. Lenaerts, M. Van Montagu, and R. W. Hedges. 1985. Genetic basis for opine secretion from crown gall tumor cells. Mol. Gen. Genet. 199:344-348.

Mikawa, T., R. Masui, T. Ogawa, H. Ogawa, and S. Kurmisu. 1995. N-terminal 33 amino acid residues of *Escherichia coli* RecA protein contribute to its self-assembly. J. Mol. Biol. 250:471-483.

Miranda, A., G. Janssen, L. Hodges, E. G. Peralta, and W. Ream. 1992. *Agrobacterium tumefaciens* transfers extremely long T-DNAs by a unidirectional mechanism. J. Bacteriol. 174:2288-2297.

Nash, H. A. 1981. Integration and excision of bacteriophage λ: the mechanism of conservative site specific recombination. Ann. Rev. Genet. 15:143-167.

Ohba, T., Y. Yoshioka, C. Machida, and Y. Machida. 1995. DNA rearrangement associated with the integration of T-DNA in tobacco: an example of multiple duplications of DNA around the integration target. Plant J. 7:157-164.

Okamoto, S., A. Toyoda-Yamamoto, K. Ito, I. Takebe, and Y. Machida. 1991. Localization and orientation of the VirD4 protein of *Agrobacterium tumefaciens* in the cell membrane. Mol. Gen. Genet. 228:24-32.

Otten, L., H. DeGreve, J. Leemans, R. Hain, P. J. J. Hooykaas, and J. Schell. 1984. Restoration of virulence of *vir* region mutants of *Agrobacterium tumefaciens* strain B653 by coinfection with normal and mutant *Agrobacterium* strains. Mol. Gen. Genet. 175:159-163.

Pansegrau, W., and E. Lanka. 1991. Common sequence motifs in DNA relaxases and nick regions from a variety of DNA-transfer systems. Nucleic Acids Res. 19:3455.

Pansegrau, W. F. Schoumacher, B. Hohn and E. Lanka. 1993. Site-specific cleavage and joining of single-stranded DNA by VirD2 protein of *Agrobacterium tumefaciens* Ti plasmid: analogy to bacterial conjugation. Proc. Natl. Acad. Sci. USA 90:11538-11542.

Pansegrau, W., W. Shroeder, and E. Lanka. 1993. Relaxase (Tral) of IncPα plasmid RP4 catalyzes a site specific cleaving-joining reaction of single-stranded DNA. Proc. Natl. Acad. Sci. USA 90:2925-2929.

Pansegrau, W., W. Shroeder, and E. Lanka. 1994. Concerted actions of three distinct domains in the DNA-cleaving joining reaction catalyzed by relaxase (Tral) of conjugative plasmid RP4. J. Biol. Chem. 269:2782-2789.

Parkinson, J. S., and E. C. Kofoid. 1992. Communication modules in bacterial signaling proteins. Annu. Rev. Genet. 26:71-112.

Pazour, G. J. and A. Das. 1990. Characterization of the VirG binding site of *Agrobacterium tumefaciens*. Nucl. Acids Res. 18:6909-6913.

Peralta, E. G., R. Hellmiss and W. Ream. 1986. *Overdrive*, a T-DNA transmission enhancer on the *Agrobacterium* tumor-inducing plasmid. EMBO J. 5:1137-1142.

Peralta, E. G., and W. Ream. 1985. T-DNA border sequences required for crown gall tumorigenesis. Proc. Natl. Acad. Sci. USA 82:5112-5116.

Pierson, L.S., and M. L. Kahn. 1984. Cloning of the integration and attachment regions of bacteriophage P4. Mol. Gen. Genet. 195:44-51.

Pohlman, R. F., H. D. Genetti, and S. C. Winans. 1994. Common ancestry between IncN conjugal transfer genes and macromolecular export systems of plant and animal pathogens. Mol. Microbiol. 14:655-668.

Powell, B. S., and C. I. Kado. 1990. Specific binding of VirG to the *vir*-box requires a c-terminal domain and exhibits a minimum concentration threshold. Mol. Microbiol. 4:2159-2166.

Powell, G. K., N. G. Hommes, J. Kuo, L. A. Castle, and R. O. Morris. 1988. Inducible expression of cytokinin biosynthesis in *Agrobacterium tumefaciens* by plant phenolics. Mol. Plant-Microbe Interact. 1:235-242.

Prasad, B. V. Y. and W. Chiu. 1987. Sequence comparisons of single-stranded DNA binding proteins and its structural implications. J. Mol. Biol. 193:579-584.

Pugsley, A. P. 1993. The complete secretory pathway in gram-negative bacteria. Microbiol. Rev. 57:50-108.

Ream, L. W., M. P. Gordon, and E. W. Nester. 1983. Multiple mutations in the T-regions of the *Agrobacterium tumefaciens* tumor inducing plasmid. Proc. Natl. Acad. Sci. USA 80:1660-1664.

Ream, W. 1989. *Agrobacterium tumefaciens* and interkingdom genetic exchange. Ann. Rev. Phytopathol. 27:583-618.

Reisert, P. 1981. Plant cell surface structure and recognition phenomena with reference to symbioses. Int. Rev. Cytol. 12(Suppl.):71-112.

Roca, A. I. and M. M. Cox. 1990. The RecA protein: structure and function. Crit. Rev. Biochem. Mol. Biol. 25:415-456.

Rogowsky, P. M., T. J. Close, J. A. Chimera, J. J. Shaw, and C. I. Kado. 1987. Regulation of the *vir* genes of *Agrobacterium tumefaciens* plasmid pTiC58. J. Bacteriol. 169:5101-5102.

Rogowsky, P. M., B. S. Powell, K. Shirasu, T. S. Lin, P. Morel, E. M. Zypriam, T. R. Steck, and C. I. Kado. 1990. Molecular characterization of the *vir* regulon of *Agrobacterium tumefaciens*: complete nucleotide sequence and gene organization of the 28.63-kbp regulon cloned as a single unit. Plasmid. 23:85-106.

Roitsch, T., J. Wang, S. Jin, and E. W. Nester. 1990. Mutational analysis of the VirG protein, a transcriptional activator of *Agrobacterium tumefaciens* virulence genes. J. Bacteriol. 172:6054-6060.

Rossi, L., B. Hohn, and B. Tinland. 1996. Integration of complete transferred DNA units is dependent on the activity of virulence E2 protein of *Agrobacterium tumefaciens.* Proc. Natl. Acad. Sci. 93:126-130.

Roth, D. B., W. B. Chang, and J. H. Wilson. 1989. Comparison of filler DNA at immune, non-immune and oncogenic rearrangements suggests multiple mechanisms of formation. Mol. Cell. Biol. 9:3049-3057.

Roth, D. B., and J. H. Wilson. 1986. Nonhomologous recombination in mammalian cells: roles for short sequence homologies in the joining reaction. Mol. Cell. Biol. 6:4295-4303.

Roth, D. B., and J. H. Wilson. 1988. Illegitimate recombination in mammalian cells p. 621-653. *In* R. Kucherlapati and G. R. Smith (ed.). Genetic recombination. Amer. Soc. Microbiol., Washington, D. C.

Scheiffele, P., W. Pansegrau, and E. Lanka. 1995. Initiation of *Agrobacterium tumefaciens* T-DNA processing. Purified proteins VirD1 and VirD2 catalyze site- and strand-specific cleavage of superhelical T-DNA border *in vitro.* J. Biol. Chem. 270:1269-1276.

Schroder, G., S. Waffenschmidt, E. W. Weiler, and J. Shroder. 1984. The T-region of the Ti plasmids codes for an enzyme synthesizing indole-3-acetic acid. Eur. J. Biochem. 138:387-391.

Sen, P., G. J. Pazour, D. Anderson, and A. Das. 1989. Cooperative binding of *Agrobacterium tumefaciens* VirE2 protein to single-stranded DNA. J. Bacteriol. 171:2573-2580.

Shamoo, Y., A. M. Friedman, M. R. Parsons, W. H. Konigsberg, and T. A. Steitz. 1995. Crystal structure of a replication fork: single-stranded DNA binding protein (T4 gp32) complexed to DNA. Nature 376:362-366.

Sheeren-Groot, E. P., K. W. Rodenberg, A. Dulk-Ras, S. C. H. J. Turk, and P. J. J. Hooykaas. 1994. Mutational analysis of the transcriptional activator VirG of *Agrobacterium tumefaciens*. J. Bacteriol. 176:6418-6426.

Shimoda, N., A. Toyoda-Yamamoto, J. Nagamine, S. Usami, M. Katayama, Y. Sakagami, and Y. Machida. 1990. Control of expression of *Agrobacterium vir*-genes by synergistic actions of phenolic signal molecules and monosaccharides. Proc. Natl. Acad. Sci. USA 87: 6684-6688.

Shirasu, K., and C. I. Kado. 1993. Membrane localization of the Ti plasmid VirB proteins involved in the biosynthesis of pilin-like conjugative structure on *Agrobacterium tumefaciens*. FEMS Microbiol. Let. 111:287-294.

Shirasu, K., Z. Koukolikova-Nicola, B. Hohn, and C. I. Kado. 1994. An inner-membrane associated virulence protein essential for T-DNA transfer from *Agrobacterium tumefaciens* to plants exhibits ATPase activity and similarities to conjugative transfer genes. Molec. Microbiol. 11:581-588.

Shirasu, K., P. Morel, and C. I. Kado. 1990. Characterization of the *virB* operon of an *Agrobacterium tumefaciens* Ti plasmidi nucleotide sequence and protein analysis. Mol. Microbiol. 4:1153-1163.

Shurvinton, C. E., L. Hodges, and W. Ream. 1992. A nuclear localization signal and the C-terminal omega sequence in the *Agrobacterium tumefaciens* VirD2 endonuclease are important for tumor formation. Proc. Natl. Acad. Sci. USA 89:11837-11841.

Shurvinton, C. E., and W. Ream. 1991. Stimulation of the *Agrobacterium tumefaciens* T-DNA transfer by *overdrive* depends on a flanking sequence but not on helical position with respect to the border repeat. J. Bacteriol. 173:5558-5563.

Stachel, S. E., E. Messens, M. Van Montagu, and P. Zambryski. 1985. Identification of the signal molecules produced by wounded plant cells that activate T-DNA transfer in *Agrobacterium tumefaciens*. Nature 318:624-629.

Stachel, S. E., and E. W. Nester. 1986. The genetic and transcriptional organization of the *vir* region of the A6 Ti plasmid of *Agrobacterium tumefaciens*. EMBO J. 5:1445-1454.

Stachel, S. E., E. W. Nester, and P. C. Zambryski. 1986a. A plant cell factor induces *Agrobacterium tumefaciens vir* gene expression. Proc. Natl. Acad. Sci. USA 83:379-383.

Stachel, S. E., B. Timmerman, and P. Zambryski. 1986b. Generation of single-stranded T-DNA molecules during the initial stages of T-DNA transfer from *Agrobacterium tumefaciens* to plant cells. Nature 322:706-712.

Stachel, S. E., B. Timmerman, and P. Zambryski. 1987. Activation of *Agrobacterium tumefaciens vir* gene expression generates multiple single-stranded T-strand molecules from the pTiA6 T-region: requirement for 5' *virD* gene products. EMBO J. 6:857-863.

Stachel, S. E., and P. Zambryski. 1986. *virA* and *virG* control the plant-induced activation of the T-DNA transfer process of *A. tumefaciens*. Cell 46:325-333.

Stephens K. M., C. Roush, and E. Nester. 1995. *Agrobacterium tumefaciens* VirB11 protein requires a consensus nucleotide-binding site for function in virulence. J. Bacteriol. 177:27-36.

Story, R. M., D. K. Bishop, N. Kleckner, and T. A. Steitz. 1993. Structural relationship of bacterial RecA protein to recombination proteins from Bacteriophage T4 and yeast. Science 259:1892-1896.

Story, R. M., I. T. Welier, and T. A. Steitz. 1992. The structure of the *E. coli recA* protein monomer and ploymer. Nature 355:318-325.

Sundberg, C., L. Meek, K. Carroll, A. Das, and W. Ream. 1996. VirE1 protein mediates export of the single-stranded DNA-binding protein VirE2 from *Agrobacterium tumefaciens* into plant cells. J. Bacteriol. 178:1207-1212.

Thomashow, L. S., S. Reeves, and M. F. Thomashow. 1985. Crown gall oncogenesis: evidence that a T-DNA gene from the *Agrobacterium* Ti plasmid pTiA6 encodes an enzyme that catalyzes synthesis of indoleacetic acid. Proc. Natl. Acad. Sci. USA 81:5071-5075.

Thompson, D. V., L. S. Melchers, K. B. Idler, R. A. Schilperoort, and P. J. J. Hooykaas. 1988. Analysis of the complete nucleotide sequence of the *Agrobacterium tumefaciens virB* operon. Nucleic Acids Res. 16:4621-4636.

Thorstenson, Y. R., G. A. Kuldau, and P. C. Zambryski. 1993. Subcellular localization of seven *virB* proteins of *Agrobacterium tumefaciens:* implications for the formation of a T-DNA transport structure. J. Bacteriol. 175: 5233-5244.

Thorstenson, Y. R., and P. C. Zambryski. 1994. The essential virulence protein VirB8 localizes to the inner membrane of *Agrobacterium tumefaciens.* J. Bacteriol. 176:1711-1717.

Tinland, B., Z. Koukolikova-Nicola, M. N. Hall, and B. Hohn. 1992. The T-DNA-linked VirD2 protein contains two distinct functional nuclear localization signals. Proc. Natl. Acad. Sci. USA 89:7442-7446.

Tinland, B., F. Schoumacher, V. Gloeckler, A. M. Bravo-Angel, and B. Hohn. 1995. *Agrobacterium tumefaciens* virulence D2 protein is responsible for precise integration of T-DNA into the plant genome. EMBO J. 14:3585-3595.

Toro, N., A. Datta, O. A. Carmi, C. Young, R. K. Prusti, and E. W. Nester. 1989. The *Agrobacterium tumefaciens virC1* gene product binds to *overdrive*, a T-DNA transfer enhancer. J. Bacteriol. 171:6845-6849.

Toro, N. A. Datta, M. Yanofsky, and E. W. Nester. 1988. Role of the *overdrive* sequence in T-DNA border cleavage in *Agrobacterium*. Proc. Natl. Acad. Sci. USA 85:8558-8562.

van Haaren, M. J. J., N. J. A. Sedee, R. A. Schilperoort, and P. J. J. Hooykaas. 1987. Overdrive is a T-region transfer enhancer which stimulates T-strand production in *Agrobacterium tumefaciens* Nucleic Acids Res. 15:8983-8997.

Van Larebeke, N., G. Engler, M. Holsters, S. Van den Elsacker, I. Zaenen, R. A. Schilperoort, and J. Schell. 1974. Large plasmid in *Agrobacterium tumefaciens* essential for crown gall inducing activity. Nature 252:169-170.

Veluthambi, K., W. Ream, and S. B. Gelvin. 1988. Virulence genes, borders and overdrive generate single-stranded T-DNA molecules from the A6 Ti plasmid of *Agrobacterium tumefaciens*. J. Bacteriol. 170:1523-1532.

Vogel, A. M., and A. Das. 1992a. Mutational analysis of *Agrobacterium tumefaciens virD2:* tyrosine 29 is essential for endonuclease activity. J. Bacteriol. 174:303-308.

Vogel, A. M., and A. Das. 1992b. The *Agrobacterium tumefaciens virD3* gene is not essential for tumorigenicity on plants. J. Bacteriol. 174:5161-5164.

Voloshin, O. N., L. Wang, and R. D. Camerini-Otero. 1996. Homologous DNA pairing promoted by a 20 amino acid peptide derived from RecA. Science 272:868-872.

Wang, K., A. Herrera-Estrella, and M. Van Montagu. 1990. Overexpression of *virD1* and *virD2* genes in *Agrobacterium tumefaciens* enhances T-complex formation and plant transformation. J. Bacteriol. 172:4432-4440.

Wang, K., S. E. Stachel, B. Timmerman, M. Van Montagu, and P. C. Zambryski. 1987. Site-specific nick in the T-DNA border sequence is a result of *Agrobacterium vir* gene expression. Science 235:587-591.

Ward, E. R., and W. M. Barnes. 1988. VirD2 protein of *Agrobacterium tumefaciens* very tightly linked to the 5' end of the T-strand DNA. Science 242:927-930.

Ward, J. E., E. M. Dale, and A. N. Binns. 1991. Activity of the *Agrobacterium* T-DNA transfer machinery is affected by the *virB* gene products. Proc. Natl. Acad. Sci. USA 88:9350-9354.

Ward, J. E., E. M. Dale, P. J. Christie, E. W. Nester, and A. N. Binns. 1990. Complementation analysis of *Agrobacterium tumefaciens* Ti plasmid *virB* genes by use of a *vir* promoter expression vector: *virB9, virB10* and *virB11* are essential virulence genes. J. Bacteriol. 172. 5187-5199.

Waters, V. L., K. H. Hirata, W. Pansegrau, E. Lanka, and D. G. Guiney. 1991. Sequence identity in the nick regions of IncP plasmid transfer origins and T-DNA borders of *Agrobacterium* Ti plasmids. Proc. Natl. Acad. Sci. USA 88:1456-1460.

Watson, B., T. C. Currier, M. P. Gordon, M. D. Chilton, and E. W. Nester. 1975. Plasmid required for virulence of *Agrobacterium tumefaciens*. J. Bacteriol. 123:255-264.

Willmitzer, L., M. Debeuckeleer, M. Lemmers, M. Van Montagu, and J. Schell. 1980. DNA from Ti plasmid present in nucleus and absent from plastids of crown gall plant cells. Nature 287:359-361.

Winans, S. C. 1992. Two way chemical signaling in *Agrobacterium*-plant interactions. Microbiol. Rev. 56:12-31.

Winans, S. C., P. Allenza, S. E. Stachel, K. E. McBride, and E. W. Nester. 1987. Characterization of the *virE* operon of the *Agrobacterium tumefaciens* Ti plasmid pTiA6. Nucleic Acids. Res. 15:825-838.

Winans, S. C., R. A. Kerstetter, and E. W. Nester. 1988. Transcriptional regulation of the *virA* and *virG* genes of *Agrobacterium tumefaciens*. J. Bacteriol. 170:4047-4054.

Winans, S. C., R. A. Kerstetter, J. E. Ward, and E. W. Nester. 1989. A protein required for transcriptional regulation of *Agrobacterium* virulence genes spans the cytoplasmic membrane. J. Bacteriol. 171:1616-1622.

Winans, S. C., N. J. Mantis, C. Chen, C. Chang, and D. C. Han. 1994. Host recognition by the VirA, VirG two component regulatory proteins of *Agrobacterium tumefaciens*. Res. In Microbiol. 145:461-473.

Yadav, N. S., J. Vanderleyden, D. R. Bennett, W. M. Barnes, and M. D. Chilton. 1982. Short direct repeats flank the T-DNA on a nopaline Ti plasmid. Proc. Natl. Acad. Sci. USA 79:6322-6326.

Yanisch-Perron, C., J. Vieira, and J. Messing. 1985. Improved M13 phage cloning vectors and host strains: nucleotide sequence of the M13, mp18 and pUC19 vectors. Gene 33:103-119.

Yanofsky, M., B. Lowe, A. Montoya, R. Rubin, W. Krul, M. Gordon, and E. Nester. 1985. Molecular and genetic analysis of factors controlling host range in *Agrobacterium tumefaciens*. Mol. Gen. Genet. 201:237-246.

Yanofsky, M. F., and E. W. Nester. 1986. Molecular characterization of a host-range-determining locus from *Agrobacterium tumefaciens*. J. Bacteriol. 168:244-250.

Yanofsky, M. F., S. G. Porter, C. Young, L. M. Albright, M. P. Gordon, and E. W. Nester. 1986. The *virD* operon of *Agrobacterium tumefaciens* encodes a site-specific endonuclease. Cell 47:471-477.

Young, C., and E. W. Nester. 1988. Association of the VirD2 protein with the 5' end of the T strands in *Agrobacterium tumefaciens*. J. Bacteriol. 170:3367-3374.

Yu, A. and E. Haggard-Ljungquist. 1993. Characterization of the binding sites of two proteins in the bacteriophage P2 site-specific recombination system. J. Bacteriol. 175:1239-1249.

Yusibov, V. M., T. R. Steck, V. Gupta, and S. B. Gelvin. 1994. Association of single-stranded transferred DNA from *Agrobacterium tumefaciens* with tobacco cells. Proc. Natl. Acad. Sci. USA 91:2994-2998.

Zambryski, P.C. 1992. Chronicles from the *Agrobacterium*-plant cell DNA transfer story. Annu. Rev. Plant Physiol. Plant Mol. Biol. 43:465-490.

Zambryski, P., A. Depicker, K. Kruger, and H. Goodman. 1982. Tumor induction by *Agrobacterium tumefaciens*: analysis of the boundaries of T-DNA. J. Mol. Appl. Gen. 1:361-370.

APPENDIX

APPENDIX

Preliminary Data

As mentioned in the introduction (see section entitled The Role of VirE2 in T-DNA Integration) VirE2 mediated genetic recombination in *E. coli* between 2 copies of the *lacZ* gene with non-overlapping deletions. No recombination occurred in the same *E. coli* background strain containing the vector alone or containing the*virE* operon with a deletion in the *virE1* gene.

Because no colonies were observed in the *E. coli* strain with the deleted *virE1* gene, immunoblot analysis was performed to verify if the VirE2 protein was present. Although VirE2 is stable in *A. tumefuciens* without VirE1 (Sundberg *et al.* 1996), VirE2 has been reported to be unstable in *E. coli* without VirE1 (McBride and Knauf 1988). An *E. coli* strain containing the *virE* operon with a frameshift mutation in the *Bgl*II site of *virE2* was also immunoblotted as well as a strain containing only the pTrc99A vector and a strain containing the entire *virE* operon.

Twenty-ml cultures were grown overnight in L-broth containing tetracycline, ampicillin and IPTG (2 mM). The cells were harvested by centrifugation (9,500 RPM, SS34 rotor, 10 minutes) and resuspended on ice in 2 ml ice-cold buffer (10 mM Tris Hcl (pH 8.0), 25 mM NaCl, 1 mM phenyl methyl sulfonyl fluoride (PMSF), 1 mM dithiothreitol). The cells were lysed in a French press at 19,600 pounds per square inch (PSI) and centrifuged (12,000 RPM, SS34 rotor, 6 minutes). The protein concentrations of the supernatants and the pellets dissolved in buffer were determined using the Bradford method dye-binding procedure (Bradford 1976, Biorad).

The supernatant and pellet fractions were loaded (100 µg of the supernatant fractions and 10 µg of the pellet fractions) on a 10% SDS-polyacrylamide gel and immunoblotted (see Protein Methods in section 2.5). The results are shown in Figure A1.1. Only when both VirE1 and VirE2 are present, does a band corresponding in size to full length VirE2 appear. This band does not appear when *virE1* is deleted or in the *E coli* strain containing the pTrc99A vector. This VirE2 protein is insoluble as it only appears in the pellet fraction. A band corresponding to truncated VirE2 is seen only in the strain containing the *virE2* operon with a frameshift mutation in *virE2*.

This truncated VirE2 protein is also insoluble as it appears only in the pellet fraction. This experiment was repeated except the cells were induced with IPTG (2 mM) for 3 hours instead of overnight. As expected, VirE2 was not present in the strain with the deletion in *virE1*. However, the truncated VirE2 protein was also not observed indicating that this truncated protein may be unstable in *E. coli*.

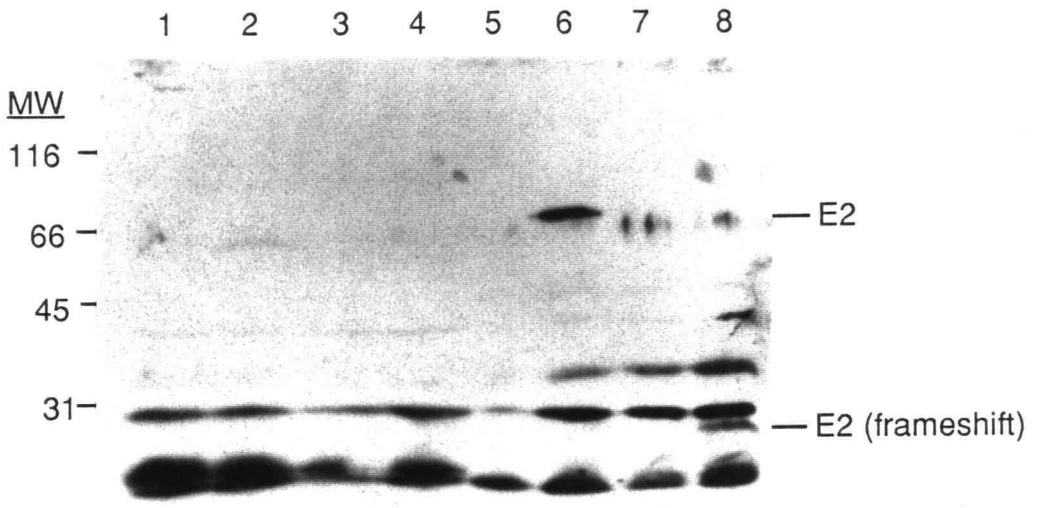

Figure A1.1. Immunoblot analysis of protein extracts from *E. coli* containing mutations in *virE1* and *virE2*.

Lane 1 vector control supernatant (WR705)
Lane 2 E1 + E2 supernatant (WR724)
Lane 3 E2 only supernatant (WR797)
Lane 4 E1 + E2(frameshift) supernatant (WR798)
Lane 5 vector control pellet (WR705)
Lane 6 E1 + E2 pellet (WR724)
Lane 7 E2 only pellet (WR797)
Lane 8 E1 + E2(frameshift) pellet (WR798)